NTNU
Det skapande universitetet

Central Processing of Plant Odor Mixtures and Single Odorants in the Moth *Heliothis virescens*

Øyvind Arne Høydal

Biologi

Hovedveiledar: Hanna Mustaparta, IBI
Medveiledar: Pål Kvello, IBI
Bjarte Løfaldlie, IBI

Noregs teknisk-naturvitskaplege universitet
Institutt for biologi

Acknowledgements

The work and writing of this thesis have been conducted at the Neuroscience Unit, Department of Biology, under the supervision of Professor Hanna Mustaparta, PhD student Bjarte Bye Løfaldli, and Dr. Pål Kvello. It has been an inspiring, exciting and fun time and I am thankful for the privilege of sharing these two years with all of you.

Especially I thank Bjarte Bye Løfaldli for introducing me to Spike 2 and Amira, and for his helpful and enthusiastic spirit. I am also thankful to Dr. Pål Kvello for his good advice and contagious cheerfulness, and to Bente Berg for sharing her knowledge and always interesting perspectives.

I would also like to give thanks to my parents, my brothers and their families for love and support through all times. Thanks to my fellow master students Siri Børø, Bente Jacobsen and Eirik Nilsen for a fair share of ridiculous conversations and for making these two years a joyful experience I will never forget.

Finally, I would like to thank Professor Hanna Mustaparta for sharing her insight and wisdom. Your enthusiasm, knowledge and cheerful spirit is an inspiration to us all.

Trondheim 15th of May

Øyvind Arne Høydal

Samandrag

Insekt nyttar luktesansen til mange formål som er avgjerande for overlevnad og reproduktiv suksess. Ein veksande kunnskapsbase tyder på at miksturar av nokre få biologisk relevante plantevolatiler kan vekke atferdsmessige responsar i insekt medan einskilde volatiler har liten effekt. Mykje forsking er gjort på nevral prosessering av binære duftblandingar i det primære luktesenteret til insekt, men ein veit lite om korleis informasjon om blandingar av mange komponentar vert handsama i høgare ordens hjernesentra. Denne studien tok sikte på å utforske prosessering av informasjon om biologisk relevante planteduftar og komplekse duftblandingar i høgare ordens luktesentra i nattflyarten *Heliothis virescens.* Insekt vart stimulerte med primære planteduftar og komplekse duftblandingar medan intracellulære registreringar vart utførte på høgare ordens nevron i laterale og superiore protocerebrum. Nokre nevron vart òg karakteriserte morfologisk ved intracellulær fargeinjeksjon, og eit av desse nevrona vart rekonstruert digitalt i tre dimensjonar og registrert inn i eit standard hjerneatlas som er konstruert for denne arten. Nevrofysiologiske analyser viste at duftblandingane vekte responsar med høgare sannsyn enn enkeltdufter i desse høgare ordens nevrona. Mange nevron skilde mellom blandingar og enkeltkomponentar ved å svare med ulik styrke på dei to typane stimuli, men det var ikkje noko fast forhold mellom responsmønstera eit nevron utviste for ei blanding og responsmønstera nevronet utviste for komponentane i blandinga. Resultata viste òg at mange nevron kunne skilje mellom to komplekse blandingar som var kjemisk nært slekta. Blandingane vakte dei sterkaste responsane I storparten av nevrona, men eit nevron svarte spesifikt på berre éin primær odorant. Desse resultata tyda på at informasjon om primære planteduftar vert integrerte i høgare ordens nevron på ein ikkje-lineær måte som er spesifikk for kvar duftblanding og kvart enkelt nevron. Vidare utviser høgare ordens nevron primært synergi for duftblandingar, men informasjon om spesifikke enkeltdufter er òg bevart i høgare hjernesentra.

Abstract

Insects use olfactory information in many tasks crucial for survival and reproduction. A growing body of evidence indicates that behavioral responses are elicited by specific mixtures of a few biologically relevant plant volatiles, even though these volatiles have little behavioral relevance when presented alone. Several studies have explored neural processing of binary blends and their constituents in the primary olfactory center of insects, but few attempts have been made to investigate how multicomponent blends are represented in higher order brain regions. The present study aimed to explore processing of multicomponent blends and single odorants in higher order olfactory centers of the moth *Heliothis virescens*. Insects were stimulated with identified primary plant odorants and multicomponent blends during intracellular recordings from higher order neurons in the superior and lateral protocerebrum. Some of the recorded neurons were morphologically characterized by dye injection, one of which was digitally reconstructed and registered into a standard brain atlas constructed for this species. Neurophysiological analysis showed that blends evoked responses with greater probability than single odorants in these higher order neurons. Many neurons distinguished between blends and single odorants by their response strengths. However, the response strengths of a particular blend could not be predicted from the responses to the constituents of the blend. In the majority of neurons, responses to the most potent blend were stronger than responses to the single odorants, an effect that was found significant when regarded over the neuronal population. Moreover, many neurons discriminated between two chemically related multicomponent blends. One neuron was unresponsive to blends and reacted exclusively to one single odorant. These results indicated that information about primary odorants is integrated in higher order neurons in a non-linear, predominantly synergistic manner, specific for any particular mixture. However, information about specific single odorants is seemingly also preserved in higher levels of odor processing.

Table of contents

1. Introduction

The chemical senses are ubiquitous in the animal kingdom, signifying their importance for survival and reproductive success. Olfaction participates in the identification of nutritious food sources and the avoidance of toxins, as well as mating and reproduction, kin recognition, social organization, predator-prey interactions, nesting and selection of oviposition sites. In mammals, olfaction is also essential for flavor perception and is intimately associated with emotions and other limbic functions (Chen & Dalton, 2005; Herz, 2005; Shepherd, 2006). The olfactory systems of many species in different phyla have been anatomically characterized. Remarkably, despite the phylogenic distance between insects and mammals, the organizations of their olfactory systems share some striking similarities. These similarities are particularly evident for the structural and functional organization of sensory neurons in the periphery and the primary olfactory centers, the antennal lobes (ALs) in insects and the olfactory bulb (OB) in vertebrates. In recent years, advances in experimental methods have led to a great expansion of our knowledge as to how odor cues in our environment are detected at the periphery and processed in the central nervous system to yield a unitary percept, ultimately affecting behavior. The relative simplicity and accessibility of the nervous system of insects make them suitable model organisms for studying general principles of neural coding of sensory information. In addition, insects make tremendous ecological impacts as pollinators, pests, and vectors of disease. The key role olfaction plays in insect behavior thus prompts a better understanding of the olfactory system of this diverse group of animals.

1.1 The olfactory system of insects

1.1.1 Odor detection at the periphery

Chemical cues are detected in the periphery by bipolar olfactory receptor neurons (ORNs) with their dendrites residing in sensilla on the antennas and the maxillary palps. In the sensilla, the dendrites of ORNs are embedded in an aqueous solution, the receptor lymph. Hydrophobic volatiles enter the receptor lymph through pores in the cuticular outer structure of the sensilla, and are transported by odorant binding proteins to receptors on the dendrites of the ORNs. The olfactory receptors (ORs), first identified in mammals, belong to the family of 7-transmembrane G-protein coupled receptors (Buck & Axel, 1991). However, the ORs of insects have adapted an inverse membrane topology, and are not structurally similar or phylogenetically related to those of

vertebrates (Robertson et al., 2003; Benton et al., 2006; Lundin et al., 2007; Kaupp, 2010). Whereas transduction in vertebrates is metabotrophic, ORs in insects are co-expressed with an obligatory subunit to form a complex acting as a ligand gated ion channel (Sato et al., 2008; Kaupp, 2010). Whether signaling through a second messenger system also occurs is a topic of debate (Larsson, et al., 2004; Kaupp, 2010). In most insects and vertebrates, each ORN express only one type of OR (Kaupp, 2010; Martin et al., 2011). This principle apparently also holds true for *H. virescens* (Krieger et al., 2002; Krieger et al., 2004). The molecular receptive range of ORNs varies among insect species. Broadly tuned ORNs have been demonstrated in the honeybee *Apis mellifera* and the fruitfly *Drosophila melanogaster* (de Bruyne et al., 1999; Sachse et al., 1999; Goldman et al., 2005), whereas narrow molecular receptive ranges have been shown for the ORNs of heliothine moths by combining chemical analysis with recordings from single ORNs (Rostelien et al., 2000; Stranden et al., 2002; Stranden et al, 2003a; Stranden et al., 2003b; Rostelien et al., 2005). ORNs in these moths respond strongly to one or two primary odorants, and weakly to a few other secondary odorants.

1.1.2 Odor processing in the ALs

ORNs expressing a particular OR converge onto one or two sphere-like structures in the ALs, called glomeruli. This mapping of ORN-types to specific glomeruli has been referred to as the molecular logic of olfaction (Axel 2005). In the glomeruli, the ORNs make excitatory synapses with projection neurons (PNs) and local interneurons (LN). LNs are structurally diverse and mediate interactions within and between glomeruli. Many LNs use gamma-amino-butyric acid (GABA) as their neurotransmitter and physiological data have shown that this neurotransmitter is inhibitory in the AL (Homberg et al., 1987; Waldrop et al., 1987; Stopfer et al., 1997; Sachse & Galizia, 2002; Berg et al., 2009; Dupuis et al., 2010). Two GABAergic subsystems, mediating fast and slow inhibition, have been identified in the ALs of the honeybee and the fruitfly (Sachse & Galizia, 2002; Wilson & Laurent, 2005). In the honeybee, LNs are also classified by structure into two main types. Homo-LNs have uniform innervations in most glomeruli, while hetero-LNs innervate one glomerulus densely and a few others in a sparser manner. It has been proposed that these two groups of LNs carry out distinct functions, with homo-LNs providing a global gain control whereas hetero-LNs refine odor representations by an asymmetric lateral inhibition (Sachse & Galizia, 2002). Distinct classes of GABAergic LNs have been found in the silk moth *Bombyx mori* (Seki & Kanzaki, 2008) and LNs containing GABA have also been demonstrated in *H. virescens* (Berg et al., 2009). Another function of inhibitory LNs, believed to be important for olfactory coding in some species, is to promote

synchrony and oscillating activity (Laurent, 2002; Ito et al, 2009; Martin & Hildebrand, 2010). Excitatory connections between glomeruli in the ALs have thus far only been demonstrated for the fruit fly, where they contribute to a broadening of the AL output (Olsen et al., 2007; Shang et al., 2007).

PNs are the functional analogs to mitral and tufted cells in the vertebrate olfactory system. These neurons receive excitatory input from ORNs and relay information to higher brain areas, most notably the Mushroom Body Calyces (MBC) and the lateral and superior protocerebrum (LP and SP, respectively) (Rø et al., 2007; Galizia & Rössler, 2010). In moths and honeybees, the PNs run mainly in three antenno-protocerebral tracts (APTs) to higher order structures: the medial, mediolateral and lateral APTs (hereinafter known as m-APT, ml-APT and l-APT, respectively) (Rø et al., 2007; Galizia & Rössler, 2010). In moths, the l-APT comprises both uniglomerular and multiglomerular PNs. Uniglomerular PNs receive input in only one glomerulus and project to the LP and MBC, while multiglomerular PNs innervate several glomeruli and send axonal arborizations to the LP and SP without entering the MBCs (Rø et al., 2007). The ml-APT consists of multiglomerular PNs, while the m-APT mostly contains uniglomerular PNs. Uniglomerular PNs in the l-APT send axonal collaterals to the LP before they terminate in the MBC. PNs in the m-APT project to the same areas, but in a contra-directional manner. A morphologically distinct group of PNs in the m-APT, thus far only identified in moths, innervate 2-4 glomeruli and follow the same projection pattern as the uniglomerular PNs (Løfaldli et al., 2010; Namiki & Kanzaki, 2011). Whereas uniglomerular PNs make excitatory synapses with their target areas, some multiglomerular PNs in the ml-APT have been shown to use GABA as their neurotransmitter (Hoskins et al., 1986; Berg et al., 2009). These PNs are highly diverse as concerns both the numbers of glomeruli they contact and the density with which they innervate each glomerulus. Because some data from the honeybee and *H. virescens* indicate that these neurons respond stronger to odor blends, it has been proposed that multiglomerular PNs provide a direct route to the lateral and superior protocerebrum, carrying combinatorial information about relevant odor mixtures innate to each species (Sun et al., 1993; Lei & Vickers, 2008; Løfaldli et al., 2012). Finally, the ALs receive modulatory input from centrifugal neurons. One particularly well characterized neuron identified in the honeybee is the ventral unpaired medial neuron of the maxillary palp (VUM_{mx}). This neuron has been shown to release octopamine to the ALs, MBCs and LP when the insect receives an appetitive reward. Electrophysiological and behavioral studies have proven this neuron to be strongly involved in appetitive associative odor

learning (Hammer, 1993; Hammer & Menzel, 1998). In *H. virescens*, a neuron with similar morphology has been found but physiological data is lacking (Rø et al., 2007). A serotonergic bilateral neuron has also been identified in this species (Zhao & Berg, 2009). This neuron received input in the AL of one hemisphere and the SP, and had extensive axonal arborizations in the contralateral AL. Recently, it was discovered that the ALs are innervated by neurons responding to sound pulses (Zhao et al., 2012).

Owing to interactions between LNs and PNs, the output from the ALs is partly decoupled from the input. This may have important implications for the processing of odor mixtures. Calcium imaging experiments from the l-APT in the honeybee showed that, while responses to mixtures could be predicted from the salience of their constituents at the input level, the representations of the more potent single odorants were suppressed at the output stage, yielding a unique mixture representation (Deisig et al., 2006; Deisig et al., 2010). Similar observations have been made in other studies, employing both calcium imaging and intracellular recordings (Krofczik et al., 2009; Yamagata et al., 2009). These studies have implied a functional division between the tracts. In this scheme, the m-APT is responsible for coding odor intensity, while the l-APT encodes specific mixtures in a concentration-invariant manner. This corresponds to two crucial tasks an insect must perform. That is, an insect seeking its host-plant from afar needs to recognize the specific combination of odorants characteristic for that plant, irrespective of the concentration and salience of any individual odorant. Depending on ecological and seasonal factors and the internal state of the insect, it must also be able to separate and choose between certain combinations of odorants that may overlap in their composition. However, in order to make inference about the relative proximity or quality of a food source or oviposition site, it is essential to preserve information about stimuli intensity and the relative quantities of the constituents in the natural mixture of odors. This dichotomy of obtaining a synthetic, concentration-invariant mixture representation on one hand while preserving information about the concentrations of single odorants on the other, might be solved through dual processing of different odor features in parallel pathways (Muller et al., 2002; Menzel et al., 2005; Krofczik et al., 2009; Yamagata et al., 2009; Galizia & Rössler, 2010).

1.1.3 Odor processing in the protocerebrum

From the ALs, information is relayed to third order neurons in higher brain centers, predominantly the MBC, LP and SP. PNs from the m-APT and the l-APT make synapses with the intrinsic neurons of the MBCs, the Kenyon cells (KCs). The MBCs contain the dendrites of the KCs while their axonal arborizations form the pedunculus and the MB lobes (MBLs) (Galizia & Rössler, 2010). In the MBLs, the KCs synapse on extrinsic neurons which in turn project widely in the protocerebrum. Some of these extrinsic neurons have been shown to provide feedback inhibition to the MBCs and the LP (Okada et al., 2007). The MBCs are heterogeneous neuropile structures receiving multimodal sensory input. Detailed knowledge of the branching patterns of PNs in the MBCs is presently not available for moth species, but PNs from the plant odor system seem to branch widely in the MBCs while some pheromone responsive PNs in *Bombyx mori* and *H. virescens* terminate in more confined areas (Homberg et al., 1988; Kanzaki et al., 2003; Rø et al., 2007; Siri Lillevoll, unpublished results). In the fruit fly, the odotopic organization of the ALs is to some degree preserved in higher order centers, as PNs receiving input from the same glomeruli terminate in circumscribed regions of the MBCs (Jefferis et al., 2001; Jefferis et al., 2007). The MBCs and MBLs are subdivided by the diversity in immunoreactivity and sizes of dendritic fields expressed by different KCs. It has been proposed that these subdivisions may allow for a segregated or parallel processing of olfactory information (Galizia & Rössler, 2010; Martin et al., 2011).

A temporal sharpening of the odor code takes place at the transition from PNs to KCs (Perez-Orive et al., 2002; Szyszka et al., 2005). Whereas PNs fire action potentials rather promiscuously, KCs respond sparsely to odor stimuli. This is partly due to the general organization of the insect olfactory system, where thousands of ORNs converge onto only a few hundreds of PNs. These PNs fan out so that each PN gives input to many of the several thousands of KCs. In the locust *Schistocera americana*, a KC is seemingly contacted by about 50% of the PNs through weak synapses, while KCs of the fruit fly and class II KCs in honeybees receive input from estimated 10 PNs (Szyszka et al., 2005; Jortner et al., 2007; Turner et al., 2008). In addition, input from inhibitory feedback and feed-forward channels, as well as intrinsic membrane properties of the KCs themselves, create only a short window of time for PNs to activate these third order neurons (Perez-Orive et al., 2002; Szyszka et al., 2005). Importantly, the MBs have been nominated key structures in the formation and retrieval of associative memories (Menzel & Giurfa, 2001; Heisenberg, 2003).

The LP is another region receiving input from the ALs. In contrast to the MBCs, PNs from all APTs project to this area. Studies on the fruit fly have shown that, similar to the MBC, PNs from a few glomeruli terminate in circumscribed areas in the LP (Tanaka et al., 2004; Jefferis et al., 2007). Furthermore, in some hymenoptera, the m-APT and l-APT terminate in separate regions with only slightly overlapping arborizations (Kirschner et al., 2006; Zube et al., 2008). In the fruit fly, third order neurons of the LP reach out to various regions of the brain, overlapping with the projections of MB extrinsic neurons (Tanaka et al., 2008). Little is known about the functional organization of the higher order centers receiving input from these third order neurons, although it has been proposed that the SP integrates sensory information and participates in decision-making (Lei et al., 2001). The LP is widely believed to be a premotoric area. Descending neurons seemingly emanate from an area ventral in the LP that has been shown to receive multimodal input, including olfactory information from the regions where PNs terminate (Tanaka et al., 2004). Another input source to the LP is extrinsic neurons of the MBs. The circuit formed by PNs, KCs and extrinsic neurons is suggested to form an associative or experience dependent pathway to the LP, while the AL-LP route constitutes a channel for naïve or inexperienced odor processing (Heimbeck et al., 2001; Keene & Wadell, 2007).

Other regions, closely associated with descending neurons, are the lateral accessory lobes (LALs) and the ventral protocerebrum (VP). These structures are bilaterally connected through a circuitry of reciprocal inhibition, resulting in long lasting excitation of one hemisphere and the silencing of the other when the insect encounters an odor plume (Iwano et al., 2010). This “flip-flopping” activity corresponds to the characteristic zig-zag searching behavior displayed by many insects as they try to locate the source of an odor plume (Kanzaki et al., 1991a; Kanzaki et al., 1991b; Lei et al., 2001; Iwano et al., 2010).

1.2 Combinatorial coding, labeled lines and parallel processing

Although the olfactory systems of many insect species are well characterized, many questions are still to be addressed as concerns how olfactory stimuli are represented in this network. Basically, odors can be coded in labeled lines or in a combinatorial fashion, but these schemes are not mutually exclusive. In a labeled line system, an odorant excites a specific population of ORNs that activate one glomerulus which in turn passes this information onto higher order brain centers in a segregate stream. From the activity in this single channel, all features of an odorant are decodable

(Galizia & Rössler, 2010). Alternatively, an odorant activates more than one population of ORNs and a corresponding set of glomeruli. In this case, the information is read out in higher levels of processing by the specific spatiotemporal glomerular pattern of activity evoked by each odorant. This is called combinatorial coding (Galizia & Szyszka, 2008; Galizia & Rössler, 2010). The pheromone system of moths provides an example where both strategies are employed. In this system, ORNs are specifically tuned to a single component which activates specific PNs. However, when single components are presented together in certain ratios, the PNs respond in an entirely different fashion, perhaps owing to lateral interactions mediated by LNs (Galizia & Rössler, 2010). Notably, a labeled line in the periphery does not necessarily translate to a labeled line in the central brain. Signals that are strictly segregated in the ORNs and even in the ALs could still be integrated by higher order neurons (Galizia & Szyszka, 2008).

The many pathways from the ALs to the brain, along with the apparent segregation in higher order neuropiles such as the MBCs, have spurred the notion of parallel odor processing. This is akin to the dual processing of different visual features by the magnocellular and parvocellular pathways in the mammalian visual system. By this notion, the parallel pathways from the ALs could carry information about different features of an odor stimulus. For instance, one channel could signal the intensity of a stimulus while the other codes for identity, or mixtures could be represented in one pathway while another extracts information about single odorants. Since odor signals are transmitted in multiple pathways to many brain regions, some of which are stratified in their design, it has been proposed that information about an odor stimulus may be analyzed under different contexts in segregate or parallel streams. The functional implications of parallel pathways for odor signaling, as well as different coding schemes for processing through multiple channels, have been thoroughly reviewed by Galizia and Rössler (2010).

1.3 Current knowledge and issues to be addressed

The work presented in this thesis is a small contribution to an ongoing and extensive research on the moth *H. virescens*, aiming to explore principles for neural coding of olfactory and gustatory information. Previous labors by the group have identified biologically relevant plant odorants for this species and shown that these activate specific ORNs, thus contributing considerably to an understanding of encoding at the periphery (Rostelien et al., 2000; Stranden et al., 2002; Stranden et al, 2003a; Stranden et al., 2003b; Rostelien et al., 2005) . Moreover, central neurons have been

morphologically and physiologically characterized by intracellular recordings and dye labeling. Integrating these neurons into a standard brain atlas (SBA) constructed for *H. virescens*, allows for the identification and exploration of neural circuits and the way they process olfactory information (Kvello et al., 2009; Løfaldli et al., 2010). Recent experiments by the group have sought to elucidate whether odor mixtures and single volatiles are differentially processed in the protocerebrum. In nature, virtually all olfactory stimuli encountered by an insect are present as mixtures of many volatiles, and a growing body of evidence indicates that mixtures, and not single odorants, constitute the behaviorally relevant signal (Mumm & Hilker, 2005; Lei & Vickers, 2008; Pinero et al., 2008; Riffel et al., 2009a; Riffel et al., 2009b). In essence, mixture processing can be elemental or configural (synthetic). In elemental processing, the mixture is represented as the linear sum of its constituents. Conversely, in synthetic processing, interactions between the constituents may yield a representation that is unique to the mixture (Kuebler et al., 2011). The majority of studies exploring the relationships between mixtures and single odorants has primarily employed binary blends, and has mostly focused on the ALs. Few studies have attempted to compare representations of blends and their constituents in protocerebral neurons, and these have mainly explored responses to pheromone stimuli. Hence, the work of this thesis aimed to investigate processing of plant odor mixtures and single volatiles in the protocerebrum. Intracellular recordings were performed while stimulating with biologically relevant plant odorants and mixtures of these odorants. A few neurons were also morphologically characterized by dye injection, one of which was digitally reconstructed and registered into the SBA.

Hypotheses

1) Neurons of the protocerebrum distinguish between blends and single odorants by their response strengths, and respond to blends with higher probability.

2) The response strength of a blend cannot be predicted from the response strengths to the blends constituents.

3) The protocerebrum comprises neurons mediating information about blends as well as neurons preserving information about specific single odorants.

4) Neurons of the protocerebrum are able to distinguish between two multicomponent blends of ten and twelve components, differing in their composition by two extra substances in the twelve component blend.

2. Materials and methods

2.1 The insects

Pupae of the moth *Heliothis virescense* (Heliothine; Lepidoptera; Noctuidae) were acquired from the Syngenta laboratory culture in Basel, Switzerland. The pupae were sorted according to sex and kept in separate incubators (Refritherm 200, Struers-Kebolab, Albertslund, Denmark) at a temperature of 25 ^{O} C, 70% humidity and a phase-shifted LD photoperiod (14:10 hours). Upon hatching, adult insects were transferred to cylindrical plexiglass containers (approximately 3400 cm^3, maximum 8 insects per container) with perforated lids for air supply. The Insects were fed *ad libitum* on a 0.15 M sucrose solution. Only 3-6 days old insects were used for experiments.

2.2 Preparation of test substances

Biologically relevant plant odors were diluted with hexane to concentrations of 10^{-5} M in decade steps. The mixtures were made as homogenous solutions where every odor was diluted by other odors in the mixture in addition to hexane. Thus, every primary odorant was present in equal amounts within a mixture, and every primary odorant was present in equal amounts when in a mixture as when alone. 100 µL of each test substance was applied to separate colorless filter papers (approximately 2 cm in diameter). Hexane was evaporated by a slow nitrogen flow, whereupon the filter papers were inserted into glass cartridges (100 mm * 5 mm) that were concealed by plastic plugs. A clean filter paper was used for control and prepared in the same manner as the odorants. The cartridges were kept in a refrigerator at 4^{o} C, and were replaced every week.

2.3 Preparation for intracellular recordings

In order to calm the insects before the experiment, moths were cooled for a period of time in a temperature of 4^{o}C, whereupon they were mounted in plastic tubes and immobilized with dental wax (Kerr Corporation, Romulus, MI, USA). Cephalic scales and hair on the head of the insects were removed with a forceps in order to expose the underlying cuticle. The antennae were fixated with tungsten clamps to prevent movement during the experiment. The cuticle between the antennae and posterior to the antennae was cut with a microknife and removed with a forceps; this provided a good dorsal view of the antennal nerves and antennal lobes, as well as most of the

protocerebrum. In order to gain readily access to the underlying brain tissue, trachea and intracranial muscle tissue were removed with a forceps. Ringer solution (150 mM NaCl, 3 mM CaCl2, 3 mM KCl, 25 mM C12H22O11, 10 mM TES buffer, pH 6.9) was applied regularly to avoid dehydration of the brain tissue.

2.4 Intracellular recordings

The moths were mounted inside a faraday cage to prevent electromagnetic interference from the external environment. A silver nitrate coated silver wire served as a reference electrode and was inserted into the right compound eye. The sharp borosilicate glass microelectrodes used to detect neuronal activity were pulled with a Flaming-Brown horizontal puller (P97; Sutter instruments, Novato, CA, USA). The tip of the glass electrodes was filled with the fluorescent dye tetramethylrhodamine-biotin dextran (Micro-Ruby, Invitrogen, Germany) and back-filled with a 0.2 M solution of potassium acetate. The resistance in the electrodes was in the range of 100-400 MΩ. The electrode was connected to a preamplifier (Axonprobe-1A, multipurpose microelectrode amplifier, Molecular Devices, CA, USA) through a chloride coated silver wire, inserted into the fluid-filled electrode. An oscilloscope displayed the flux of electric currents flowing to and from the electrode. This signal was digitalized by a data acquisition unit CED (Micro 1401 mk II, Cambridge Electronic Design Limited, Cambridge, UK). Spike2 (version 7, CED) was used as recording software and analyzing tool. A custom written script running in Spike2 contained stimuli codes and magnetic valve commands to control odor stimulation. The glass electrode was inserted into the brain with the aid of a micromanipulator. In some cases, parts of the neurolemma had to be removed with a fine forceps or perforated with a sharpened tungsten needle in order to reach the neurons of the protocerebrum with the sharp electrode. The dorsal LP was most often the site of insertion, but some recordings took place in the more ventral lateral areas or the superiomedial protocerebrum.

During recording, the left antenna was exposed to a continuous airstream at 400 ml/min, flowing from a glass tube with the same shape and size as the cartridges containing the test substances. Upon stimulation with an odorant, a cartridge containing the odorant was connected with a tube controlled by a separate valve and directed against the left antenna. Activation of the valve caused a puff of air to be led through the cartridge holding the odor, with a flow rate of 100 ml/min and duration of 300 ms. The time-delay from opening of the valve to the odor reached the antenna was estimated to 200 ms; this delay was compensated for in the Spike2 script. The script recorded

activity from 200 ms prior to stimulation until 10 seconds following onset. Stimulations with any particular odorant were at least 10 seconds apart. This allowed the neuron to return to spontaneous activity and helped prevent adaptation to the test substance.

2.5 Test protocol

The inherent instability of intracellular recordings imposes limits on the time available for testing. Hence, it was not feasible in any of the recordings to test the complex blends against every one of their single constituents. The emphasis put on randomization of tested substances and repetitive trials for each stimulus added to the challenge of this task. Hence, some priorities had to be made on the substances that were to be included in the test protocol. Control (puff of purified air) was always tested twice prior to stimulation with any of the odorants. When possible, air was also tested at the end of each recording. Among the odorants, blend 12 and blend 10 had first priority and were tested before any of the single odorants in a pseudo-random fashion. In addition to the two larger blends, the binary blend of linalool and hexenylacetate, blend 2, was frequently tested. This allowed, in many cases, to compare the responses of a blend to both of its single constituents. The four most frequently tested single odorants were racemic Linalool, 2-Phenylethanol, (3Z) Hexenyl acetate and (-)-Germacrene D (hereinafter referred to as linalool, phenylethanol, hexenylacetate and germacrene D, respectively). These were selected because previous experiments had proven these the most effective at eliciting neuronal responses. Also, germacrene D is one of the two substances that are added to blend 10 in order to yield blend 12. The other primary odorant distinguishing blend 12 form blend 10, farnesene, was unfortunately not available during the experimentation period. Some of the other single odorants were also included infrequently to ensure that they really had a lower response probability than the selected odorants. Like the large blends, the single odorants were also tested in a pseudo-random fashion. A table of the compositions of the tested blends is included in appendix I.

2.6 Intracellular staining and preparations for visualization of stained neurons

Following intracellular recording, dye was injected iontophoretically by passing a positive current (0.5-3 nA, 2 Hz) through the recording electrode. Staining lasted until contact with the neuron was lost, typically 5-15 minutes. Only one staining was attempted in each preparation. After staining, the animal was kept overnight in a temperature of 4^{O} C, thus allowing the dye to diffuse throughout the neuron. On the next day, the brains were dissected in Ringer solution (150 mM NaCl, 3 mM CaCl2, 3 mM KCl, 25 mM C12H22O11, 10 mM TES buffer, pH 6.9), whereupon they were fixated in 4% paraformaldehyde (24 hours, 4^{O} C) to prevent degradation of the neuronal tissue. Following fixation, the brains were rinsed in phosphate buffered saline (PBS; in mM: 684 NaCL, 13 KCl, 50.7 Na_2HPO_4 and 5 KH2PO4, pH 7.2) for 10 minutes. Streptavidin-Cy3 (Jackson Immunoresearch, West Grove, PA, USA; diluted 1:200 in PBS; 24 hours at 4^{O}C, or 2 hours at room temperature) was applied for enhancement of the fluorescent labeling. The brains were subsequently rinsed with PBS and dehydrated in an increasing series of ethanol (50, 70, 90, 96, 100 %) in steps of 10 minutes each, before the brains could be made transparent with methyl 2-hydroxybenzoate (methyl salicylate). Next, the brains were placed in a methyl salicylate bath in a centrally located hole on custom cut aluminium plates, covered by double sided cover glass. In order to check for successful staining, the preparations were studied under a fluorescence light microscope (Leitz Aristoplan, Wetzlar, Germany). Stained preparations were rehydrated in a decreasing series of ethanol (100, 96, 90, 70, 50 %) and rinsed with PBS in steps of 10 minutes each, whereupon another series of dehydration and application of the degreasing agent xylol (5 minutes) followed. Once again, the preparations were rehydrated and washed in PBS before incubation with collagenase diluted in PBS (1 mg/ml PBS at 36^{O}C for 30 minutes). Next, the preparations were preincubated in normal goat serum (NGS; Sigma, ST. Louis, MO, USA; 10 %) diluted in triton X PBS (PBStx; 0.1 %) for 30 minutes. Triton X is a detergent that increases the permeability of the cell membranes, thus facilitating the entrance of intracellular antigens. SYNORF 1, diluted in PBStx (0.1%) and NGS (10 %), was next applied. Incubation with SYNORF 1 lasted for 48 hours at 4^{O} C. SYNORF 1 is a monoclonal mouse antibody against the presynaptic terminal protein synapsin and thus aids the identification of synaptic neuropiles. NGS blocks binding of unspecific proteins. The preparations were washed in PBS (6 repetitions of 20 minutes each) and then incubated with CY5-conjugated goat anti-mouse secondary antibody (Jackson Immunoresearch), diluted in PBStx (1:500), for 48 hours at 4^{O} C. CY5 is a hydrophilic fluorescent dye that binds to the primary antibody. The preparations were next rinsed

with PBS (6 repetitions of 1 hour each) and dehydrated in an increasing ethanol series as before, until methyl salicylate was applied to clear the brains. As a last preparation before confocal laser scanning microscopy, the brains were placed on aluminium plates, frontally positioned, in a methyl salicylate bath concealed by double sided cover glass.

2.7 Confocal laser-scanning microscopy

Stained neurons were visualized by the use of a confocal laser-scanning microscope (Leica TCS SP5; Leica Microsystems CMS GmbH, Mannheim, Germany). The preparations were scanned in frontal view with a DPSS laser. The objective used was a 10x dry objective (HCX PL APO CS; 0.4 NA). The DPSS laser excites in wavelengths 440-800 nm, whereas Micro-Ruby, the dye used for intracellular staining, has peak excitation at 550 nm. The brains were scanned with a resolution of 1024x1024 pixels in the XY-plane. An optimization formula in the Leica software was used to decide the inter-slice distance (z-step size); this resulted in step sizes in the range of 2 – 3.5 µm. Whole-brain scans were performed at a rate of 200 – 400 Hz, whereas rates of 100 – 200 Hz were used for areas containing dendritic- or axonal arborizations. Adjustments of Gauss-filtering and light intensity were made to improve the visualization of the stained neurons. Scanning yielded a stack of images that were saved as a Leica Image File (.lif) and converted to Amira Mesh format (.am) in Amira (Amira 4.1; Amira Visage Imaging Inc., San Diego, CA, USA). The Z-axis dimension was multiplied with a factor of 1.6 in order to compensate for the refraction index of methyl salicylate.

2.8 Three-dimensional reconstruction and transformation into the SBA

Confocal images of the stained neurons served as templates for 3d-reconstructions in the Amira software. A skeleton tool was used to semi-automatically reconstruct the neuron (Schmitt et al., 2004; Evers et al., 2005). Following reconstruction of the stained neuron, the segmentation editor in Amira was used to reconstruct selected neuropile structures as label images. These label images were then affine- and elastically registered to label images of the corresponding neuropiles in the SBA of *H virescens*. Thus, the label images of neuropiles in the preparations would share coordinates with label images in the SBA. The reconstructed neuron was then affine- and elastically registered into the SBA, using the adjusted parameters obtained from the label images. The procedure used for registration of the reconstructed neuron into the SBA, was similar to that described by Brandt et al. (2005).

2.9 Neurophysiological analyses

2.9.1 Preliminary analysis and selection criteria for inclusion to final analysis

In a preliminary analysis, the recorded data were visually inspected and responses were classified as excitatory, inhibitory or mixed (consisting of both inhibitory and excitatory segments). From this preliminary sorting, 47 neurons passed onto the next stage and were analyzed for response strength according to the procedures described in the next sections. For a neuron to be included in the final analysis, it had to meet the following criteria:

1. The neuron had to be tested at least twice with mechanosensory control (airpuff).
2. The neuron had to be tested with the two large blends (blend 12 and blend 10)
3. The neuron had to respond to at least one of the single odorants or blends, and the response had to be repeated at least once (see section 2.9.3 for the proper definition of a response).

A total of 33 neurons fulfilled the criteria. Thirty-two neurons were selected for the comparison of blend 12 and blend 10. Twenty-five neurons were analyzed for differences between blends and single odorants with respect to response strength. One neuron responded exclusively to one single odorant. 20 of the 32 neurons were inspected for latencies in their responses to blend 12 and blend 10, and 11 of these were also examined for similarities in the frequency distributions of responses to blend 12 and blend 10.

2.9.2 Spike sorting

A wave form analysis tool in Spike 2 was used to sort out spikes from the recordings. In cases where multiple wave forms, representing spikes from more than one source, were evident, the spike types that did not respond to odor stimuli were filtered out. Filtered spikes were next transformed into discrete time events in separate channels. These event channels were used for estimation of spontaneous activity and response strength.

2.9.3 Analyses of response strengths

Employing the event correlation option in Spike 2, the time events were exported as bin-wise frequencies (bin length 50 ms) into a template sheet in Excel for further analysis. Spontaneous activity was estimated from the averaged spike rates of all responses 200 ms prior to stimulus onset and 1500 ms following the first 400 ms after the end of a predefined response window. In neurons where the spontaneous activity changed considerably during the recording, two or more spontaneous activities were estimated. Frequency bins for the responses were treated in a similar manner. The predefined response windows were in most cases 600 ms or 1400 ms, but on the few occasions where responses were considerably longer, other window lengths were used. A common response window, set to accommodate the longest response, was used for all responses within the same recording.

Response strength was expressed as the mean deviation from spontaneous activity (MDS). By this approach, all negative and positive deviations from spontaneous activity were averaged over all bins in the response window. Thus, inhibitory and excitatory parts of a response would not cancel each other out. MDS was calculated as:

$$MDS = \frac{1}{n}\sum_{i=1}^{n} r_i - r_{sp} \qquad (1)$$

Where MDS is the mean difference from spontaneous activity, r_i is the frequency of bin *i,* r_{sp} is the estimated spontaneous activity, and *n* is the number of bins.

Excitatory and inhibitory MDS was treated separately when identifying responses qualitatively and when quantifying response strengths. Thus, when characterizing excitatory responses, any negative deviation from spontaneous activity was set to zero. Conversely, positive deviations were set to zero for inhibitory responses. In order to be considered an excitatory response, the excitatory (e)MDS had to exceed the standard deviation (SD) of the estimated spontaneous activity by a factor of at least 2. For an inhibitory response, the absolute value of the inhibitory (i)MDS had to be at least 2 times the SD of the estimated spontaneous activity. A mixed response demanded that eMDS and iMDS each exceeded the SD by a factor of at least 2.

When comparing stimuli with respect to response strength, a single neuron was considered to distinguish between two stimuli if either the excitatory or inhibitory average MDS values differed by an amount that exceeded the pooled SD of all responses in that neuron. Pooled SD was calculated as:

$$S_P = \sqrt{\frac{\sum_{i=1}^{k}((n_i - 1)S_i^2)}{\sum_{i=1}^{k}(n_i - 1)}} \quad (2)$$

Where S_p is the pooled SD, n_i is the number of trials for the ith stimulus, and S_i^2 is the variance of the (n_i – 1) trials for the ith stimulus.

The pooled SD approach was used because an insufficient number of test trials within a recording would not allow proper significance testing on the single neuron level.

Statistical tests comparing response strengths and associations between odorants on the population level were conducted in Ecxel or Matlab. As a preliminary step, prior to statistical inference on differences in response strengths and correlation coefficients, Shapiro-Wilk tests were used to check the underlying distributions for normality. Since the null hypothesis of normality had to be rejected for all distributions (all $P<0.001$), non-parametric tests were employed in all cases. A two-sample Wilcoxon signed rank test was used to check for significant differences in response strengths to blends and single components, and to different combinations of odorants, regarded over the population of neurons. The test compared the responses of the strongest blend with the strongest single odorant in each neuron over the population of neurons. In neurons where enough data were available, the two or three strongest blends were compared with the two or three strongest single odorants. Likewise, for two particular odorants, responses were compared for all neurons responding to both odorants. A Wilcoxon rank sum test was also conducted on all responses to blends and single odorants over the population of neurons.

Spearman rank order correlations on response strengths were calculated over the population of neurons for every combination of odorants where sufficient data existed. This aimed to see if any association could be found between any two particular odorants. A permutation test was used for statistical inference. Spearman rank order correlations were chosen as they are robust in the presence of outliers and skewed distributions. However, one caveat when performing statistical inference over a neuronal population is that neurons may be fundamentally different in their

properties. For instance, the MDS potential of inhibitory responses is limited by the neurons spontaneous activity. Thus, for inhibitory responses, one might expect that MDS values in neurons with high spontaneous activities exceed MDS values in neurons with low spontaneous activities. Since the Spearman method correlates ranked variables, this may create a bias towards higher correlation coefficients. Statistical inference is therefore to be taken with precaution and the correlation coefficients are rather to be regarded as descriptive. Dunn-Sidak corrections for multiple testing were applied for alpha levels in the comparisons of response strengths and correlation coefficients. The corrected alpha level is given as:

$$\alpha` = 1 - (1 - \alpha)^{1/k} \quad (3)$$

Where α` is the corrected alpha, and *k* is the number of two-by-two comparisons. Corrections for multiple testing are often used to compensate for the possibility of some results coming out as significant by mere chance. However, these corrections may also severely inflate the risk of committing type II errors. Hence, the tables presented in the results are uncorrected, but corrected tables are given in the appendix.

2.9.4 Mixture effects and mixture indexes

Mixture processing can be elemental (linear) or configural (synthetic). In elemental processing, the responses of a blend are the linear sum of the responses to its constituents. In synthetic processing, interactions imposed by the constituents yield a representation unique to the mixture. Synthetic mixture effects are classified as synergistic (or best mixture effect) if the response to the mixture is stronger than the most effective single odorant, suppressive if the response to the mixture is weaker than the strongest single odorant and hypoadditive if the response to the mixture is similar to the strongest of its single constituents (Krofczik et al., 2009; Deisig et al., 2006; Duchamp-Viret et al., 2003). In order to examine the occurrences of mixture effects, the response strengths of the blends were compared with the response strength of the strongest single odorant. Using the pooled SD approach (equation 2), a relationship was deemed synergistic if the MDS of the blend exceeded the MDS of the single odorant by an amount that exceeded the pooled SD; suppression was the case if the MDS of the single odorant was larger by an amount that exceeded the pooled SD, and the relationship was termed hypoadditive if the difference in response strength was anywhere in between synergy and suppression. Notably, the terms synergy and hypoadditivity are

applied with reserve because every constituent of a blend was not tested, except for the binary blend of linalool and hexenylacetate in some neurons. Hence, in most cases, the only mixture effect reported with certainty is suppression.

A color coded mixture index was constructed to visualize how the various blends related to the single odorants. The index was calculated as:

$$I_{BS} = \frac{(B - S)}{(B + S)} \quad (4)$$

Where I_{BS} is the index, B is the MDS of the blend and S is the MDS of the single odorant. The index assumes values between 1 and -1 and will be positive for a synergistic relationship, negative in case of suppression, and close to zero for hypoadditivity. However, the value of the index cannot be used to exactly determine the kind of mixture effect since the pooled SD may vary considerably between neurons. The index values were expressed as color intensity with dark red representing 1 and dark blue representing -1. The indexes only compared responses of the same mode. That is, excitatory responses to blends were compared with excitatory responses to single odorants, and inhibitory responses to blends were compared with inhibitory responses to single odorants.

An index was also constructed to evaluate the relationships between blends. This index was calculated as:

$$I_{BB} = \frac{(B_l - B_m)}{(B_l + B_m)} \quad (5)$$

Where I_{BB} is the index, B_l is the MDS of the larger blend, and B_m is the MDS of the minor blend. Like the index in equation 4, this index also assumes values between 1 and -1. Index values were represented as color intensity in the same way as described for the index in equation 4. In this case, the index will be positive if responses to the more complex blend are stronger, negative if responses to the less complex blend are stronger and close to zero if the two blends are equally potent.

2.9.5 Latency analysis

Latencies for excitatory responses was evaluated by measuring manually in Spike 2 the time interval from odor onset to the first spike where the next time segment exhibited considerable positive deviation from spontaneous activity. For inhibitory responses, latencies were measured from odor onset to the last spike where the next time segment exhibited a markedly negative deviation from spontaneous activity. Latency could not be decided for some inhibitory responses in neurons with low spontaneous activity, because the last spike occurred before odor onset. A neuron was considered to differentiate between blend 12 and blend 10 if the mean latency of one blend differed from the mean latency of the other by an amount of time that exceeded the pooled SD of latencies for all responses by a factor of 2. Pooled SD was calculated as in equation 2.

2.9.6 Interval histograms

Interval histograms were constructed for 11 neurons in order to assess similarities in the frequency distributions of responses to blend 12 and blend 10. The histograms were made using the interval histogram option in Spike 2. Data were then transported into Excel for further processing. Interval histograms display counts for which any particular interval occurs between two spikes. Since the length of the interval between spikes is the inverse of the frequency, the interval histogram in essence shows the distribution of frequencies in a response. Bin sizes of 0.5 ms were used for all responses. The underpinning principle of an interval histogram is displayed in illustration 1.

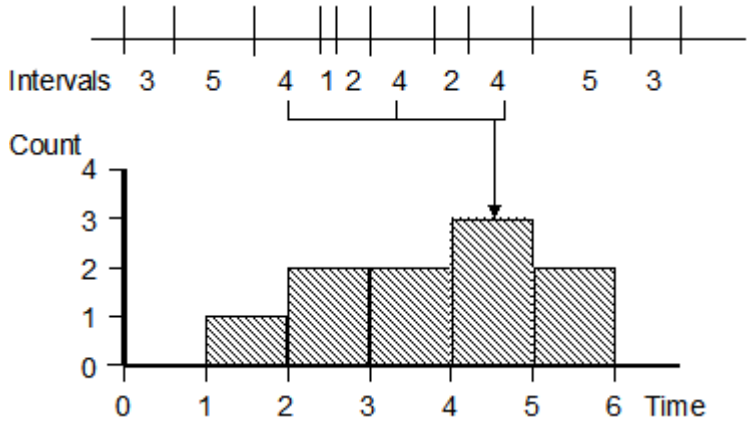

Illustration 1. The principle behind the interval histogram. The histogram displays counts for which any particular interval between two spikes occurs.

3. Results

The results presented here are based on data from 47 olfactory neurons of the protocerebrum of the moth *H. virescens.* Intracellular recordings were performed during stimulation of the antennae with odor blends and their constituents. The recorded neurons were analyzed for their tuning breadths, response strengths and temporal characteristics**.** A total of 33 neurons were included into the analysis, as these met the criteria for sufficient testing (methods). Thirty-two neurons were selected for comparing responses to blend 12 and blend 10. Twenty-five neurons were included in the analysis of response strengths to blends and single odorants. One neuron responded exclusively to one single odorant; this neuron was successfully stained, and so provided insight to higher order processing of single odorants. Intracellular staining was performed on seven of the 33 selected neurons. However, in several of the preparations additional neurons were stained or staining was incomplete. One of the stained neurons, N26, was fully reconstructed in three dimensions and registered into the SBA.

3.1 General physiological description of olfactory neurons

Most neurons exclusively exhibited either excitatory or inhibitory responses. Mixed excitatory-inhibitory responses were seen in only one neuron (N7), and one neuron responded with inhibition to the two complex blends and linalool, but was excited by germacrene D (N33). Opposite response modes were also observed for blend 12 and blend 10 in N16. Stimulations with airpuffs generally elicited responses of the same modes as the odorants. In only one neuron (N4) did air elicit an excitatory response while the odorants caused inhibition. The spontaneous activity varied considerably between neurons, ranging from 0 - 65 Hz. On a few occasions, abrupt shifts in spontaneous activity occurred during recording. These shifts were in most cases sporadic, but sometimes lasted throughout the recording. The baseline firing mode also varied. Some neurons displayed a tonic firing mode, whereas regular or irregular bursting activities were observed in others. No consistent relationship was found between baseline firing mode, spontaneous activity and the response modes a neuron exhibited.

3.2 Comparing blends and single odorants

3.2.1 Response profiles

The 33 neurons differed by their tuning breadths. Twenty-five neurons responded to at least one blend and one single odorant. Thirteen neurons responded to more than one single odorant. The blends caused responses in 32 neurons, three of which reacted to only one blend and none of the single odorants. One neuron showed no response to any of the blends, and responded exclusively to one single odorant. Twelve neurons also responded to flashes of light (not shown). The response profiles and test protocols for each of the 33 neurons are shown in figure 1.

The blends as a group evoked responses more frequently than the single odorants. Both the summated response probabilities and the weighted average response probabilities were higher for the blends with 0.97 and 0.75 for the blends against 0.54 and 0.78 for the single odorants, respectively. Linalool was the single odorant which most frequently evoked responses, while responses to germacrene D were scarcest. Among the blends, blend 10 most reliably evoked responses in 91% of the recorded neurons. Blend 12 and blend 5 frequently elicited responses with response scores of 76% and 83%, respectively, whereas blend 2 and blend 9 had the lowest response scores at 50%. However, blend 9 was only tested in two of the recordings. Airpuffs elicited responses in 30% of the recorded neurons. Table 1 gives an overview of the number of neurons for which a particular odorant was tested, and how frequently it caused a response. The table also includes the percentages of excitatory and inhibitory responses for each odorant, and the summated and weighted average response probabilities of blends and single odorants.

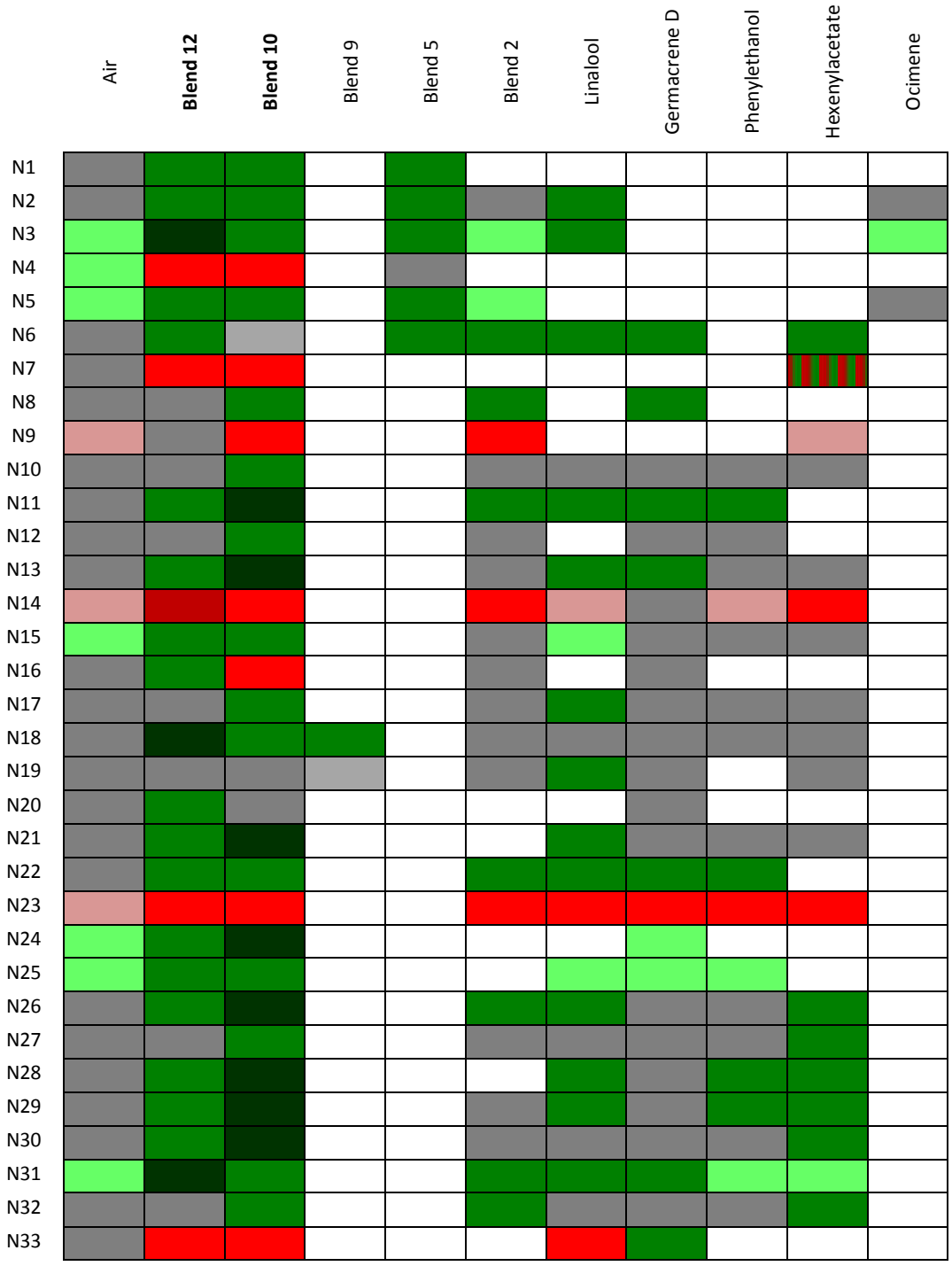

Figure 1. Response profiles for each of the 33 selected neurons. Green: excitation; red: inhibition; red-green stripes: mixed response; grey: tested but no response; white: not tested; light colors: responses to control (airpuff), and odor responses that are not considerable different from air; dark colors: in neurons where the responses to blend 12 and blend 10 are markedly different, the blend that caused the strongest response is presented in dark color.

Table 1. Overview of the number of neurons tested for each odorant and control, and the number of neurons responding to each stimulus. Percentages of excitatory and inhibitory responses for odorants and control are also included, as well as the summated and weighted average response probabilities for blends and single odorants.

Single odorants	Nr. of neurons tested	Nr. of neurons responding	% responding	% excitation	% inhibition
Linalool	23	18	78 %	83 %	17 %
Germacrene D	26	10	38 %	90 %	10 %
Phenylethanol	19	8	42 %	69 %	31 %
Hexenylacetate	19	12	63 %	75 %	33 %
Ocimene	3	1	33 %	100 %	0 %
Sum	**123**	**49**			
Weighted average response probability single odorants	**P(r): 0,54**				
Summated response probability single odorants	**P(r): 0,78**				
Blends	Nr. of neurons tested	Nr. of neurons responding	% responding	% excitation	% inhibition
Blend 12	33	25	76 %	80 %	20 %
Blend 10	33	30	91 %	77 %	23 %
Blend 9	2	1	50 %	100 %	0 %
Blend 5	6	5	83 %	100 %	0 %
Blend 2	24	12	50 %	75 %	25 %
Sum	**98**	**73**			
Weighted average response probability blends	**P(r): 0,75**				
Summated response probability blends	**P(r):0,97**				
Control	Nr. of neurons tested	Nr. of neurons responding	% responding	% excitation	% inhibition
Airpuff	33	10	30 %	70 %	30 %
Response probability	**P(r): 0,3**				

3.2.2 Response strengths to blends and single odorants

Response strength was expressed as the mean deviation from spontaneous activity (MDS), measured in hertz (Hz). Considerable variation in MDS values was observed between neurons, ranging from 3-69 Hz for excitatory responses and 3-22 Hz for inhibitory responses. The highest MDS value (69 Hz) was seen for blend 10 in N27, and the lowest values were found for phenylethanol and germacrene D in N23 (MDS<3 Hz). A general tendency for stronger responses to the blends was observed (figure 2). In fifteen neurons, the MDS of the strongest blend was considerably higher than that of the most effective single odorant. In the remaining ten neurons, the MDS values for the most potent blends and single odorants differed by an amount less than the pooled SD. However, the highest MDS was seen for one of the blends in all but one neuron. Figure 2 gives an overview of the MDS values of blends (A) and single odorants (B) for each of the 33 neurons.

Regarded over the neuronal population, the response strengths to blends proved significantly stronger than to single odorants (Wilcoxon signed rank test, $P<0.001$; Wilcoxon rank sum test, $P<0.001$). Responses to blend 10 were found to be significantly stronger than to any of the single odorants (Wilcoxon signed rank test, $P<0.002$, except for hexenylacetate and germacrene D, $P<0.01$). Blend 12 was significantly stronger than phenylethanol and germacrene D (Wilcoxon signed rank test, $P<0.002$) but was not significantly stronger than hexenylacetate or linalool (Wilcoxon signed rank test, $P>0.05$). Comparisons of the blends did not yield any significant differences. However, a tendency for neurons to respond more vigorously to blend 10 was observed. Correcting for multiple testing made little difference, except for blend 10 not being significantly stronger than hexenylacetate and germacrene D ($P>0.0018$, Dunn-Sidak correction, $\alpha`=0.0018$). Comparisons of the group-wise response strengths to blends and single odorants, and any pair-wise combination of odorants, are summarized in table 2. Table 2 is uncorrected for multiple testing, but a corrected table is given in the appendix (table 5).

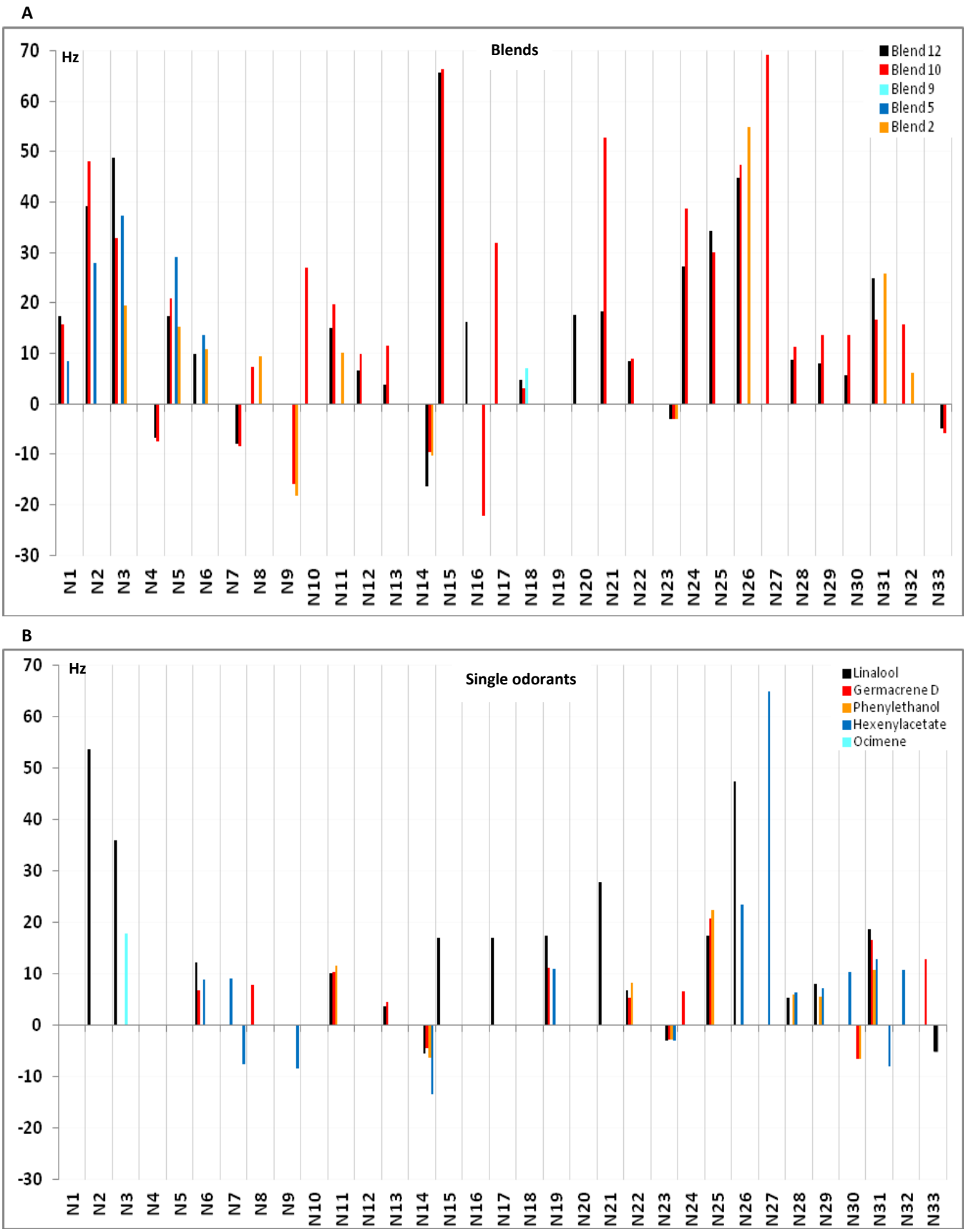

Figure 2. MDS values for blends (A) and single odorants (B) in each of the 33 neurons. MDS values (measured in Hz) are shown on the ordinate, while the abscissa show the identities of the neurons. The zero line represents spontaneous activity. Positive and negative values represent excitation and inhibition respectively. Notice the general tendency for higher MDS values for the blends. **A)** MDS values for the various blends in each of the 33 neurons. Black: blend 12; red: blend 10; bright blue: blend 9; blue: blend 5; orange: blend 2. **B)** MDS values for the various single odorants. Black: linalool; red: germacrene D; orange: phenylethanol; blue: hexenylacetate; bright blue: ocimene.

Table 2. Overview of differences in response strengths, as determined by the Wilcoxon signed rank test, regarded over the neuronal population. For each combination of odorants, if one odorant is significantly stronger than the other, the table displays the color of the stronger odorant (α=0.05). Grey color: no significant difference. The table is uncorrected for multiple comparisons. A corrected table is given in the appendix (table 5).

MDS <>	Blends	Blend 12	Blend 10	Blend 5	Blend 2	Linalool	Germacrene D	Hexenylacetate
Singles	P<0,001							
Blend 12								
Blend 5								
Blend 2								
Linalool			P<0,002					
Germacrene D		P<0,002	P<0,01					
Hexenylacetate			P<0,01					
Phenylethanol		P<0,002	P<0,002					

3.2.3 Correlations of response strengths

In order to check for associations between the tested blends and single odorants, MDS values were correlated for all combinations of odor stimuli.

Significant positive correlations were found for the majority of odorant pairs. However, when correcting for multiple comparisons, only a few combinations came out as significant. Linalool was significantly positively correlated with blend 12, blend 10 and blend 2. A significant positive correlation was also seen between blend 12 and blend 10. Thus, for any of these pairs, if the response strength of a neuron to one odor stimulus increased or decreased, the response strength to the other odor would tend to increase or decrease in a similar manner. Negative associations were not found for any correlated pair. That is, for no combination of odorants was there a tendency for increments in the response strengths of one odorant to be accompanied by decrements in response strengths of another; nor would excitatory responses to a given odor stimulus tend to occur alongside inhibitory responses to another odorant. Due to a lack of responses, correlations could not be performed between blend 5 and the three single odorants germacrene D, hexenylacetate and phenylethanol, or between blend 2 and phenylethanol. However, considering that the numbers of responses varied greatly for each correlated odorant pair, and that different properties of individual neurons may affect the value of the correlation

coefficients, statistical inference should be taken with precaution and comparisons of coefficients should be avoided. The important finding from this analysis was that no consistent *negative* associations could be found between any of the odorants. An overview of the Spearman rank order coefficients are given in table 3. Table 3 is uncorrected for multiple comparisons, but a corrected table is given in the appendix (table 6).

Table 3. Spearman's rho for each correlated pair of odorants. Green: significant (α=0.05). White: not significant. Blank grey: insufficient data. The table is uncorrected for multiple comparisons. A corrected table is given in the appendix (table 6).

Correlation	Blend 12	Blend 10	Blend 5	Blend 2	Linalool	Germacrene D	Hexenylacetate
Blend 12							
Blend 10	0,87						
Blend 5	0,81	0.4					
Blend 2	0,86	0,78					
Linalool	0,85	0,82		0,95			
Germacrene D	0,45	0,32		0,70	0,61		
Hexenylacetate	0,73	0,95		0,82	0,81	0,40	
Phenylethanol	0,89	0,83			0,60	0,80	0,80

3.2.4 Mixture effects

In order to investigate whether neuronal responses to different blends could be predicted from responses to their constituents, the occurrences of mixture effects were explored.

Linear mixture responses were not observed in any of the 25 neurons. When considering the most potent blend and single odorant in each neuron, fifteen neurons exhibited synergy, whereas hypoadditivity was observed in ten. However, all neurons were tested for more than one blend and in many cases these related differently to the most effective single odorant. In seven neurons, the responses to every mixture tested were considerably greater than to the most potent single odorant. Hypoadditivity was observed for at least one of the blends in fifteen neurons, but in only three did all blends respond in this manner. Suppression was seen for at least one of the blends in nine neurons, but no neuron exhibited this mixture effect exclusively. Thus, within a single neuron, one kind of mixture effect could be observed for one blend, while a different effect was seen for another. Figure 3 gives an overview of the numbers of neurons where any particular mixture effect was observed (3A) and the numbers of neurons that exclusively exhibited only one particular mixture effect (3B).

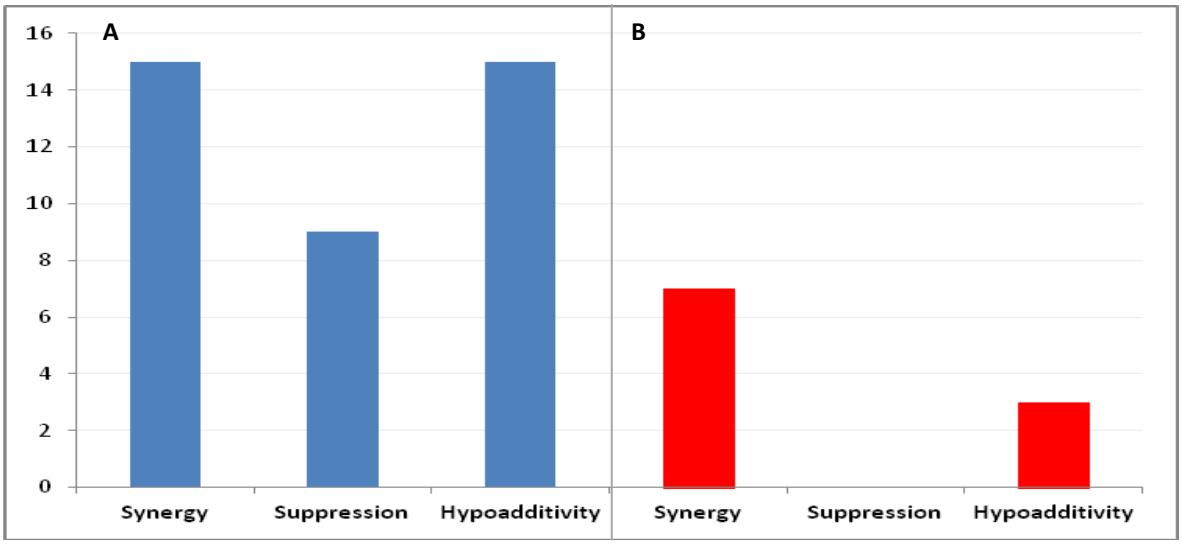

Figure 3. A) The numbers of neurons where a particular mixture effect was observed. **B)** The numbers of neurons that exhibited only one particular mixture effect.

Color coded mixture indexes were constructed to visualize how the various blends related to the single odorants (figure 4), and to other blends (figure 5).

The indexes showed no consistent rule as to how a neuron would respond to a blend, given the responses to its constituents. For example, the blend of hexenylacetate and linalool, blend 2, was suppressed in N3 and N14, but caused synergy in N26 and N31 (figure 4). Moreover, the response strengths of the blends did not scale with their degree of complexity. That is, there was no tendency for stronger or weaker responses to occur if a blend contained more or fewer components. This is demonstrated in N6 (figure 5) where the three components added to blend 5 yielded a more effective combination than the less complex blend 2. However, the five extra volatiles in the ten component blend imposed interactions that resulted in the ablation of responses to blend 10. The two additional components in blend 12 then “rescued” this blend from ablation. Similarly, the strongest responses in N18 (figure 5) were to blend 9, but blend 12 was more potent than blend 10. This neuron was also tested for phenylethanol, a volatile present in blend 10 but not in blend 9. No response was observed for this single odorant so the difference between these blends could not be attributed to an inhibitory response to phenylethanol. The only neuron where response strengths and blend complexity showed any association was N26, in which response strengths apparently diminished with increasing complexity (figure 4 and 5). One neuron (N33, figure 6) responded with inhibition to blend 12, blend 10 and linalool, but was excited by germacrene D. Inhibition lasted longer for blend 10 than blend 12, perhaps attributed to an excitatory contribution from germacrene D. This implied a summating, although non-linear, integration. Spike trains from N33 are displayed in figure 6. In summary, responses to any given blend could not be predicted from the responses to the constituents of the blend or from its degree of complexity. Furthermore, a variety of integration principles was employed by different neurons.

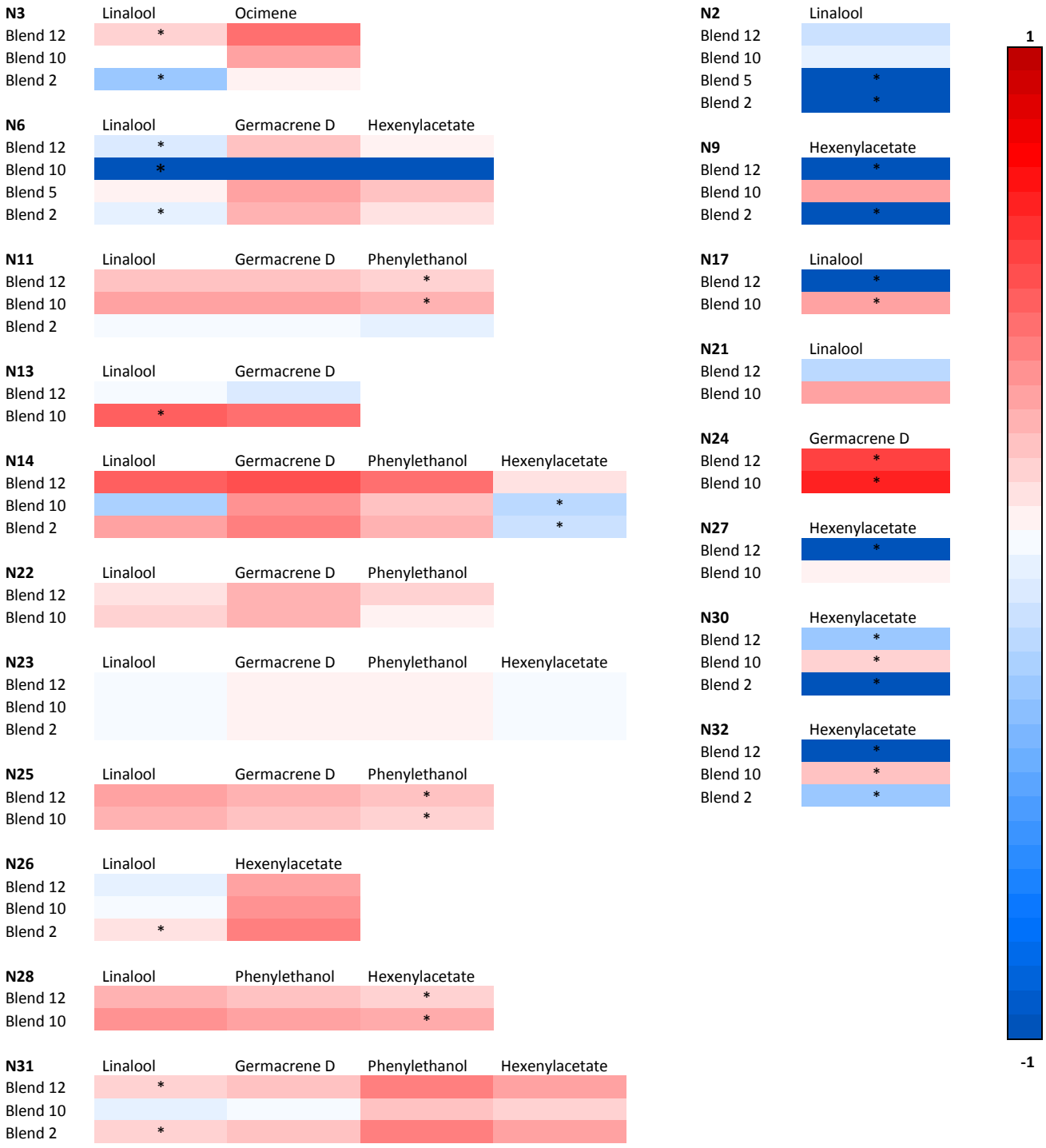

Figure 4. The color coded mixture index shows how blends relate to their constituent. Left column: indexes for neurons where more than two blends and more than two single odorants have responded. Right column: same as left column, but for neurons where only one single odorant has responded. The index compares only responses of the same modes. In case of a synergistic relationship the index value is positive and assumes a red color. For suppressive responses, the index is negative, represented in blue. The index will be close to zero and virtually colorless for hypoadditive responses. Color intensity indicates the degree to which one odorant is stronger than the other. Because the pooled SD varies between neurons, the type of mixture effect cannot exactly be determined from the color intensity. Asterisks (*) mark the cases where the difference between the blend and the strongest of its single constituents exceeds the pooled SD. This is only the case if the single odorant is included in the particular blend. Hence, for N13 and N24 the relationship between blend 10 and germacrene D is not deemed synergistic because germacrene D is not a constituent of blend 10.

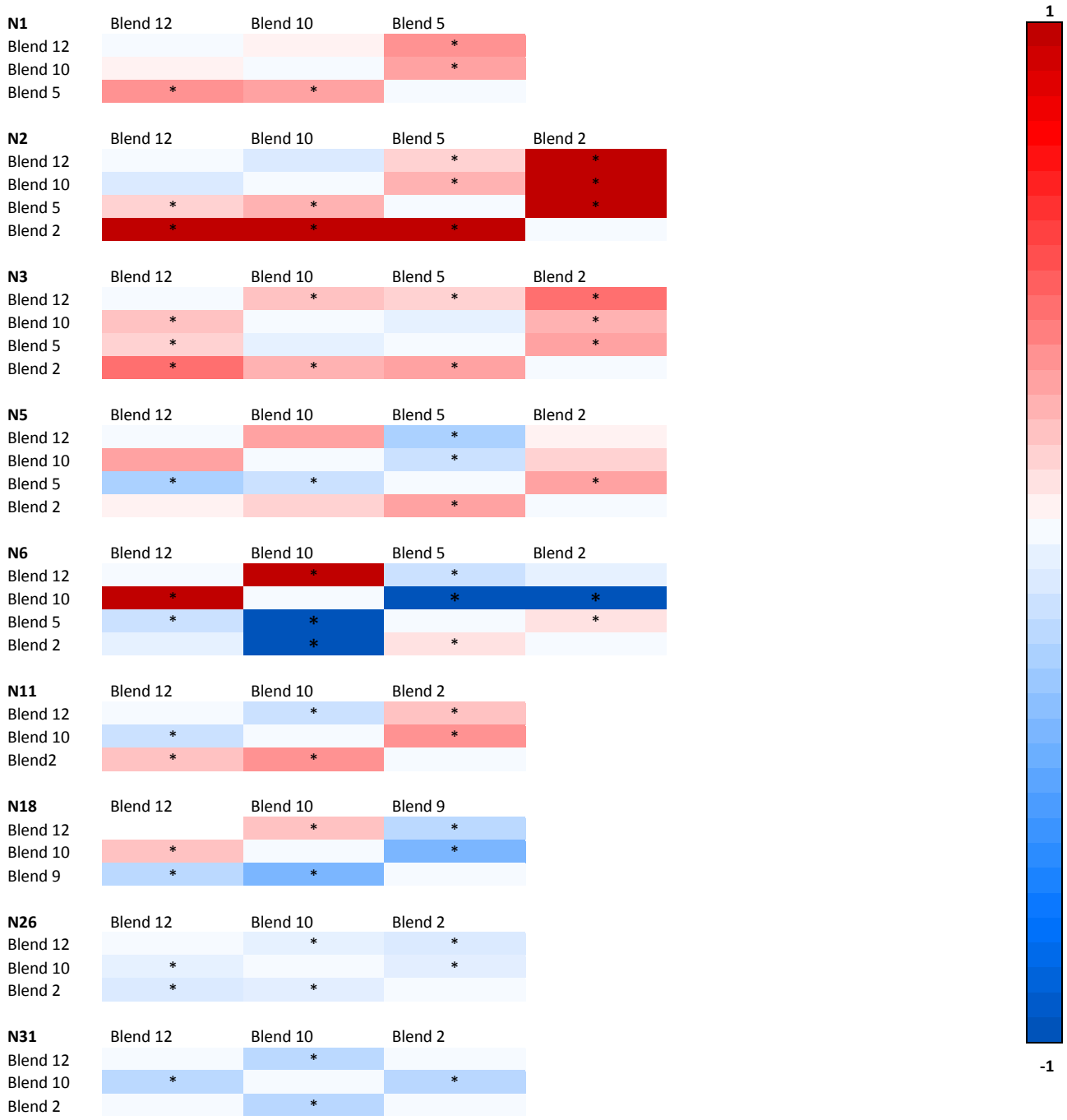

Figure 5. Color coded index showing the strength relationships between blends. The index compares only responses of the same modes. In cases where the more complex blend is stronger, the index will have a positive value and assume a red color. If the less complex blend is stronger, the index will have a negative value, represented in blue. If the two blends are equal in response strength, the index will be close to zero and virtually colorless. Color intensity indicates the degree to which two blends differ in strength. Because the pooled SD varies between neurons, color intensity cannot be used to exactly determine if one blend is stronger than the other. Asterisks (*) mark the cases where the difference between two blends exceeds the pooled SD.

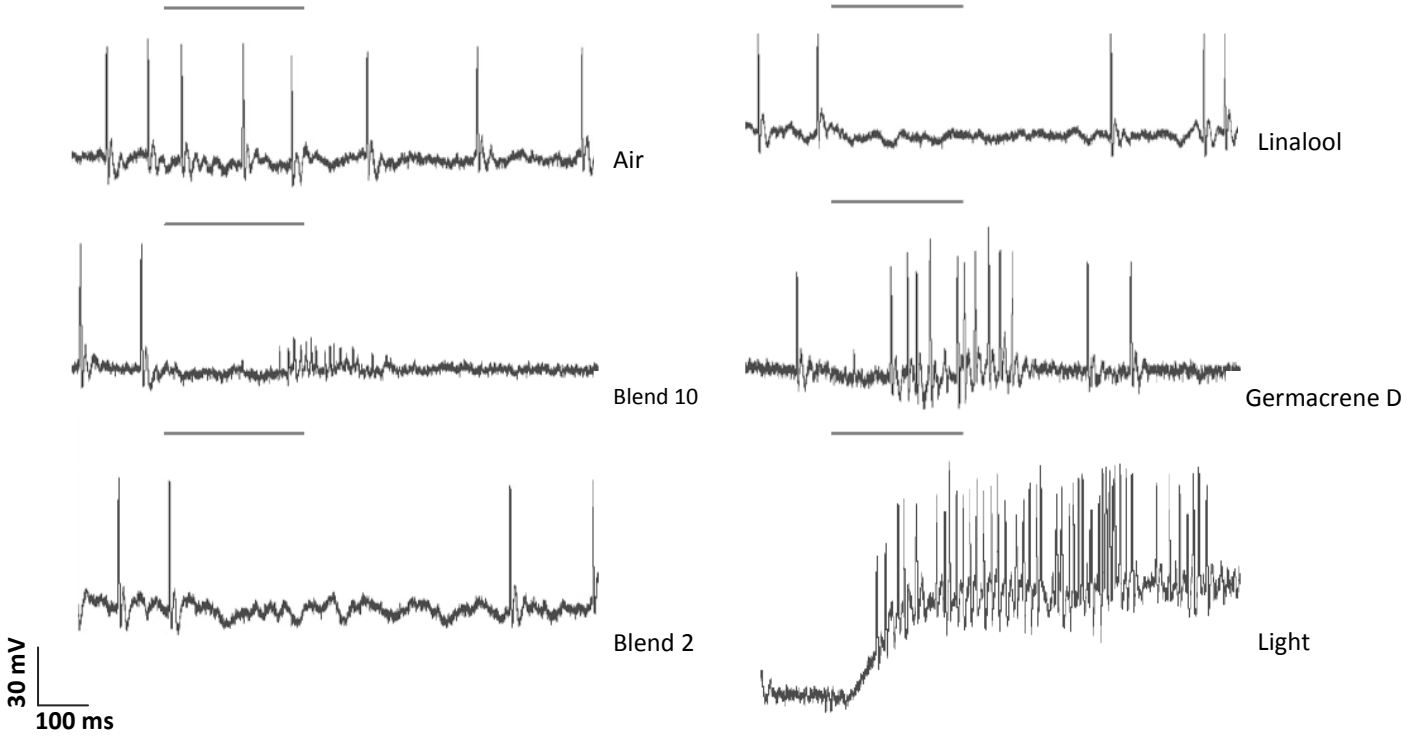

Figure 6. Spike trains from N33. This neuron responded with inhibition to blend 12, blend 10 and linalool, while germacrene D caused an excitatory response. Inhibition to blend 10 was longer compared to blend 12 and linalool, perhaps attributed to an excitatory contribution from germacrene D. The neuron also exhibited ON and OFF responses to light (ON response is shown in figure). Horizontal bar marks the stimulation period (300 ms).

3.3 Comparing blend 12 and blend 10

Aiming to see whether single neurons are able to discriminate between blend 12 and blend 10, the response profiles of 32 neurons were analyzed; twenty-three neurons were investigated for differences in response strengths; twenty neurons were included in latency analysis, and the frequency distributions of responses to the two blends were evaluated in eleven neurons. A summary of the relationships between blend 12 and blend 10 as regards response profiles, response strengths, and temporal expressions is given in table 4.

3.3.1 Response profiles of blend 12 and blend 10

Both blends frequently elicited neuronal responses, but their response profiles clearly differed (figure 1). Blend 10 conferred responses on 30 of the 33 neurons, and thus had a response probability of 0.91. Blend 12 caused responses in 25 neurons, yielding a response probability of 0.76. The conditional probability of a response to blend 12 given a response to blend 10 was 0.79. If a neuron had already responded to blend 12, the probability of observing a response to blend 10 was 0.95. Twenty-three neurons responded to both blends. Response modes of the two blends were the same in most neurons. The exception was N16 which responded with excitation to blend 12 and inhibition to blend 10. Seven neurons responded to blend 10 and not to blend 12, whereas two neurons responded to blend 12 and not blend 10.

3.3.2 Response strengths of blend 12 and blend 10

Twenty-three neurons were inspected for differences in response strengths to blend 12 and blend 10. The response of one blend was regarded stronger than the other if the average difference in MDS values exceeded the pooled SD of all responses in that neuron. Response strengths were considerably different in twelve neurons, blend 12 being the most potent in four and blend 10 in eight. Considered over the neuronal population, no significant difference could be found between the two blends, but there was a tendency for stronger responses to blend 10 (Wilcoxon signed rank test, $P = 0.14$). Figure 7 gives an overview of the MDS values of blend 12 and blend 10 in the 23 neurons responding to both blends.

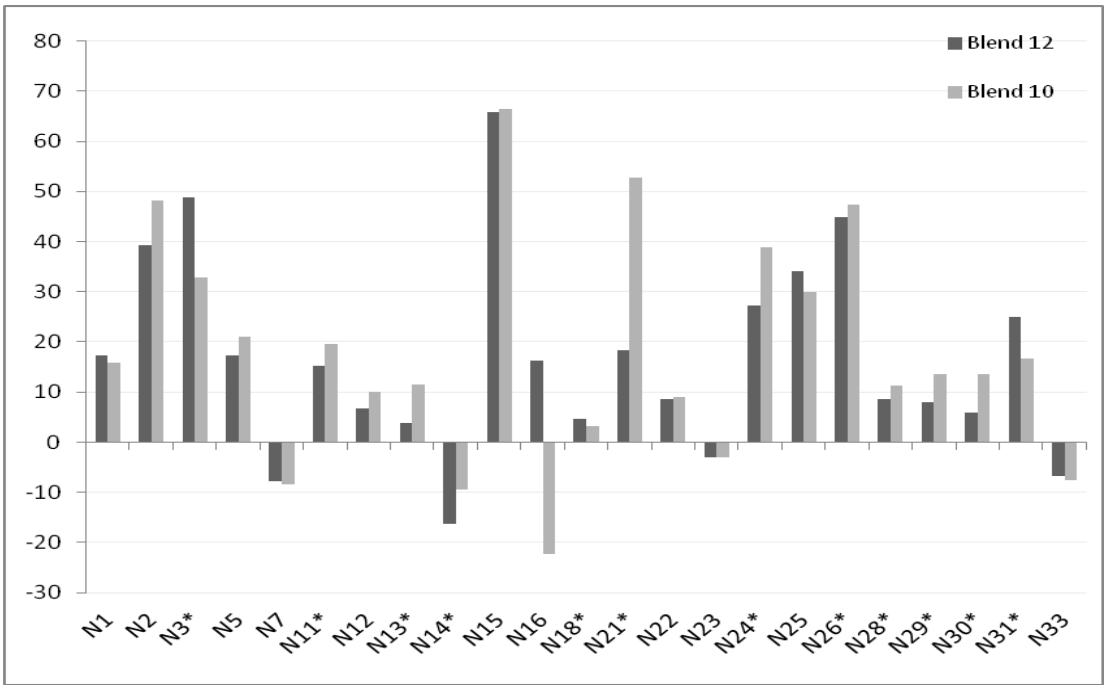

Figure 7. MDS values for blend 12 and blend 10 in neurons that responded to both blends. The ordinate shows MDS values (Hz) and the abscissa shows the identities of the neurons. Dark shade: blend 12; light shade: blend 10. Asterisks (*) mark the neurons where one of the blends responded stronger than the other by an amount that exceeded the pooled SD.

3.3.3 Latency analysis

Latencies were measured in 20 neurons. Latencies of the two blends were regarded as different if the mean latencies differed by an amount that exceeded the pooled SD of all latencies in that neuron by a factor of at least two. Different latencies were observed in seven neurons, three of which also differed with respect to response strengths (figure 7). Figure 8 gives an overview of the measured latencies for blend 12 and blend 10.

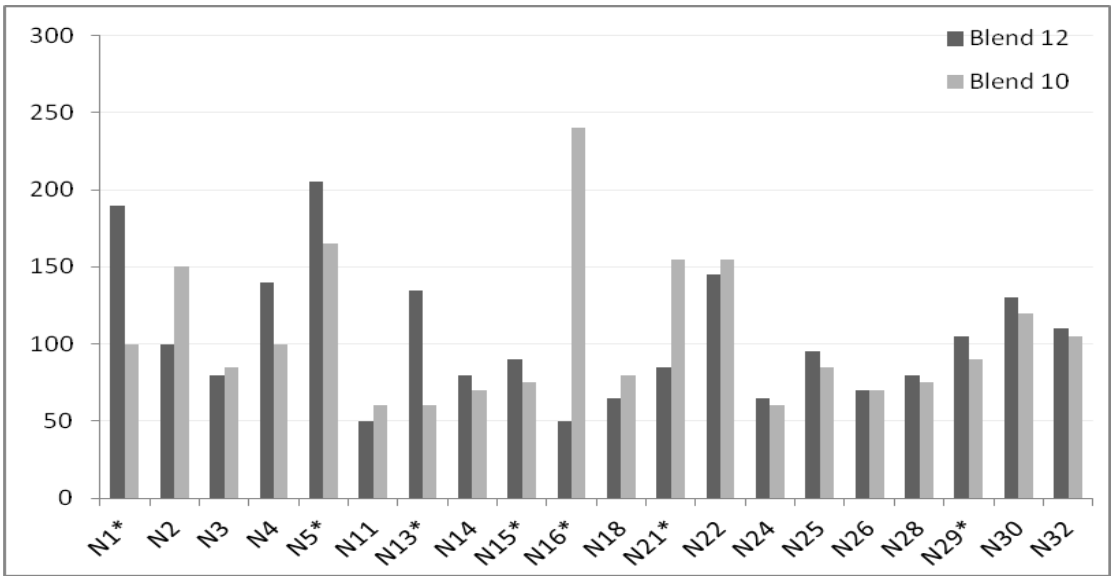

Figure 8. Mean response latencies, measured in milliseconds, for 20 neurons responding to blend 12 and blend 10. The ordinate shows time (ms). Identities of the 20 neurons are shown on the abscissa. Dark shade: blend 12; light shade: blend 10. Asterisks (*) mark the neurons where the differences in mean latencies exceeded the pooled SD by a factor of two.

3.3.4 Interval histograms

Interval histograms were constructed for eleven neurons in order to assess similarities in the frequency distributions of responses to blend 12 and blend 10. A considerable degree of overlap was observed in the frequency distributions of four neurons (N2, N15, N25 and N26), and some similarities were seen in two (N1 and N24). The remaining five neurons showed little or no overlap in their distributions. Variations were also observed when comparing repetitions of the same blend. This seemed partly to be attributed to adaptation, and in neurons were no similarities were found between blends, at least some degree of overlap was seen for repetitions of the same stimulus. The interval histogram for N15 is shown in figure 9. Histograms for all eleven neurons are given in the appendix.

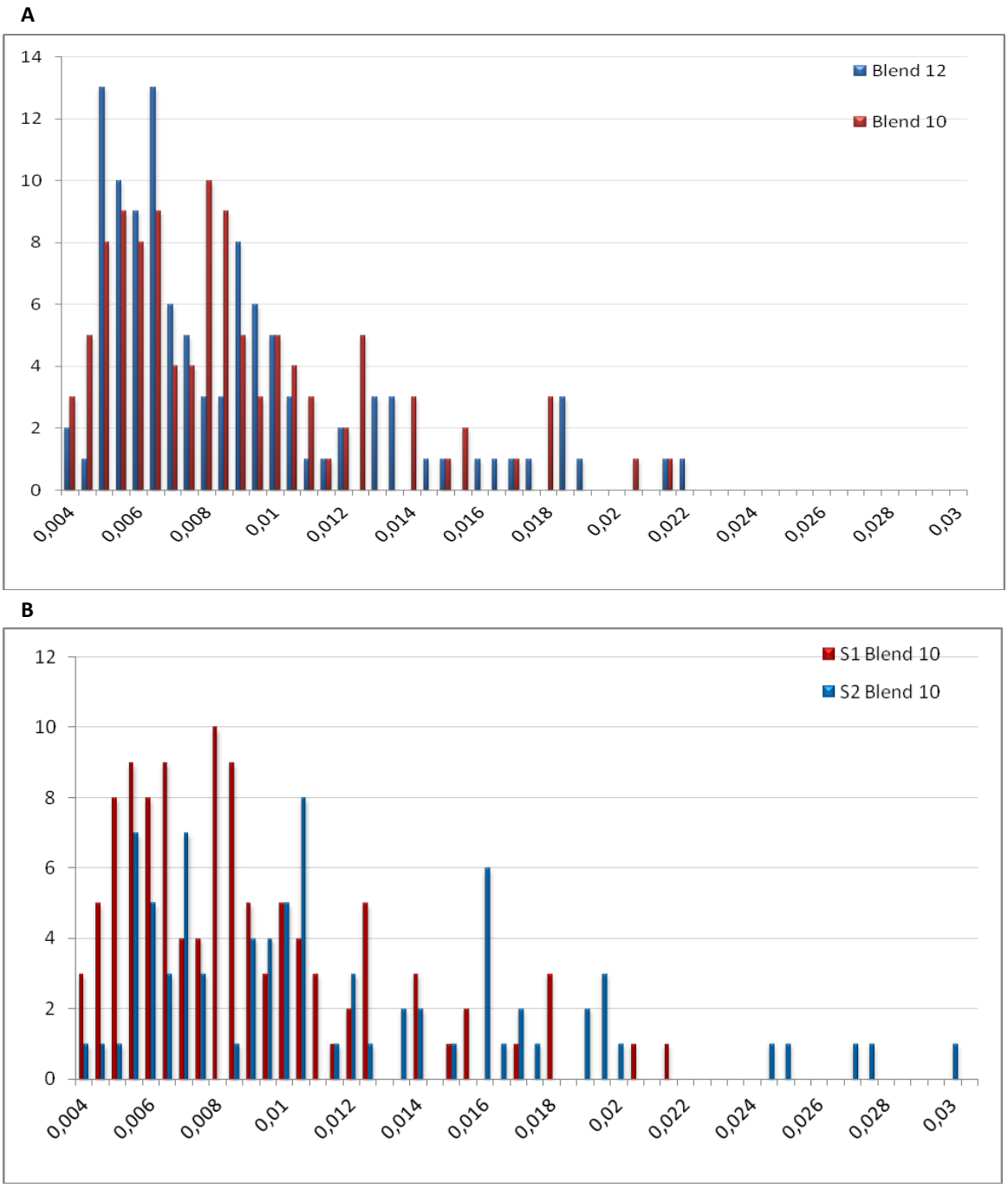

Figure 9. Interval histogram for N15. The ordinate shows the counts for which a particular interval betweeen spikes occurred. The length of the intervals (in secunds) are shown on the abscissa. **A**) This neuron displayed a high degree of overlap in their interval distributions for responses to blend 12 and blend 10. Blue: blend 12; red: blend 10. **B**) Variations in interval distributions also occurred for two responses to the same stimuli. Red: first stimulation (S1) with blend 10; blue. Second stimulation (S2) with blend 10.

Table 4. Schematic overview of the relationship between blends 12 and 10 as regards response profiles, response probabilities, response strengths and temporal expressions.

Blend 12		Percentage (%)
Neurons tested	33	
Neurons responding	25	76 %
P(r) Blend 12	0,76	91 %
Blend 10		
Neurons tested	33	
Neurons responding	30	91 %
P(r) Blend 10	0,91	91 %
Blend 12 & Blend 10		
Neurons responding to B12 & B10	23	72 %
Neurons responding to B12, not B10	2	6 %
Neurons responding to B10, not B12	7	22 %
B12 strongest	4	12 %
B10 strongest	8	24 %
P(B12|B10)	0,79	79 %
P(B10|B12)	0,95	95 %
Neurons with different latencies for B12 & B10	7	30 %
Neurons with overlapping frequency distributions	4	36 %
Neurons with some overlap	2	18 %
Neurons with no overlap	5	46 %

3.4 Representations of blends and single odorants in the moth brain

When combined with morphological characterization, the physiological profiles of single neurons provide valuable information about how blends and single odorants are represented at different levels of processing. Here, the physiological profiles of three morphologically characterized neurons are presented. All three neurons displayed characteristic response profiles that give important clues as to how blends and single odorants are represented in the insect brain.

3.4.1 PN, N26

N26 received its input in the ALs and projected via the m-APT to its output areas in the MBC and LP (figure 11 A-L). Three PNs were stained, but the intracellular recordings clearly showed only one kind of spike. Thus, the physiological profile presented in figure 11 M reflects the responses from one neuron. Due to excessive staining in the AL, it was difficult to determine the glomerular innervation pattern with certainty. At least two glomeruli in the medial posterior part of the AL were innervated. One glomerulus seemed to be densely innervated and another more sparsely. A cell body connected with the dendritic arborizations of the PN was located to the medial cell cluster (figure 11 G). The three PNs followed almost identical paths to the MBC and LP where they terminated in overlapping areas. All three PNs were digitally reconstructed in three dimensions and registered into the SBA.

N26 had no spontaneous activity and responded with excitation to linalool, hexenylacetate, blend 12, blend 10 and blend 2. Neither germacrene D or phenylethanol, nor control, elicited any response. All response patterns contained a primary high-frequent burst of 7-10 spikes followed by a silent intermittent period whereupon a train of spikes ensued that outlasted the stimulus period by hundreds of milliseconds. The intermittent silent period after the first barrage of spikes was almost lacking for the first stimulation of linalool (figure 11 M), but was clearly observed for the second stimulation also with this odorant. Latency was 70 ms for all responses. With respect to response strengths, linalool was most potent among the primary odorants. The response strengths of blend 10 and linalool were identical, while blend 12 scored a somewhat lower MDS value. The strongest response was elicited by the mixture of the two primary odorants, blend 2. While the other odorants consistently had eight spikes in the first barrage (except for hexenylacetate which had seven), blend 2 had ten. The binary blend also exhibited a higher density of spikes in the part of

the response that followed the intermittent silent period. Thus, synergy could be reported with certainty for this neuron. MDS values for N26 are displayed in figure 10

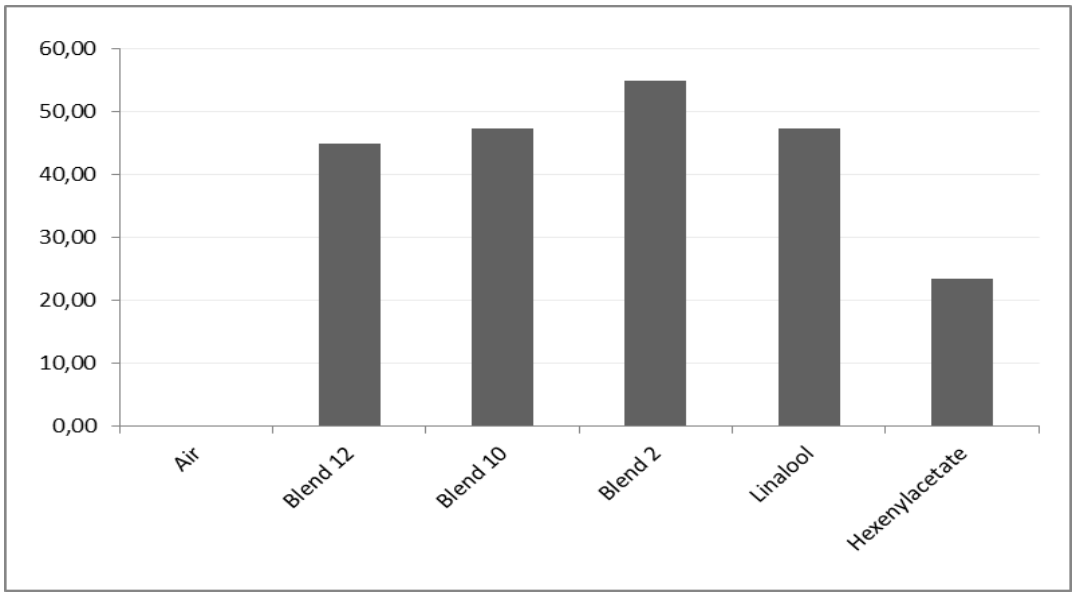

Figure 10. Response strengths, expressed as MDS, for responses of N26 to air, blend 12, blend 10, blend 2, linalool and hexenylacetate. The ordinate shows MDs values in Hz, while odor identities are displayed on the abscissa. Notice that blend 10 is identical to the strongest single odorant, linalool, while blend 12 is somewhat weaker. Synergy is observed for blend 2.

3.4.2 Bilateral LAL neuron, N19

N19 had smooth, putatively dendritic, arborizations in the ventral and medial protocerebrum and LAL of the left hemisphere. Its main neurite projected via the LAL commissure (LALco) to the contralateral LAL where it gave off varicose, putatively axonal, arborizations (Figure 12 A-C). The cell body of N19 was located in the left hemisphere, ventral and anterior to the MBC. This neuron had an irregular bursting spontaneous activity, but responded repeatedly with excitatory bursts to stimulation with linalool. Four blends and three single odorants were also tested, but all failed to elicit a response. Confocal images of N19, as well as spike trains from stimulations with the various blends and linalool are shown in figure 12.

3.4.3 Protocerebral neuron, N30

The cell body of N30 was located dorsal and posterior to the AL of the left hemisphere. The neuron projected in the SP, with some arborizations in the ipsilateral MBLs and the central body. One neurite crossed the midline over to the right hemisphere. Two additional neurons were weakly stained, the cell body of one residing behind the left antennal lobe alongside that of the neuron with the strongest staining. The third cell body was located in the superior protocerebrum. Of the four single odorants and three blends tested, excitatory responses were elicited by stimulations with blend 10, blend 12 and hexenylacetate. Germacrene D and phenylethanol did not cause any response. Blend 10 evoked a response that was somewhat stronger than to hexenylacetate, whereas blend 12 caused only a weak excitation. Neither linalool, nor the binary blend from linalool and hexenylacetate managed to cause a response. Thus, blend 2 was suppressed, and this suppression could not be accounted for by linalool responding in an antagonistic manner to hexenylacetate. Figure 13 shows the morphology of N30, as well as spike trains from stimulations with the various odorants.

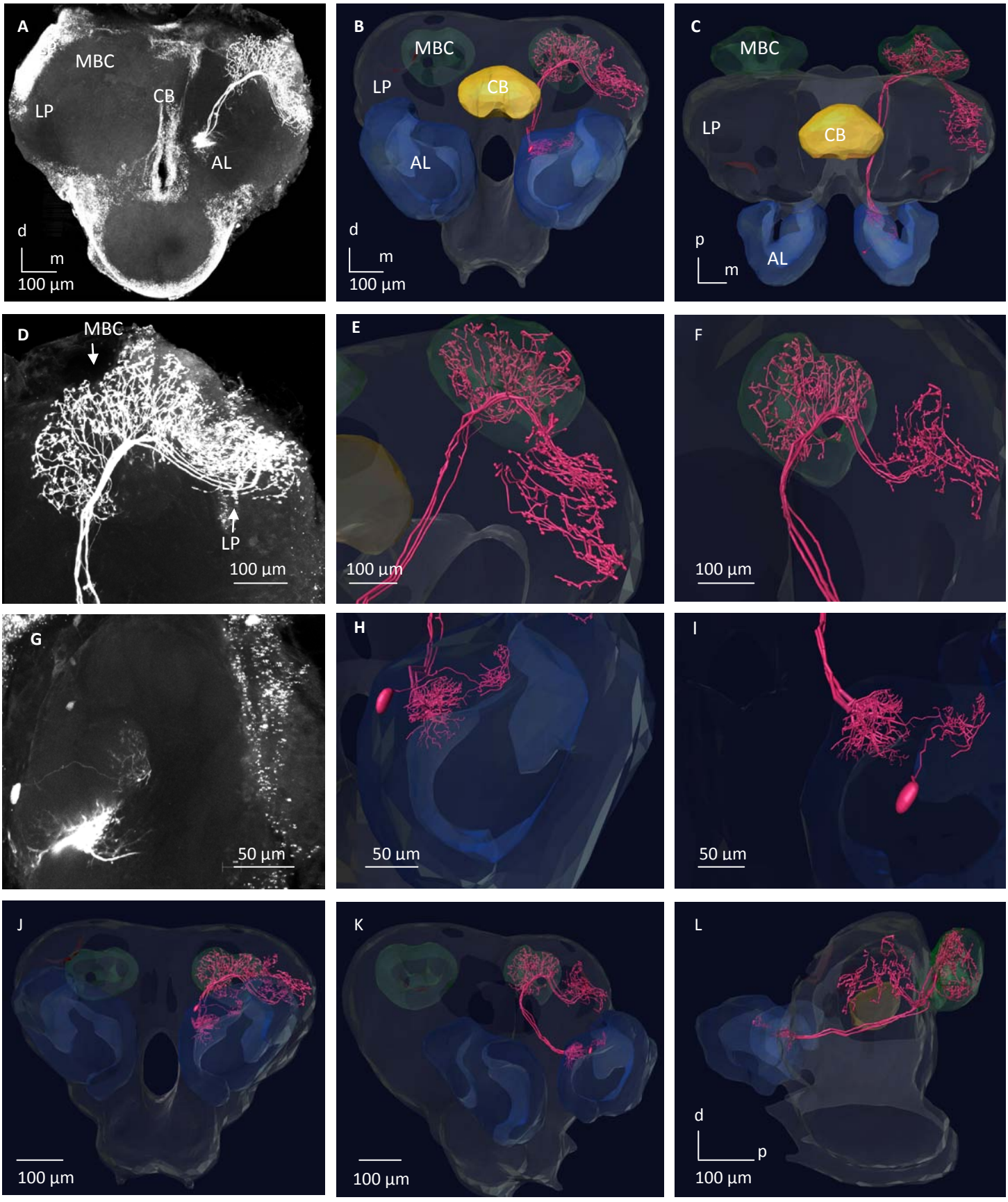
A
MBC
CB
LP
AL
d
m
100 µm
B
MBC
LP
CB
AL
d
m
100 µm
C
MBC
LP
CB
p
m
AL
D
MBC
LP
100 µm
E
100 µm
F
100 µm
G
50 µm
H
50 µm
I
50 µm
J
100 µm
K
100 µm
L
d
p
100 µm

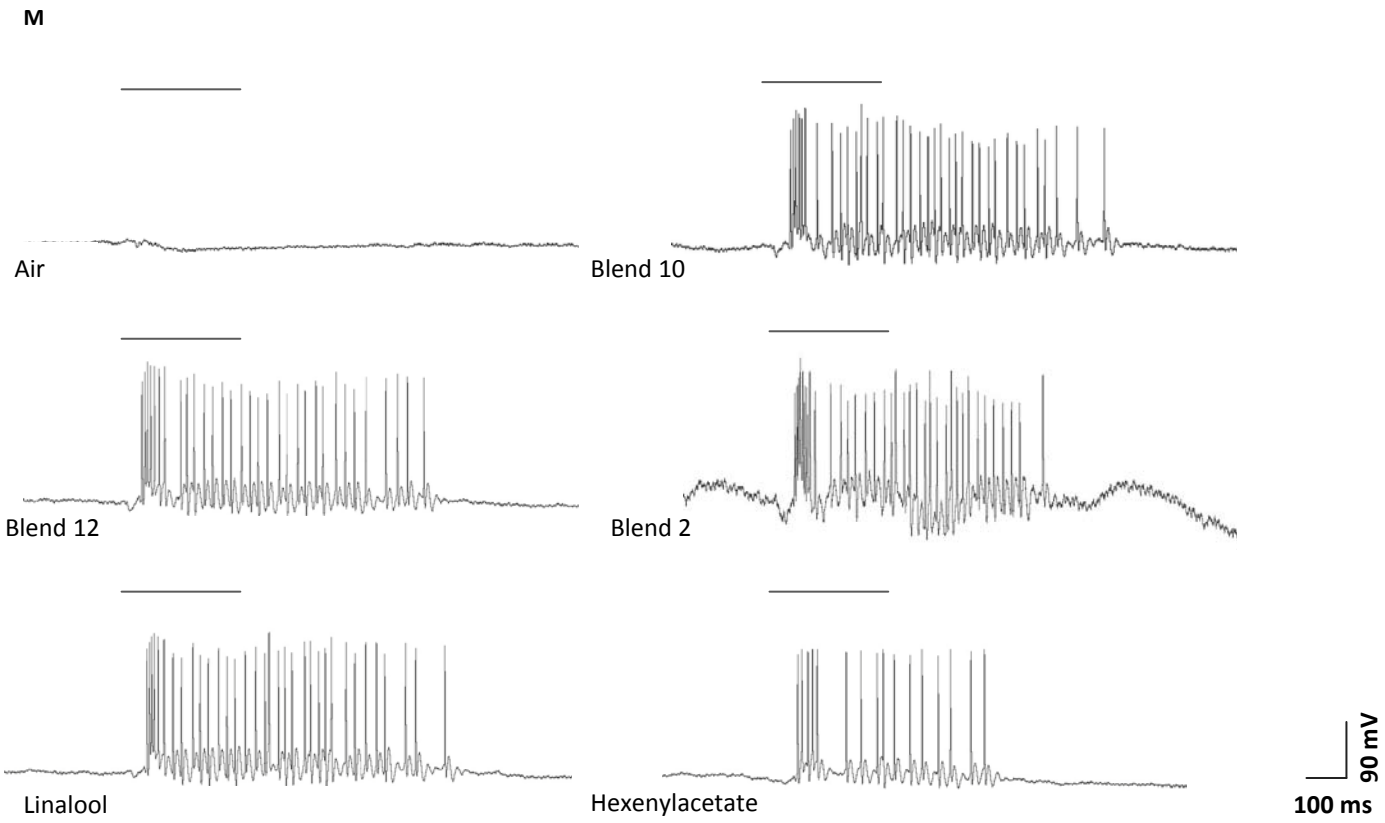

Figure 11. **A**) Confocal image. Whole brain scan in frontal view showing the projection pattern from the input area in the left AL to the output areas in the MBC and the LP. **B**) Frontal view of digital reconstruction of N26 transformed into the SBA**. C**) Digital reconstruction in dorsal view. **D**) Confocal image of innervation pattern in MBC and LP. **E, F)** Digital reconstruction. Innervation patterns in MBC and LP. **G**) Confocal image showing innervation patterns in glomeruli of the AL. Cell body resides in the medial cell cluster. **H, I**) Digital reconstruction. Innervation patterns in the ALs. **J**) Digital reconstruction. Whole brain in frontal view. **K**) Digital reconstruction. Whole brain seen in angle from the right . **L**) Digital reconstruction. Whole brain in sagittal view. **M**) Spike trains from stimulations with control (air), blend 12, blend 10, blend 2, linalool and hexenylacetate. Notice the stronger response elicited by blend 2 compared to its constituents linalool and hexenylacetate. Horizontal bars mark the stimulation period (300 ms). Abbreviations: MBC – mushroom body calyx; LP – lateral protocerebrum; CB – central body; AL – antennal lobe; p – posterior; d – dorsal; m – medial. SBA – standard brain atlas.

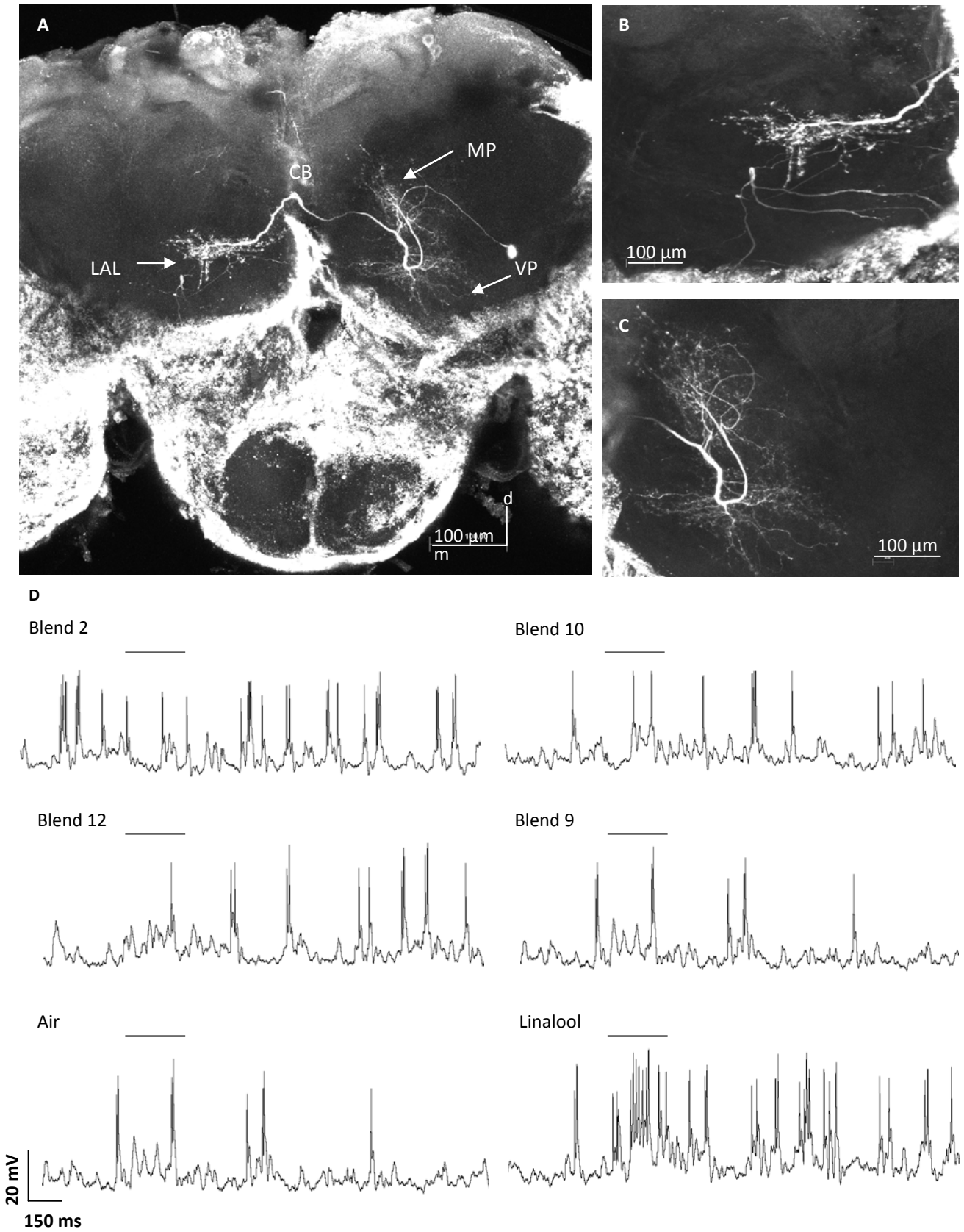

Figure 12. A-C) Confocal images of N19. **A**) Whole brain scan showing the projection pattern of N19 from its putative input areas in the left LAL, MP and VP, via its primary neurite in the LALco to its putative output area in the contralateral LAL. Cell body resides in the left hempisphere, ventrally and anteriorally located from the MBs. **B**) Output area in the LAL of the right hemisphere. **C**) Input areas in the left LAL and medial protocerebrum. **D**) Spike trains from stimulation with control (air), blends 12, 10, 9, 2, and linalool. Notice that the single odorant linalool elicits an excitatory burst whereas neither air nor any of the blends cause any response. Horizontal bars mark the stimulation period (300 ms). Abbreviations: CB – central body; LAL – lateral accessory lobe; MP – medial protocerebrum; VP – ventral protocerebrum; MB – mushroom body; LALco – lateral accessory lobe commissure; d – dorsal; m - medial.

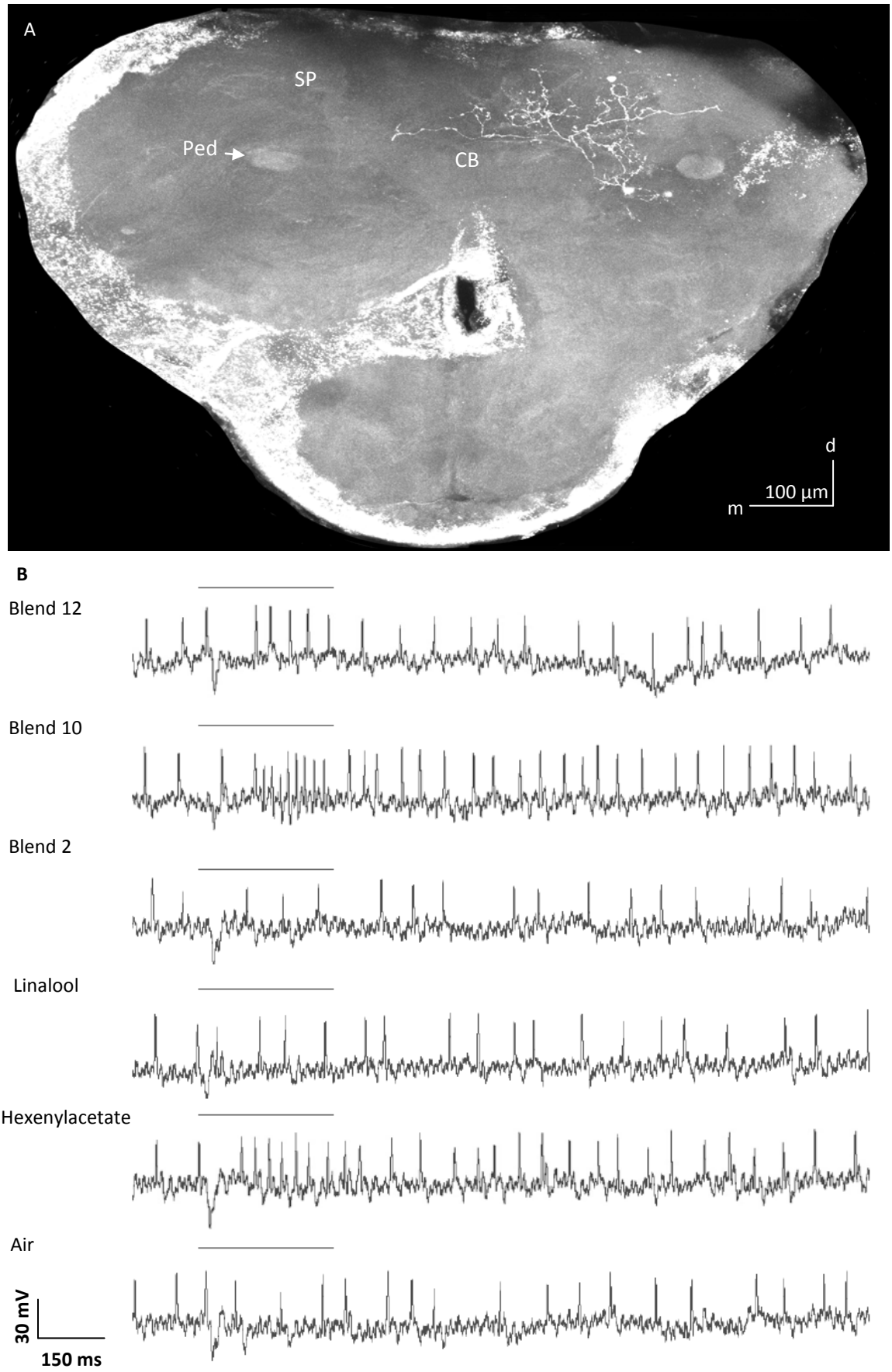

Figure 13. A) Confocal image of N30 in frontal view. The neuron projected in the SP of the left hemisphere. One neurite extended over the midline to the right hemisphere. The cell body was located posterior to the AL in the left hemisphere**. B**) Spike trains from stimulations with control (air), blends 12, 10 and 2, as well as the primary odorants linalool and hexenylacetate. Notice the much stronger response of blend 10 over blend 12, and the suppression of blend 2 compared to hexenylacetate. Horizontal bar marks the stimulation period (300 ms). Abbreviations: CB – central body; Ped – pedunculus; SP – superior protocerebrum; d – dorsal; m – medial.

4. Discussion

4.1 Differential processing of blends and single odorants

Intracellular recordings from 33 olfactory neurons of the protocerebrum revealed that many neurons seem to discriminate between odor mixtures and their constituents. Considered over the population of neurons, responses to blends were significantly stronger than to single odorants and blends evoked responses with higher probability. These observations corroborate the findings of Løfaldli et al. (2012) where the same mixtures and single odorants were used as test substances. In agreement with their results, all three types of mixture interactions were observed in the present study, synergy being the most prominent. The idea of stronger responses to multi-component blends in higher order integrative neurons is appealing in light of behavioral and electrophysiological experiments on various insects, including moth species. Several studies have shown that mixtures are discriminated from their constituents (Hopkins & Young, 1990; Laska & Hudson, 1991; Dekker et al., 2002; Deisig et al., 2010) and that single volatiles have little behavioral relevance when presented alone, but become significant in the context of other odor cues (Mumm & Hilker, 2005; Pinero et al., 2008; Riffel et al., 2009a; Riffel et al., 2009b). An attractive hypothesis would be that synergy in protocerebral neurons, frequently observed in this study and by Løfaldli et al. (2012), constitute a neural correlate to the behavioral saliencies of odor mixtures. That is, behavior could be implemented by higher order neurons integrating information about specific combinations of odorants into signals strong enough to elicit a behavioral response. In line with this notion, a morphologically characterized descending output neuron from the LP responded robustly to blend 10, whereas stimulations with blends of lesser complexity or single odorants were ignored or caused only weak reactions (Løfaldli et al., 2012).

A putative connection between best mixture effects and the behavioral saliencies of plant blends have been explored in only a few studies. Pinero et al. (2008) observed strong synergy in glomeruli of female fruit moths when stimulating with a behaviorally effective 5-component attractant, but this synergy was not evident for responses to reduced mixtures that did not cause attraction. In a study on the hawk moth, synergy was observed in some units of the ALs when stimulating with a synthetic mixture that effectively evoked attraction. Attraction persisted even for low concentrations of this mixture but synergy faded. The authors therefore concluded that the units

responding with synergy could not be responsible for the behavioral effect of the mixture (Riffel et al, 2009a).

The notion of synergy as a neural correlate for mixture-driven behavior does not require that this synergy is present already at the level of the ALs. Indeed, there seem to be a difference between representations of blends and single odorants in the ALs and the protocerebrum. The protocerebral neurons presented in this study often exhibited best mixture effects and responded to more than one single component. Moreover, response probabilities were markedly higher for blends, and some neurons were blend specific. Similar observations were made by Løfaldli et al. (2012) when recording from the protocerebrum of the same species. In contrast, previous recordings from the ALs in *H. virescens* (Løfaldli et al., unpublished results) showed sparse responses to odorants, and intracellular and multiunit recordings from the ALs of the hawk moth have demonstrated predominantly suppressive and hypoadditive mixture effects, as well as sparse responses to blends (Riffel et al., 2009a; Kuebler et al, 2011; Capurro et al., 2012). Comparable results have been reported for honeybees (Krofczik et al., 2009; Yamagata et al., 2009; Deisig et al., 2010). The apparent disparity between odor representations in the protocerebrum and ALs indicates that higher order neurons integrate information from several channels originating in the ALs. In the honeybee, suppression in PNs of the l-APT has been shown to facilitate concentration-invariance and mixture-separability (Deisig et al., 2010) while rising concentration dependence has been demonstrated in the m-APT (Krofczik et al., 2009; Yamagata et al., 2009), implying a functional division between the two tracts. Thus, even if synergy should be a neural correlate of mixture-driven behavior, the synergistic mixture representation in descending neurons might not have to mirror the mixture interactions of the AL. Rather, the ALs may facilitate separation of similar mixtures through suppression and extract different odor features for further processing in parallel pathways.

Synergy for selective mixtures in higher order neurons may be accomplished through synchronous firing of spatially defined PNs onto downstream neurons. Information from the ALs about a given odor is seemingly conveyed and processed in multiple channels. Ultimately, behavior could be implemented through the synchronous convergence of processed information from these parallel pathways onto descending neurons. Synchrony has now found acceptance as an essential coding feature in neuronal systems (Singer, 1999). In the pheromone system of hawk moths, synchrony has been proposed to act in tandem with a rate code so that the presence and intensity of a

pheromone component is represented by the firing rates of its congruent PNs, while the coincidence of components in a mixture is encoded by the coordinated firing of PNs (Lei et al., 2002; Martin & Hildebrand, 2010). These coding principles may also be applicable to the plant odor system. Indeed, Riffel and collaborators (2009b) found that the degree of synchronous firing of AL neurons in response to various odor stimuli, as well as the mean firing rate, correlated best with the behavioral effects of these odorants. Moreover, studies on moths have shown that the behavioral impact of an attractant is lost if its constituents are distributed to differently located sources, thus impeding the synchronous detection of the mixture (Andersson et al., 2011). Martin and Hildebrand (2010) propose that synchronization of output from the ALs is attributed to asymmetric lateral inhibitory networks, and that predefined genetically programmed inhibitory connections may underlie the innate odor preferences exhibited by some moths.

Although the majority of neurons in the present study responded with synergy to at least one of the blends, suppressive or hypoadditive responses were often observed for some other blend in these neurons. When contemplating the mixture indexes (figure 4 and 5) it seems that no consistent rule dictated the way a neuron responded to a given mixture. Rather, the impression was that responses to a blend rarely could be predicted from its complexity or from the responses to its constituents. Correlations of response strengths showed no negative associations, implying that no pair of odorants consistently opposed each other to yield suppressive mixture effects. The rather inconsistent logic of mixture effects was well demonstrated for blend 2. Some neurons responded with synergy and others with suppression to this blend, but the suppressive effects could never be explained by its constituents causing responses of opposite modes. An example is N30 (figure 13) which responded with excitation to hexenylacetate, but reacted to neither blend 2 nor linalool. Putatively, the inhibitory effect of linalool could be presynaptic to the neurons conveying the hexenylacetate signal. The fact that some neurons responded with synergy to a particular mixture while the same mixture was suppressed in others, might partly be explained by the spatial arrangement of inhibitory connections being different in the various subsystems.

However, a more elegant solution to the conundrum of mixture effects might be to impose a temporal format on mixture coding, taking into account the system as a whole. In this scheme, differential representations of mixtures in higher order neurons reflect the timing and synchrony of inputs from different processing streams. Consider, for instance, an output neuron of the LP. This neuron will receive information about the same odor stimulus from the l-APT and the m-APT, but in

opposite order. It will also receive combinatorial information from multiglomerular PNs in the ml-APT and the l-APT, as well as indirect input from the experience dependent pathway of the MBs. Odor induced inhibition is present in most of these pathways: LNs in the ALs, MB extrinsic neurons mediating inhibition to the calyces and LP, and GABA-reactive multiglomerular PNs of the ml-APT. The inhibition mediated by these areas could readily promote a synchronous flow of information. If the notion of a genetically programmed network of inhibitory connections in the ALs is extended to other brain areas, then innate preferences for certain mixtures could be a result of synergistic signals implemented through the coordinated convergence of parallel pathways. Conversely, if excitatory and inhibitory contributions from different streams are desynchronized, they will annul each other as they converge onto the same neurons. Simply put, the response to a mixture in a given neuron could be a reflection of the degree of synchrony within and between the subsystems from which the neuron receives its input. Thus, when a neuron reacting vigorously to a ten component blend is unresponsive when presented to a mixture of two more components, it might be because the two extra components cause interactions which disrupt the pattern of synchronous input to that neuron. Likewise, when a volatile like hexenylacetate cause excitatory responses alone but is ignored in blend 2, it might be because the addition of linalool disrupts the pattern of synchrony. Thus, the ablated response to blend 2 does not require an inhibitory contribution from linalool *per se*. Such a system would be flexible. Learning a rewarded odor has been shown to change the spatiotemporal pattern of activation in the ALs and MBs (Daly et al., 2004; Okada et al., 2007; Szyszka et al., 2008; Denker et al., 2010). Changing the pattern of odor evoked synchrony on a short term or long term basis could facilitate shifts in odor preferences. Likewise, desynchronizing odor evoked patterns could impede their relevance in a given context, for example at the sound detection of a predative bat. Indeed, modulatory neurons innervating the ALs have been shown to react to sound stimuli in *H. virescens* (Zhao et al., 2012). Further research is needed to explore the behavioral significance of synergistic mixture representations in higher order neurons, and how these are connected with the degree of synchronous output from the ALs and other subsystems of the olfactory network.

4.2 Representations of blends and single odorants in the moth brain

An important question concerning odor coding in the insect brain is how information about blends and single odorants is preserved throughout the levels of processing. Three morphologically and physiologically characterized neurons presented in this study provide some insight to the central representations of blends and single odorants in *H. virescens*, and may have implications for the understanding of odor processing in this species.

4.2.1 PN, N26

The PN, N26, received its input in the AL of the left hemisphere and projected via the m-APT to its output areas in the ipsilateral MBC and LP (figure 11 A and B). The confocal images showed the axonal arborizations of three PNs. Similar to previously described uniglomerular PNs in *H. virescens* (Rø et al., 2007; Løfaldli et al., 2010), the axon terminals branched widely in the MBC and LP, and innervated overlapping areas. N26 responded with excitation to the two single odorants linalool and hexenylacetate, as well as three blends, blend 12, blend 10 and blend 2. Synergy was observed for the binary blend of linalool and hexenylacetate. This effect was lost when stimulating with blend 10, so the responses to this mixture were equally strong with those to the strongest single odorant, linalool. Blend 12 was suppressed with respect to linalool, but this effect was rather weak. The diminishing response strengths to the complex blends, relative to blend 2, likely reflect an increase of unspecific global inhibition with rising odor complexity. This is in agreement with results from the ALs of honeybees demonstrating that increasing the number of components in a mixture also enhances overall suppression (Deisig et al., 2010). The behavioral significance of AL synergies, as that observed for blend 2 in N26, is unknown. Linalool and hexenylacetate have both been proposed to mediate attraction in unmated females, and linalool has been shown to effectively induce learning in appetitive conditioning experiments (Rostelien et al., 2003; Jørgensen et al., 2007; Meagher & Landholt, 2008). The synergy in N26 may thus signal the coincidence of two compounds associated with the same biologically relevant signal. As discussed above, few attempts have been made to address the putative importance of best mixture effects in the ALs. Pinero and colleagues proposed these synergies to be neural correlates to the behavioral saliencies of mixtures (Pinero et al., 2007). This notion was rejected in another study because synergy in the AL units faded at low mixture concentrations while the behavioral effects of the mixture persisted (Riffel et al., 2009b). Arguably, those units might still have relevance for the up-close interplay between

insects and their host plants. For instance, high concentrations of certain combinations of odorants could signal the quality of a particular plant, and the insect may use this information to choose the better of several closely located oviposition sites or nectarine sources. Indeed, honeybees have demonstrated the ability to discriminate between rewarded and unrewarded odor stimuli from different cultivars of the same flower, based on the relative ratios of volatiles expressed by each plant lineage (Wright et al., 2005).

The two primary odorants that evoked responses in N26 have not been found to activate the same ORNs (Rostelien et al., 2005). Since the confocal images showed staining in three glomeruli, it is plausible that N26 received input from two or three glomeruli, corresponding to previously identified oligoglomerular PNs in *H. virescens* (Løfaldli et al., 2010) and *B. mori* (Namiki & Kanzaki, 2011). This could explain a broadening of the molecular receptive range for this PN, relative to the cognate ORNs of each primary odorant. The difference in response strengths to the two primary odorants might be a reflection of the glomerular innervations pattern. Since one glomerulus was densely innervated, and sparse innervations were seen for one or two glomeruli, it is possible that the former received input from linalool specific ORNs while the latter got input from hexenylacetate specific ORNs.

Most PNs innervating the MBC in the m-APT and l-APT are uniglomerular, but the projections of oligoglomerular PNs follow the same route to the MBC and LP (Rø et al., 2007; Løfaldli et al., 2010; Namiki & Kanzaki, 2011). Several physiological functions may be suggested for these PNs. They may signal, by synergy, the coincidence or ratios of a few biologically relevant odors, or they may be concentration-dependent. Since oligoglomerular PNs of this sort have been demonstrated only in the m-APT, it is tempting to speculate whether subsets of oligoglomerular PNs with different concentration thresholds confers the same concentration-dependence onto the moth m-APT as that indicated for the honeybee (Krofczik et al., 2009; Yamagata et al., 2009). This would mean that a functional segregation of the APTs could be preserved across species despite considerable anatomical discrepancies. Unfortunately, the neuron was not tested for more than one odor-concentration. Another function of oligoglomerular neurons might be to increase the transmission efficacy onto the Kenyon cells of the MBC. The Kenyon cells have modest excitability and are only sparsely activated in a very confined time window (Homberg et al., 1987; Perez-Orive et al., 2002; Szyzska et al., 2005). Given the sparse and weak connections between PNs and Kenyon cells, oligoglomerular PNs responding to more than one primary odorant could amplify odor signaling to

these third order neurons which need the coincidence input of many PNs to be activated (Szyszka et al., 2005; Jortner et al., 2007; Turner et al., 2008). This signal enhancement would come without requirement of extra space because these neurons would also participate in the signaling of other odorants. Furthermore, because oligoglomerular PNs could promote synchronous signaling of a few biologically relevant plant odors, they could be involved in innate odor preferences. Finally, an important consequence of these PNs is that odor coding to a larger extent becomes combinatorial already at the level of the ALs of *H. virescens*, despite the narrow tunings of ORNs in these moths.

4.2.2 Protocerebral neuron, N30

Downstream of the ALs, a neuron innervating the SP, MBLs and the dorsal central body displayed interesting mixture interactions. This higher order neuron responded vigorously to blend 10 and somewhat weaker to hexenylacetate. Blend 12 caused only a weak reaction, while blend 2 was ignored. Thus, a robust response to hexenylacetate was ablated in blend 2 despite no reaction to linalool alone. Moreover, the extra eight components added to yield blend 10 both reinstated and enhanced the response to this blend, while the additional two components in blend 12 rendered a response that was considerably weaker than the single odorant. The physiological profile of N30 demonstrates the complexity of mixture representations in higher levels of processing. Evidently, higher order neurons are able to signal the presence of specific single volatiles as well as representing combinations of these volatiles in a manner unique to each mixture. The synergistic representation of blend 10 is interesting in light of previously identified neurons of the ALs and protocerebrum of *H.virescens*. Løfaldli et al. (2012) found that this mixture is represented throughout many levels of odor processing from the ALs to descending output neurons. The authors suggest that convergent streams carrying information about this blend onto the SP and LP from all three APTs and the indirect MB-pathway, implies a parallel context dependent processing in different areas, ultimately being decoded by descending neurons. N30 thus adds to the number of morphologically characterized neurons connecting higher order brain areas, showing a unique representation of the ten component mixture. In addition to the SP and MB lobes, this neuron also innervated the central complex, a structure thought to be involved in spatial processing and limb coordination (Loesl et al., 2002; Heinze & Homberg, 2007). This is in agreement with a notion of context dependent processing of odor features in parallel or separate streams.

4.2.3 Bilateral LAL neuron, N19

In an area downstream of the LP, a bilateral neuron, N19, exhibited a peculiar response profile. This neuron had its cell body located laterally in the left hemisphere, had smooth arborizations in the ipsilateral LAL and medial protocerebrum, and projected to the contralateral LAL. The morphology of this neuron is reminiscent of bilateral neurons connecting the two LALs in the silk moth (Iwano et al., 2010), and the turnip moth *Agrotis segetum* (Lei et al., 2001). The LALs are connected with descending output neurons, and it is believed that the activity of LAL-associated bilateral neurons underlies the characteristic zig-zag searching behavior of moths following an odor plume (Kanzaki et al., 1991a; Kanzaki et al., 1991b; Lei et al., 2001; Iwano et al., 2010). N19 responded with excitation only to the single odorant linalool, whereas the four blends tested were unable to evoke any response. This was somewhat surprising, given that the information entering this region is highly processed. A morphologically similar neuron previously identified in *H. virescens* also exhibited a rather narrow tuning for two monoterpenes and a monoterpene-mixture containing these two single odorants (Bente Berg, personal communication). Interestingly, the mixture evoked a somewhat stronger response than the most potent single odorant in that neuron. Another bilateral neuron, identified by Løfaldli et al. (unpublished), arborized more laterally and dorsally in the protocerebrum and responded vigorously to hexenylacetate while reacting only weakly to blend 10 and control. In male turnip moths, Lei and coworkers (2001) found several LAL-associated neurons responding explicitly to one specific pheromone component. However, they also observed neurons reacting to two or three components, blend specific neurons, and generalists responding to every tested substance. The different tuning characteristics exhibited by the array of LAL-associated neurons had all previously been demonstrated for PNs of this species (Hansson et al., 1994; Hartlieb et al., 1996). The authors therefore concluded that some representations in the ALs are preserved as labeled lines in higher order neurons. Notably, their study mainly explored pheromone responses in male moths. There may be considerable differences between the handling of pheromone and plant odor information, as well as differences between genders. Nevertheless, their results revealed the presence of higher order neurons, specifically tuned to single components.

Although more data is needed to draw any conclusions, the physiological profile of N19 presented here, together with the findings of Løfaldi et al. (2012), implies that information about single plant odorants is preserved in higher levels of processing. However, it is not clear whether such

representations of single odorants are implemented through labeled lines or if they follow a combinatorial logic. An uninterrupted labeled line from ORNs to the protocerebrum is not likely because the presence of the specific component in the blend would then necessarily trigger a response in the neuron. As N19 responded to none of the linaool-containing blends, it is conceivable that constituents of the blends imposed interactions in the ALs so that the effect of linalool was ablated. This ablation would probably be attributed to a very specific asymmetrical lateral inhibition, considering that the mere addition of hexenylacetate was adequate to hinder a response to blend 2. Without interference from other odorants, the linalool signal would transmit from ORNs to higher order neurons as a labeled line in this scheme. Interference mediated by other odorants could also emanate from other sources, such as the LP or MBs. In this sense, the bilateral neuron would receive input from an array of channels, one being a labeled line signaling the presence of a single odorant, like linalool, and others mediating highly processed information. Alternatively, coding is solely combinatorial throughout the system so that even single odorants are coded by overlapping patterns of activation in the ALs and refined through the higher levels of processing. In this case, the ablation of linalool in a blend could be caused by hexenylacetate desynchronizing the input from this combinatorial signal.

In nature, a single odorant will rarely be the sole source of odor signals. What then could be the purpose of bilateral neurons responding to specific single components only when other odorants are not present? A plausible explanation would be that such neurons do not respond exclusively when an odorant is presented alone, but rather when a single odorant or specific combinations of these are present in relative higher amounts than other sets of odorants. That is, these neurons may be involved in a system evaluating the relative concentrations, ratios or saliencies of specific constituents within a mixture. Because most experimental set-ups utilize homogenous blends, this would ablate the response to the single component within the blend. The morphological characteristics of bilateral neurons, as well as their close association with descending neurons, make them ideally suited to affect decision-making based on differences in the compositions of two or more odor sources. Since some of these neurons also respond to 2-3 components or blends, it is conceivable that synergistic representations in the ALs observed in some studies (Pinero et al., 2008; Riffel et al.,2009a; Kuebler et al., 2011), or the best mixture effect exhibited by N26, are preserved in these bilateral neurons and contribute to specify behavior. This would fit with a model of parallel processing of different odor features where behavior is driven by homogenous

concentration-invariant mixture representations, while a concentration-dependent and ratio-sensitive subsystem modulates and specifies this behavior. Stimulating with ratio-shifted blends while conducting multi-unit recordings from the ALs and the LALco could unravel the relationship between odor representations in these subsystems. If any correlations are found between these areas, behavioral experiments (for example two-choice wind tunnels), using homogenous and ratio-shifted blends could be used to evaluate the behavioral significance of this relationship.

4.3 Differential processing of multi-component blends

How readily can insects distinguish between chemically related odors? The ability to separate between mixtures with overlapping compositions is certainly advantageous for insects that need to change behavior with seasonable, ecological and physiological variables. For example, the hawk moth feeds primarily from flowers of A*. palmeri*, but switches to its larval host plant *D. wrightii* when these are abundant (Riffel, 2008). Thus, the hawk moth must be able to separate between the odorant compositions of the two plants and switch preferences from one to the other. *H. virescens* is a highly polyphageous species with larvae feeding on plants of tobacco, tomato, cotton, sunflower and soybean (Fitt, 1989). The ovipositing female must thus change preferences in accord with the shifting abundances of these plants.

As shown in the present study, more than one fourth of the neurons completely discriminated between blend 10 and blend 12, responding to one while ignoring the other. Of the remaining neurons, one third markedly differed with respect to response strengths. How these disparities in the representations of single neurons are reflected on behavior, remains to be investigated. Some studies have found little difference between the behavioral effects of full floral extracts and synthetic mixtures of a few key components (Pinero et al, 2008; Riffel et al, 2009a; Riffel et al., 2009b). However, the mixtures used in this study comprise volatiles which are not necessarily released from the same plant, and may signal different messages depending on the context. An example of contextual odor perception is demonstrated in the fruit fly, where CO_2 participates in the odor complement of fermenting fruit, but is also involved in the signaling of an intraspecific repellant (Galizia and Szyszka, 2008). In the present study, it is possible that the internal states of the moths might have influenced neural responses to the two blends. The females used for experiments were unmated but many of them still laid eggs after a few days. As some neurons did not discriminate between the blends, it is conceivable that the younger moths perceived blend 12

and blend 10 as almost identical, while the two extra substances in blend 12, farnesene and germacrene D, became significant fragments of the mixture for older insects ready for egg-laying. Germacrene D has been shown to be important in the search for oviposition site, as well as oviposition in mated *H. virescens* (Mozuraitis et al., 2002). Thus, the significance of this substance in blend 12 might have changed with the motivational states of the moths. Alternatively, the two blends could be processed differently in a context dependent manner in parallel streams. In this case they would be regarded as similar in some channels and dissimilar in others, depending on the context in which each channel processes odor information. However, these hypotheses are not mutually exclusive. For example, a neuron may integrate information about the two blends, conveyed by separate channels. Depending on external or internal factors, the contributions of each channel to the recipient neuron might change.

Temporal features of the responses to blend 12 and blend 10 might give further clues as to whether information about these blends is differentially processed. In this study, more than one third of the neurons responded with different latencies to stimulations with the two blends. Stimulus identification by latency patterns has been proposed as a coding mechanism in many neural systems (Wise & Cain, 1999; Gollisch & Meister, 2008; Fontaine & Peremans, 2009). Intracellular recordings from the ALs of the hawk moth demonstrated significant latency differences between mixtures and single odorant in the ALs, and recordings from the honeybee have indicated that AL neurons exhibiting synthetic mixture responses differ in their lag to response onset compared to neurons responding in an elemental manner (Kuebler et al., 2011; Meyer & Galizia, 2012). Latencies may reflect dynamics of the processing network, so disparities for this temporal trait might imply that the two blends are represented by different neural ensembles comprising some common elements.

The distribution of spike frequencies of a response is another feature that could contribute to the separation of related blends. Approximately half of the neurons examined in the present study showed similarities for this temporal aspect. However, variations were also evident for responses to the same stimulus, so it could not be concluded that the spike frequency distribution is employed by single neurons to discriminate between related odor stimuli. One should also consider the possibility that the various subsystems of the olfactory network utilize different readout mechanisms. That is, a recipient neuron in one region may be tuned to input in certain frequency bands, whereas neurons in other regions are mostly concerned with the mean firing rate.

Unfortunately little is known about the logic of temporal coding in the various relays of information transfer in the insect brain. Most studies addressing this issue have focused on coding in the ALs and the transmission of odor information from PNs onto KCs. In the honeybee, it has been implied that only the first 200 ms of PN responses are important for the activation of KCs (Szyszka et al., 2005). In this case, only the spiking frequency of the ensemble during the first 200 ms of the response would be of matter to KCs. This implies a high degree of redundancy with respect to spike events. However, it has been suggested that the later part of the response hold relevant information for other target areas, such as the LP (Galizia & Szyszka, 2008). In the locust, odor identity seems to be encoded by the spike timing of evolving ensembles of neurons, locked to specific phases of a global 20 Hz oscillating local field potential (LFP) in the ALs, KCs and MB lobes (Perez-Orive et al., 2003, Laurent, 2002; Cassenaer & Laurent, 2007). Thus, for the locust, the distribution of spike frequencies would not matter so much as spike-timing relative to the LFP. In the moth, however, oscillations in the ALs and MBs have been shown to be incoherent, and the spiking activities of PNs only weakly entrained to the LFP (Christensen et al., 2003). Rather, central odor representations in the moth seem to be coordinated through non-oscillatory synchronizations of PNs, although this view has been challenged (Christensen et al., 2003; Ito et al., 2009; Daly et al., 2011). Stimulating with innately attractive mixtures have been shown to reliably evoke specific patterns of synchronous activity in the ALs of hawk moths, and the degree of synchrony correlated with the behavioral impacts of the mixtures (Riffel et al., 2009b). The disparities in latencies and spike frequency distributions shown for blend 12 and blend 10 in this study might well reflect dissimilarities in the ensembles representing these blends and the synchronous patterns they emit. It would be interesting to employ a Pavlovian learning paradigm or two-choice wind-tunnel experiments to see how differences in the neural representations of these two blends are reflected on behavior. Such experiments could also elucidate the influence of factors such as age and physiological state on odor perception and odor preferences. By stimulating with the two mixtures while performing multiunit recordings in a classical conditioning setup, or paired with electromyography from flight muscles, the contributions of response features such as synergy or synchrony to behavior could be unraveled.

4.4 Limitations to the study

A challenge when performing intracellular recordings is the limited time available for testing. In the present study, it was not feasible to test the multicomponent blends against all constituents in any recording. Hence, one cannot exclude the possibility that the often observed stronger response to one of the blends was not attributed to an untested substance within the mixture. However, given the frequent occurrences of best mixture effects, and considering that the tested single odorants have been found the most effective at eliciting neuronal responses, it is likely that several of the observations are true synergies. Moreover, synergy and hypoadditive responses could be reported with certainty for the binary blend in some neurons, and in one neuron it was shown that the difference in response strengths of two complex blends (blend 10 and blend 9) was not attributed to the one volatile distinguishing their chemical composition.

Another concern is that some of the recorded neurons might not have received their inputs in the protocerebrum. Staining was accomplished in only a few neurons so it is possible that some of the neurons were PNs with dendrites residing in the ALs. However, six of the seven neurons stained in the present study were clearly not PNs. The reconstructed PN, N26, was obtained in one of a few experiments where the electrode was inserted into the more anterioventral area of the LP. In addition, morphologically characterized neurons in previous recordings from the LP and SP have predominantly been protocerebral neurons. Hence, it is likely that the majority of the recordings presented in this study are neurons receiving their inputs in the protocerebrum.

Finally, there is some degree of uncertainty as concerns the validity of the latency analyses. Confounding factors, such as fluctuations in the airstream conveying the odor stimulus to the antennae, might have affected the results. Ideally, one would want a device to detect the arrival of the odor stimulus on the antennae in order to ensure that a neurons lag to response onset is not attributed to external factors. However, many of the recorded neurons showed remarkably little variation for responses to a particular odorant, and in some cases showed great variations for responses to different odorants. Thus, it is plausible that at least some of the latencies disparate to blend 12 and blend 10, reflect real temporal differences in the representations of these blends.

4.5 An integrative model of olfaction

In an attempt to unify the results of the present study with previous findings in *H. virescens* and current views on olfactory coding in other insect species, an integrative model of olfaction is proposed. The model takes basis in the olfactory system of moths, and heavily alludes to behavioral and experimental data from moth species. However, inspiration is also drawn from current knowledge and ideas from research on honeybees and fruit flies.

In this model, different features of an odor mixture are processed in parallel pathways in a context dependent manner. Behavior is implemented by synergistic representations of specific mixtures in descending neurons. These synergies are a result of the synchronization within and between the pathways converging onto the descending neurons. General behavior is mediated by homogenous, concentration-invariant mixture representations, while concentration-dependent, ratio-sensitive pathways modulate and specify this behavior. Innate attraction or repulsion to certain odor mixtures is promoted by synchronous representations facilitated by predefined inhibitory connections and PNs receiving combinatorial input. Associative and non-associative synaptic plasticity can serve to synchronize or desynchronize the representations of a given mixture, thus facilitating short term or long term shifts in odor preferences. This system is also apt for modulation by other sensory systems so that the behavioral salience of an odor mixture rapidly can be regulated under different contexts, such as imminent danger. Finally, applying this temporal aspect increases coding space and facilitates the handling of odor signals so that both generalization and discrimination for related mixtures are allowed in different contexts. It should be noted that the emphasis put on synchrony in this model does not preclude important contributions from other coding mechanisms, such as the mean or instantaneous firing rate of neurons in each subsystem. Indeed, a synergistic response in an integrative neuron would not only be a function of the degree of synchrony between the input channels, but also their firing rate. A schematic overview over some aspects of the model is given in figure 14.

In the future, further attempts should be made to unravel the contributions of different coding mechanisms on behavior, taking into account the system as a whole. Behavioral assays, combined with genetic interventions and neurophysiological methods exploring the dynamics of single cells and ensembles, might provide some answers to the mysteries of neural circuits, and the sway they hold over animal behavior.

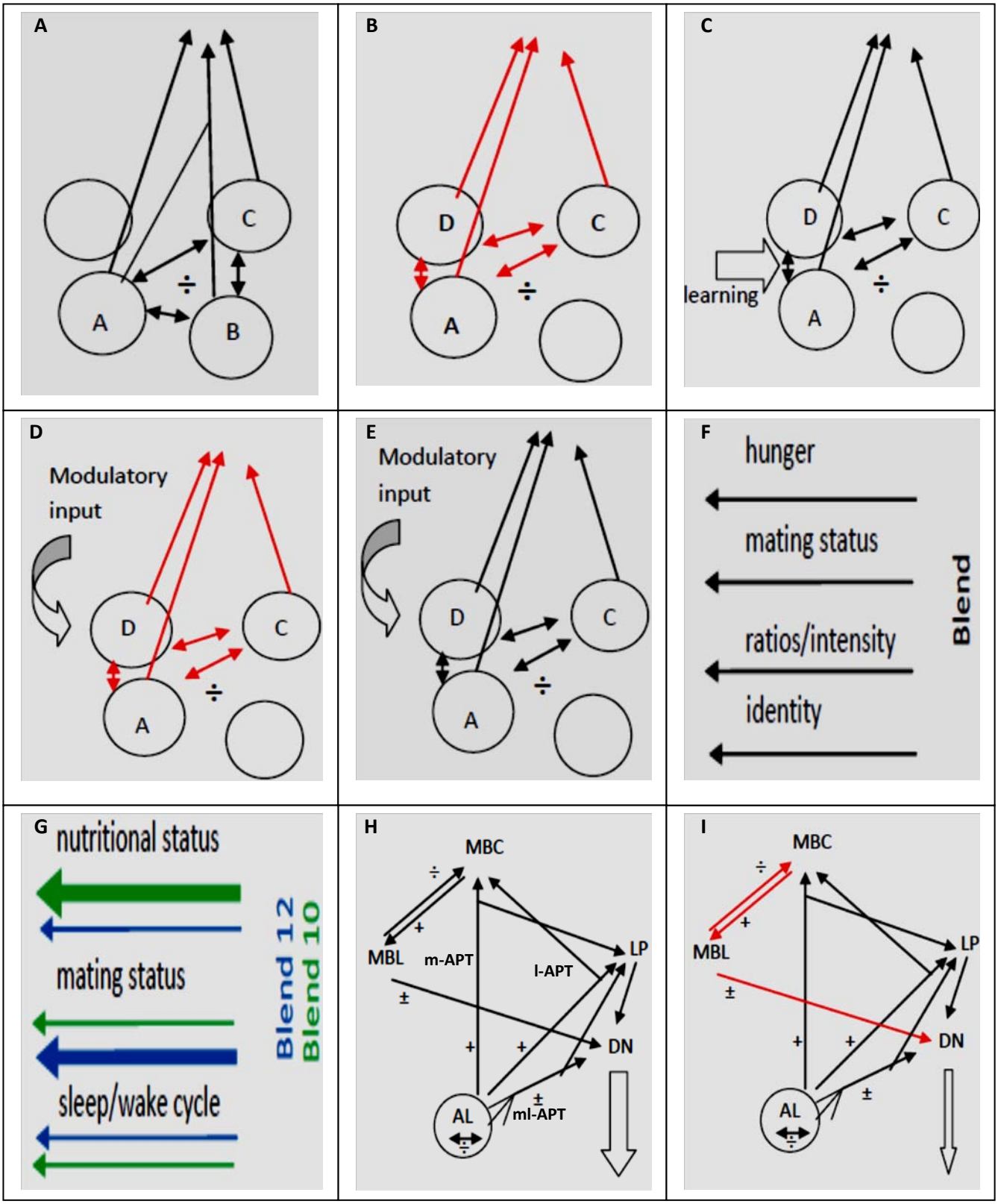
A
C
A
B
B
D
C
A
C
D
C
learning
A
D
Modulatory
input
D
C
A
E
Modulatory
input
D
C
A
F
hunger
mating status
ratios/intensity
identity
Blend
G
nutritional status
mating status
sleep/wake cycle
Blend 12
Blend 10
H
MBC
MBL
m-APT
l-APT
LP
DN
AL
ml-APT
I
MBC
MBL
LP
DN
AL

Figure 14. Schematic overview over important aspects of the model. **A)** Innately attractive mixture [A-B-C] evoke synchronous (black) output from glomeruli of the ALs owing to predefined inhibitory (÷) connections, as well as oligoglomerular PNs receiving combinatorial input from associated biologically relevant volatiles [A-B]. **B)** Unsynchronized (red) output evoked by behaviorally ineffective mixture [A-C-D]. **C)** Learning modulates synaptic plasticity and changes inhibitory connections. This improves synchrony of the activity pattern evoked by mixture [A-C-D], increasing its behavioral salience. **D, E)** Modulation by other sensory modalities or hormonal influence may change the pattern of synchrony on a long term or short term basis. **F)** Parallel pathways processing different features of a blend (identity/ratio/intensity) and/or in different contexts (nutritional status/mating status etc). **G)** Depending on the context in which each channel processes information, different blends may have different saliencies (represented by arrow size), while in other channels they are similar. **H)** A descending neuron (DN) in the LP receives input from many channels: direct combinatorial information from inhibitory or excitatory (±) multiglomerular PNs and indirect input from uniglomerular PNs via LP neurons and extrinsic neurons from the experience dependent MB pathway. Synchrony (black) within and between the subsystems creates a strong synergistic signal in the DN. **I)** If one pathway is out of sync the output from the DN is reduced. In **I**, the experience dependent pathway via the MBs is out of sync (red), as could be the case when an insect has learned that a particular odorant is *not* rewarded. The principles in **I** and **H** are shown for the DN, but is applicable to all neurons receiving input from many channels. Abbreviations: AL – antennal lobes; DN – descending neuron; LP – lateral protocerebrum; MBC – mushroom body calyces; MBL – mushroom body lobes; m-APT – medial antenno-protocerebral tract; l-APT – lateral antenno-protocerebral tract; ml-APT – mediolateral antenno-protocerebral tract.

5. Conclusions

Intracellular recordings from the protocerebrum of *H. virescens* showed that blends evoke responses with higher probability than single odorants in protocerebral neurons. Analyses of response strengths revealed that the majority of neurons responded stronger to blends than to single odorants, an effect that was found significant when regarded over the neuronal population. These results corroborate previous findings from the protocerebrum of this species, but contrasts observations from the primary olfactory center of *H. virescens* and other insect species. The apparent disparity between odor representations in the protocerebrum and the ALs might indicate that higher order neurons integrate information from several separate channels conveying information about primary odorants from the ALs. The prominence of blend synergies in protocerebral neurons could potentially constitute a neural correlate to mixture-driven behaviors, but this hypothesis remains to be investigated. A higher order neuron identified in the present study, responded exclusively to one primary odorant, implying that information about specific primary plant odorants is also preserved in protocerebral neurons. Furthermore, a morphologically characterized oligoglomerular PN was shown to respond to two primary odorants which do not activate the same ORNs. This demonstrated that odor coding to some extent is combinatorial already at the level of the ALs in this species. Elemental mixture processing was not observed in any of the recorded neurons, and no consistent rule seemed to dictate the response patterns to a blend relative to its constituents. Many neurons were also shown to completely discriminate between two chemically related multicomponents blends, and some distinguishing between them by their response patterns. These results imply that integration by higher order neurons is nonlinear and specific for each mixture in each neuron. Attempting to unify the results from the present study with experimental data on olfactory coding and behavior in moths and other insect species, an integrative model of olfaction is proposed, emphasizing both temporal and spatial aspects of sensory coding. By employing behavioral assays combined with genetic interventions and neurophysiological methods on single cells and neuronal ensembles, future investigations might unravel the logic of olfactory coding and elucidate how different coding features contribute to the behavioral output.

Abbreviations

AL – Antennal lobe

APT – Antenno-protocerebral tract

CB – Central body

GABA – gamma-amino-butyric acid

KC – Kenyon cell

LAL – Lateral accessory lobe

LALco – Lateral accessory lobe commissure

LFP – Local field potential

LN – Local interneuron

LP – Lateral protocerebrum

MBC – Mushroom body calyces

MBL – Mushroom body lobes

MDS – Mean deviation from spontaneous activity

MP – Medial protocerebrum

OR – Olfactory receptor

ORN – Olfactory receptor neuron

PN – Projection neuron

SD – Standard deviation

SP – Superior protocerebrum

VP – Ventral protocerebrum

References

ANDERSSON, M. N., BINYAMEEN, M., SADEK, M. M. & SCHLYTER, F. 2011. Attraction modulated by spacing of pheromone components and anti-attractants in a bark beetle and a moth. *J Chem Ecol,* 37**,** 899-911.

AXEL, R. 2005. Scents and sensibility: a molecular logic of olfactory perception (Nobel lecture). *Angew Chem Int Ed Engl,* 44**,** 6110-27.

BENTON, R., SACHSE, S., MICHNICK, S. W. & VOSSHALL, L. B. 2006. Atypical membrane topology and heteromeric function of Drosophila odorant receptors in vivo. *PLoS Biol,* 4**,** e20.

BERG, B. G., SCHACHTNER, J. & HOMBERG, U. 2009. Gamma-aminobutyric acid immunostaining in the antennal lobe of the moth Heliothis virescens and its colocalization with neuropeptides. *Cell Tissue Res,* 335**,** 593-605.

BRANDT, R., ROHLFING, T., RYBAK, J., KROFCZIK, S., MAYE, A., WESTERHOFF, M., HEGE, H. C. & MENZEL, R. 2005. Three-dimensional average-shape atlas of the honeybee brain and its applications. *J Comp Neurol,* 492**,** 1-19.

BUCK, L. & AXEL, R. 1991. A novel multigene family may encode odorant receptors: a molecular basis for odor recognition. *Cell,* 65**,** 175-87.

CAPURRO, A., BARONI, F., OLSSON, S. B., KUEBLER, L. S., KAROUT, S., HANSSON, B. S. & PEARCE, T. C. 2012. Non-linear blend coding in the moth antennal lobe emerges from random glomerular networks. *Front Neuroeng,* 5**,** 6.

CASSENAER, S. & LAURENT, G. 2007. Hebbian STDP in mushroom bodies facilitates the synchronous flow of olfactory information in locusts. *Nature,* 448**,** 709-13.

CHEN, D. & DALTON, P. 2005. The effect of emotion and personality on olfactory perception. *Chem Senses,* 30**,** 345-51.

CHRISTENSEN, T. A., LEI, H. & HILDEBRAND, J. G. 2003. Coordination of central odor representations through transient, non-oscillatory synchronization of glomerular output neurons. *Proc Natl Acad Sci U S A,* 100**,** 11076-81.

DALY, K. C., CHRISTENSEN, T. A., LEI, H., SMITH, B. H. & HILDEBRAND, J. G. 2004. Learning modulates the ensemble representations for odors in primary olfactory networks. *Proc Natl Acad Sci U S A,* 101**,** 10476-81.

DALY, K. C., GALAN, R. F., PETERS, O. J. & STAUDACHER, E. M. 2011. Detailed Characterization of Local Field Potential Oscillations and Their Relationship to Spike Timing in the Antennal Lobe of the Moth Manduca sexta. *Front Neuroeng,* 4**,** 12.

DE BRUYNE, M., CLYNE, P. J. & CARLSON, J. R. 1999. Odor coding in a model olfactory organ: the Drosophila maxillary palp. *J Neurosci,* 19**,** 4520-32.

DEISIG, N., GIURFA, M., LACHNIT, H. & SANDOZ, J. C. 2006. Neural representation of olfactory mixtures in the honeybee antennal lobe. *Eur J Neurosci,* 24**,** 1161-74.

DEISIG, N., GIURFA, M. & SANDOZ, J. C. 2010. Antennal Lobe Processing Increases Separability of Odor Mixture Representations in the Honeybee. *J Neurophysiol,* 103**,** 2185-2194.

DEKKER, T., STEIB, B., CARDE, R. T. & GEIER, M. 2002. L-lactic acid: a human-signifying host cue for the anthropophilic mosquito Anopheles gambiae. *Med Vet Entomol,* 16**,** 91-8.

DENKER, M., FINKE, R., SCHAUPP, F., GRUN, S. & MENZEL, R. 2010. Neural correlates of odor learning in the honeybee antennal lobe. *Eur J Neurosci,* 31**,** 119-33.

DUCHAMP-VIRET, P., DUCHAMP, A. & CHAPUT, M. A. 2003. Single olfactory sensory neurons simultaneously integrate the components of an odour mixture. *Eur J Neurosci,* 18**,** 2690-6.

DUPUIS, J. P., BAZELOT, M., BARBARA, G. S., PAUTE, S., GAUTHIER, M. & RAYMOND-DELPECH, V. 2010. Homomeric RDL and heteromeric RDL/LCCH3 GABA receptors in the honeybee antennal lobes: two candidates for inhibitory transmission in olfactory processing. *J Neurophysiol,* 103**,** 458-68.

EVERS, J. F., SCHMITT, S., SIBILA, M. & DUCH, C. 2005. Progress in functional neuroanatomy: precise automatic geometric reconstruction of neuronal morphology from confocal image stacks. *J Neurophysiol,* 93**,** 2331-42.

FITT, G. P. 1989. The Ecology of Heliothis Species in Relation to Agroecosystems. *Annu Rev Entomol,* 34**,** 17-52.

FONTAINE, B. & PEREMANS, H. 2009. Bat echolocation processing using first-spike latency coding. *Neural Netw,* 22**,** 1372-82.

GALIZIA, C. G. & RÖSSLER, W. 2010. Parallel olfactory systems in insects: anatomy and function. *Annu Rev Entomol,* 55**,** 399-420.

GALIZIA, C. G. & SZYSZKA, P. 2008. Olfactory coding in the insect brain: molecular receptive ranges, spatial and temporal coding. *Entomol Exp Appl,* 128**,** 81-92.

GOLDMAN, A. L., VAN DER GOES VAN NATERS, W., LESSING, D., WARR, C. G. & CARLSON, J. R. 2005. Coexpression of two functional odor receptors in one neuron. *Neuron,* 45**,** 661-6.

GOLLISCH, T. & MEISTER, M. 2008. Rapid neural coding in the retina with relative spike latencies. *Science,* 319**,** 1108-11.

HAMMER, M. 1993. An Identified Neuron Mediates the Unconditioned Stimulus in Associative Olfactory Learning in Honeybees. *Nature,* 366**,** 59-63.

HAMMER, M. & MENZEL, R. 1998. Multiple sites of associative odor learning as revealed by local brain microinjections of octopamine in honeybees. *Learn Mem,* 5**,** 146-56.

HANSSON, B. S., ANTON, S. & CHRISTENSEN, T. A. 1994. Structure and Function of Antennal Lobe Neurons in the Male Turnip Moth, Agrotis-Segetum (Lepidoptera, Noctuidae). *J Comp Physiol A Neuroethol Sens Neural Behav Physiol,* 175**,** 547-562.

HARTLIEB, E., ANTON, S. & HANSSON, B. S. 1997. Dose-dependent response characteristics of antennal lobe neurons in the male moth Agrotis segetum (Lepidoptera: Noctuidae). *J Comp Physiol A Neuroethol Sens Neural Behav Physiol,* 181**,** 469-476.

HEIMBECK, G., BUGNON, V., GENDRE, N., KELLER, A. & STOCKER, R. F. 2001. A central neural circuit for experience-independent olfactory and courtship behavior in Drosophila melanogaster. *Proc Natl Acad Sci U S A,* 98**,** 15336-41.

HEINZE, S. & HOMBERG, U. 2007. Maplike representation of celestial E-vector orientations in the brain of an insect. *Science,* 315**,** 995-7.

HEISENBERG, M. 2003. Mushroom body memoir: From maps to models. *Nat Rev Neurosci,* 4**,** 266-275.

HERZ, R. S. 2005. Odor-associative learning and emotion: effects on perception and behavior. *Chem Senses,* 30 Suppl 1**,** i250-1.

HOMBERG, U., KINGAN, T. G. & HILDEBRAND, J. G. 1987. Immunocytochemistry of GABA in the brain and suboesophageal ganglion of Manduca sexta. *Cell Tissue Res,* 248**,** 1-24.

HOMBERG, U., MONTAGUE, R. A. & HILDEBRAND, J. G. 1988. Anatomy of antenno-cerebral pathways in the brain of the sphinx moth Manduca sexta. *Cell Tissue Res,* 254**,** 255-81.

HOPKINS, T. L. & YOUNG, H. 1990. Attraction of the Grasshopper, Melanoplus-Sanguinipes, to Host Plant Odors and Volatile Components. *Entomol Exp Appl,* 56**,** 249-258.

HOSKINS, S. G., HOMBERG, U., KINGAN, T. G., CHRISTENSEN, T. A. & HILDEBRAND, J. G. 1986. Immunocytochemistry of GABA in the antennal lobes of the sphinx moth Manduca sexta. *Cell Tissue Res,* 244**,** 243-52.

ITO, I., BAZHENOV, M., ONG, R. C., RAMAN, B. & STOPFER, M. 2009. Frequency transitions in odor-evoked neural oscillations. *Neuron,* 64**,** 692-706.

IWANO, M., HILL, E. S., MORI, A., MISHIMA, T., ITO, K. & KANZAKI, R. 2010. Neurons associated with the flip-flop activity in the lateral accessory lobe and ventral protocerebrum of the silkworm moth brain. *J Comp Neurol,* 518**,** 366-88.

JEFFERIS, G. S. X. E., MARIN, E. C., STOCKER, R. F. & LUO, L. Q. 2001. Target neuron prespecification in the olfactory map of Drosophila. *Nature,* 414**,** 204-208.

JEFFERIS, G. S. X. E., POTTER, C. J., CHAN, A. I., MARIN, E. C., ROHLFING, T., MAURER, C. R. & LUO, L. Q. 2007. Comprehensive maps of Drosophila higher offactory centers: Spatially segregated fruit and pheromone representation. *Cell,* 128**,** 1187-1203.

JØRGENSEN, K., STRANDEN, M., SANDOZ, J. C., MENZEL, R. & MUSTAPARTA, H. 2007. Effects of two bitter substances on olfactory conditioning in the moth Heliothis virescens. *J Exp Biol,* 210**,** 2563-73.

JORTNER, R. A., FARIVAR, S. S. & LAURENT, G. 2007. A simple connectivity scheme for sparse coding in an olfactory system. *J Neurosci,* 27**,** 1659-69.

KANZAKI, R., ARBAS, E. A. & HILDEBRAND, J. G. 1991a. Physiology and morphology of descending neurons in pheromone-processing olfactory pathways in the male moth Manduca sexta. *J Comp Physiol A,* 169**,** 1-14.

KANZAKI, R., ARBAS, E. A. & HILDEBRAND, J. G. 1991b. Physiology and morphology of protocerebral olfactory neurons in the male moth Manduca sexta. *J Comp Physiol A,* 168**,** 281-98.

KANZAKI, R., SOO, K., SEKI, Y. & WADA, S. 2003. Projections to higher olfactory centers from subdivisions of the antennal lobe macroglomerular complex of the male silkmoth. *Chem Senses,* 28**,** 113-30.

KAUPP, U. B. 2010. Olfactory signalling in vertebrates and insects: differences and commonalities. *Nat Rev Neurosci,* 11**,** 188-200.

KEENE, A. C. & WADDELL, S. 2007. Drosophila olfactory memory: single genes to complex neural circuits. *Nat Rev Neurosci,* 8**,** 341-54.

KIRSCHNER, S., KLEINEIDAM, C. J., ZUBE, C., RYBAK, J., GRUNEWALD, B. & ROSSLER, W. 2006. Dual olfactory pathway in the honeybee, Apis mellifera. *J Comp Neurol,* 499**,** 933-952.

KRIEGER, J., GROSSE-WILDE, E., GOHL, T., DEWER, Y. M., RAMING, K. & BREER, H. 2004. Genes encoding candidate pheromone receptors in a moth (Heliothis virescens). *Proc Natl Acad Sci U S A,* 101**,** 11845-50.

KRIEGER, J., RAMING, K., DEWER, Y. M., BETTE, S., CONZELMANN, S. & BREER, H. 2002. A divergent gene family encoding candidate olfactory receptors of the moth Heliothis virescens. *Eur J Neurosci,* 16**,** 619-28.

KROFCZIK, S., MENZEL, R. & NAWROT, M. P. 2009. Rapid odor processing in the honeybee antennal lobe network. *Front Comp Neurosci,* 2, 9.

KUEBLER, L. S., OLSSON, S. B., WENIGER, R. & HANSSON, B. S. 2011. Neuronal processing of complex mixtures establishes a unique odor representation in the moth antennal lobe. *Front Neural Circuits,* 5**,** 7.

KVELLO, P., LOFALDLI, B. B., RYBAK, J., MENZEL, R. & MUSTAPARTA, H. 2009. Digital, Three-dimensional Average Shaped Atlas of the Heliothis Virescens Brain with Integrated Gustatory and Olfactory Neurons. *Front Syst Neurosci,* 3**,** 14.

LARSSON, M. C., DOMINGOS, A. I., JONES, W. D., CHIAPPE, M. E., AMREIN, H. & VOSSHALL, L. B. 2004. Or83b encodes a broadly expressed odorant receptor essential for Drosophila olfaction. *Neuron,* 43**,** 703-14.

LASKA, M. & HUDSON, R. 1991. A Comparison of the Detection Thresholds of Odor Mixtures and Their Components. *Chem Senses,* 16**,** 651-662.

LAURENT, G. 2002. Olfactory network dynamics and the coding of multidimensional signals. *Nat Rev Neurosci,* 3**,** 884-95.

LEI, H., ANTON, S. & HANSSON, B. S. 2001. Olfactory protocerebral pathways processing sex pheromone and plant odor information in the male moth Agrotis segetum. *J Comp Neurol,* 432**,** 356-70.

LEI, H., CHRISTENSEN, T. A. & HILDEBRAND, J. G. 2002. Local inhibition modulates odor-evoked synchronization of glomerulus-specific output neurons. *Nat Neurosci,* 5**,** 557-65.

LEI, H. & VICKERS, N. 2008. Central processing of natural odor mixtures in insects. *J Chem Ecol,* 34**,** 915-27.

LOESEL, R., NASSEL, D. R. & STRAUSFELD, N. J. 2002. Common design in a unique midline neuropil in the brains of arthropods. *Arthropod Struct Dev,* 31**,** 77-91.

LØFALDLI, B. B., KVELLO, P. & MUSTAPARTA, H. 2010. Integration of the antennal lobe glomeruli and three projection neurons in the standard brain atlas of the moth heliothis virescens. *Front Syst Neurosci,* 4**,** 5.

LØFALDLI, B. B., KVELLO, P., KIRKERUD, N, MUSTAPARTA, H. 2012. A putative neuronal circuit handling information about a ten component plant odor blend in the brain of *H. virescens*. *Front Syst Neurosci,* submitted.

LUNDIN, C., KALL, L., KREHER, S. A., KAPP, K., SONNHAMMER, E. L., CARLSON, J. R., HEIJNE, G. & NILSSON, I. 2007. Membrane topology of the Drosophila OR83b odorant receptor. *FEBS Lett,* 581**,** 5601-4.

MARTIN, J. P., BEYERLEIN, A., DACKS, A. M., REISENMAN, C. E., RIFFELL, J. A., LEI, H. & HILDEBRAND, J. G. 2011. The neurobiology of insect olfaction: sensory processing in a comparative context. *Prog Neurobiol,* 95**,** 427-47.

MARTIN, J. P. & HILDEBRAND, J. G. 2010. Innate recognition of pheromone and food odors in moths: a common mechanism in the antennal lobe? *Front Behav Neurosci,* 4.

MEAGHER, R. L. & LANDOLT, P. J. 2008. Attractiveness of binary blends of floral odorant compounds to moths in Florida, USA. *Entomol Exp Appl,* 128**,** 323-329.

MENZEL, R., GALIZIA, G., MULLER, D. & SZYSZKA, P. 2005. Odor coding in projection neurons of the honeybee brain. *Chem Senses,* 30 Suppl 1**,** i301-2.

MENZEL, R. & GIURFA, M. 2001. Cognitive architecture of a mini-brain: the honeybee. *Trends Cogn Sci,* 5**,** 62-71.

MEYER, A. & GALIZIA, C. G. 2012. Elemental and configural olfactory coding by antennal lobe neurons of the honeybee (Apis mellifera). *J Comp Physiol A Neuroethol Sens Neural Behav Physiol,* 198**,** 159-71.

MOZURAITIS, R., STRANDEN, M., RAMIREZ, M. I., BORG-KARLSON, A. K. & MUSTAPARTA, H. 2002. (-)-Germacrene D increases attraction and oviposition by the tobacco budworm moth Heliothis virescens. *Chem Senses,* 27**,** 505-9.

MULLER, D., ABEL, R., BRANDT, R., ZOCKLER, M. & MENZEL, R. 2002. Differential parallel processing of olfactory information in the honeybee, Apis mellifera L. *J Comp Physiol A Neuroethol Sens Neural Behav Physiol,* 188**,** 359-70.

MUMM, R. & HILKER, M. 2005. The significance of background odour for an egg parasitoid to detect plants with host eggs. *Chem Senses,* 30**,** 337-43.

NAMIKI, S. & KANZAKI, R. 2011. Heterogeneity in dendritic morphology of moth antennal lobe projection neurons. *J Comp Neurol,* 519**,** 3367-86.

OKADA, R., RYBAK, J., MANZ, G. & MENZEL, R. 2007. Learning-related plasticity in PE1 and other mushroom body-extrinsic neurons in the honeybee brain. *J Neurosci,* 27**,** 11736-47.

OLSEN, S. R., BHANDAWAT, V. & WILSON, R. I. 2007. Excitatory interactions between olfactory processing channels in the Drosophila antennal lobe. *Neuron,* 54**,** 89-103.

PEREZ-ORIVE, J., MAZOR, O., TURNER, G. C., CASSENAER, S., WILSON, R. I. & LAURENT, G. 2002. Oscillations and sparsening of odor representations in the mushroom body. *Science,* 297**,** 359-65.

PINERO, J. C., GIOVANNI GALIZIA, C. & DORN, S. 2008. Synergistic behavioral responses of female oriental fruit moths (Lepidoptera:Tortricidae) to synthetic host plant-derived mixtures are mirrored by odor-evoked calcium activity in their antennal lobes. *J Insect Physiol,* 54**,** 333-43.

RIFFELL, J. A., ALARCON, R., ABRELL, L., DAVIDOWITZ, G., BRONSTEIN, J. L. & HILDEBRAND, J. G. 2008. Behavioral consequences of innate preferences and olfactory learning in hawkmoth-flower interactions. *Proc Natl Acad Sci U S A,* 105**,** 3404-9.

RIFFELL, J. A., LEI, H., CHRISTENSEN, T. A. & HILDEBRAND, J. G. 2009a. Characterization and Coding of Behaviorally Significant Odor Mixtures. *Curr Biol,* 19**,** 335-340.

RIFFELL, J. A., LEI, H. & HILDEBRAND, J. G. 2009b. Neural correlates of behavior in the moth Manduca sexta in response to complex odors. *Proc Natl Acad Sci U S A,* 106**,** 19219-26.

RØ, H., MULLER, D. & MUSTAPARTA, H. 2007. Anatomical organization of antennal lobe projection neurons in the moth Heliothis virescens. *J Comp Neurol,* 500**,** 658-75.

ROBERTSON, H. M., WARR, C. G. & CARLSON, J. R. 2003. Molecular evolution of the insect chemoreceptor gene superfamily in Drosophila melanogaster. *Proc Natl Acad Sci U S A,* 100 Suppl 2**,** 14537-42.

RØSTELIEN, T., BORG-KARLSON, A. K. & MUSTAPARTA, H. 2000. Selective receptor neurone responses to E-beta-ocimene, beta-myrcene, E,E-alpha-farnesene and homo-farnesene in the moth Heliothis virescens, identified by gas chromatography linked to electrophysiology. *J Comp Physiol A,* 186**,** 833-47.

RØSTELIEN, T., STRANDEN, M., BORG-KARLSON, A. K. & MUSTAPARTA, H. 2005. Olfactory receptor neurons in two Heliothine moth species responding selectively to aliphatic green leaf volatiles, aromatic compounds, monoterpenes and sesquiterpenes of plant origin. *Chem Senses,* 30**,** 443-61.

SACHSE, S. & GALIZIA, C. G. 2002. Role of inhibition for temporal and spatial odor representation in olfactory output neurons: a calcium imaging study. *J Neurophysiol,* 87**,** 1106-17.

SACHSE, S., RAPPERT, A. & GALIZIA, C. G. 1999. The spatial representation of chemical structures in the antennal lobe of honeybees: steps towards the olfactory code. *Eur J Neurosci,* 11**,** 3970-82.

SATO, K., PELLEGRINO, M., NAKAGAWA, T., VOSSHALL, L. B. & TOUHARA, K. 2008. Insect olfactory receptors are heteromeric ligand-gated ion channels. *Nature,* 452**,** 1002-6.

SCHMITT, S., EVERS, J. F., DUCH, C., SCHOLZ, M. & OBERMAYER, K. 2004. New methods for the computer-assisted 3-D reconstruction of neurons from confocal image stacks. *Neuroimage,* 23**,** 1283-98.

SEKI, Y. & KANZAKI, R. 2008. Comprehensive morphological identification and GABA immunocytochemistry of antennal lobe local interneurons in Bombyx mori. *J Comp Neurol,* 506**,** 93-107.

SHANG, Y., CLARIDGE-CHANG, A., SJULSON, L., PYPAERT, M. & MIESENBOCK, G. 2007. Excitatory local circuits and their implications for olfactory processing in the fly antennal lobe. *Cell,* 128**,** 601-12.

SHEPHERD, G. M. 2006. Smell images and the flavour system in the human brain. *Nature,* 444**,** 316-321.

SINGER, W. 1999. Neuronal synchrony: a versatile code for the definition of relations? *Neuron,* 24**,** 49-65, 111-25..

STOPFER, M., BHAGAVAN, S., SMITH, B. H. & LAURENT, G. 1997. Impaired odour discrimination on desynchronization of odour-encoding neural assemblies. *Nature,* 390**,** 70-4.

STRANDEN, M., BORG-KARLSON, A. K. & MUSTAPARTA, H. 2002. Receptor neuron discrimination of the germacrene D enantiomers in the moth Helicoverpa armigera. *Chem Senses,* 27**,** 143-52.

STRANDEN, M., LIBLIKAS, I., KONIG, W. A., ALMAAS, T. J., BORG-KARLSON, A. K. & MUSTAPARTA, H. 2003a. (-)-Germacrene D receptor neurones in three species of heliothine moths: structure-activity relationships. *J Comp Physiol A Neuroethol Sens Neural Behav Physiol,* 189**,** 563-77.

STRANDEN, M., ROSTELIEN, T., LIBLIKAS, I., ALMAAS, T. J., BORG-KARLSON, A. K. & MUSTAPARTA, H. 2003b. Receptor neurones in three heliothine moths responding to floral and inducible plant volatiles. *Chemoecology,* 13**,** 143-154.

SUN, X. J., FONTA, C. & MASSON, C. 1993. Odor Quality Processing by Bee Antennal Lobe Interneurons. *Chem Senses,* 18**,** 355-377.

SZYSZKA, P., DITZEN, M., GALKIN, A., GALIZIA, C. G. & MENZEL, R. 2005. Sparsening and temporal sharpening of olfactory representations in the honeybee mushroom bodies. *J Neurophysiol,* 94**,** 3303-13.

SZYSZKA, P., GALKIN, A. & MENZEL, R. 2008. Associative and non-associative plasticity in kenyon cells of the honeybee mushroom body. *Front Syst Neurosci,* 2**,** 3.

TANAKA, N. K., AWASAKI, T., SHIMADA, T. & ITO, K. 2004. Integration of chemosensory pathways in the Drosophila second-order olfactory centers. *Curr Biol,* 14**,** 449-57.

TANAKA, N. K., TANIMOTO, H. & ITO, K. 2008. Neuronal assemblies of the Drosophila mushroom body. *J Comp Neurol,* 508**,** 711-755.

TURNER, G. C., BAZHENOV, M. & LAURENT, G. 2008. Olfactory representations by Drosophila mushroom body neurons. *J Neurophysiol,* 99**,** 734-46.

WALDROP, B., CHRISTENSEN, T. A. & HILDEBRAND, J. G. 1987. GABA-mediated synaptic inhibition of projection neurons in the antennal lobes of the sphinx moth, Manduca sexta. *J Comp Physiol A,* 161**,** 23-32.

WILSON, R. I. & LAURENT, G. 2005. Role of GABAergic inhibition in shaping odor-evoked spatiotemporal patterns in the Drosophila antennal lobe. *J Neurosci,* 25**,** 9069-79.

WISE, P. M. & CAIN, W. S. 1999. Latency and accuracy of same-different discriminations of odor quality. *Fechner Day 99: The End of 20th Century Psychophysics, Proceedings*, 395-400.

WRIGHT, G. A., LUTMERDING, A., DUDAREVA, N. & SMITH, B. H. 2005. Intensity and the ratios of compounds in the scent of snapdragon flowers affect scent discrimination by honeybees (Apis mellifera). *J Comp Physiol A Neuroethol Sens Neural Behav Physiol,* 191**,** 105-14.

YAMAGATA, N., SCHMUKER, M., SZYSZKA, P., MIZUNAMI, M. & MENZEL, R. 2009. Differential odor processing in two olfactory pathways in the honeybee. *Front Syst Neurosci,* 3**,** 16.

ZHAO, X. C. & BERG, B. G. 2009. Morphological and physiological characteristics of the serotonin-immunoreactive neuron in the antennal lobe of the male oriental tobacco budworm, Helicoverpa assulta. *Chem Senses,* 34**,** 363-72.

ZHAO, X. C., PFUHL, G., SURLYKKE, A., TRO, J., BERG, B.G. 2012. A multisensory centrifugal neuron in the olfactory pathway of heliothine moths. *J Comp Neurol,* in press.

ZUBE, C., KLEINEIDAM, C. J., KIRSCHNER, S., NEEF, J. & ROSSLER, W. 2008. Organization of the olfactory pathway and odor processing in the antennal lobe of the ant Camponotus floridanus. *J Comp Neurol,* 506**,** 425-441.

APPENDIX

Table 5. Compositions of the blends used in this study. Shaded areas: single component is included in the mixture. Blank area: single component is not included in the mixture.

Single components	Blends				
	B2	B5	B9	B10	B12
3Z-Hexenol					
3Z-Hexenyl acetate					
Ocimene					
Linalool					
Geraniol					
3-Carene					
E-verbenol					
Methyl benzoate					
Hexanol					
Phenylethanol					
Farnesene					
Germacrene D					

Interval Histograms

Interval histograms over the first stimulations with blend 12 and blend 10 in eleven neurons.

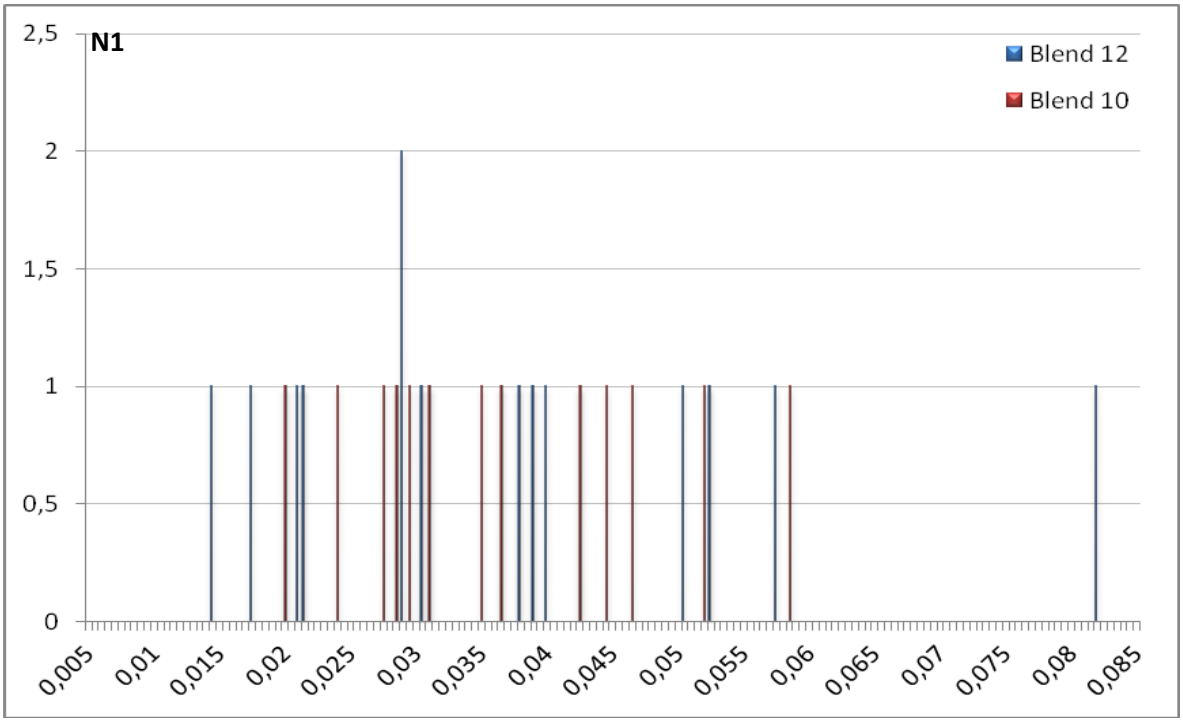

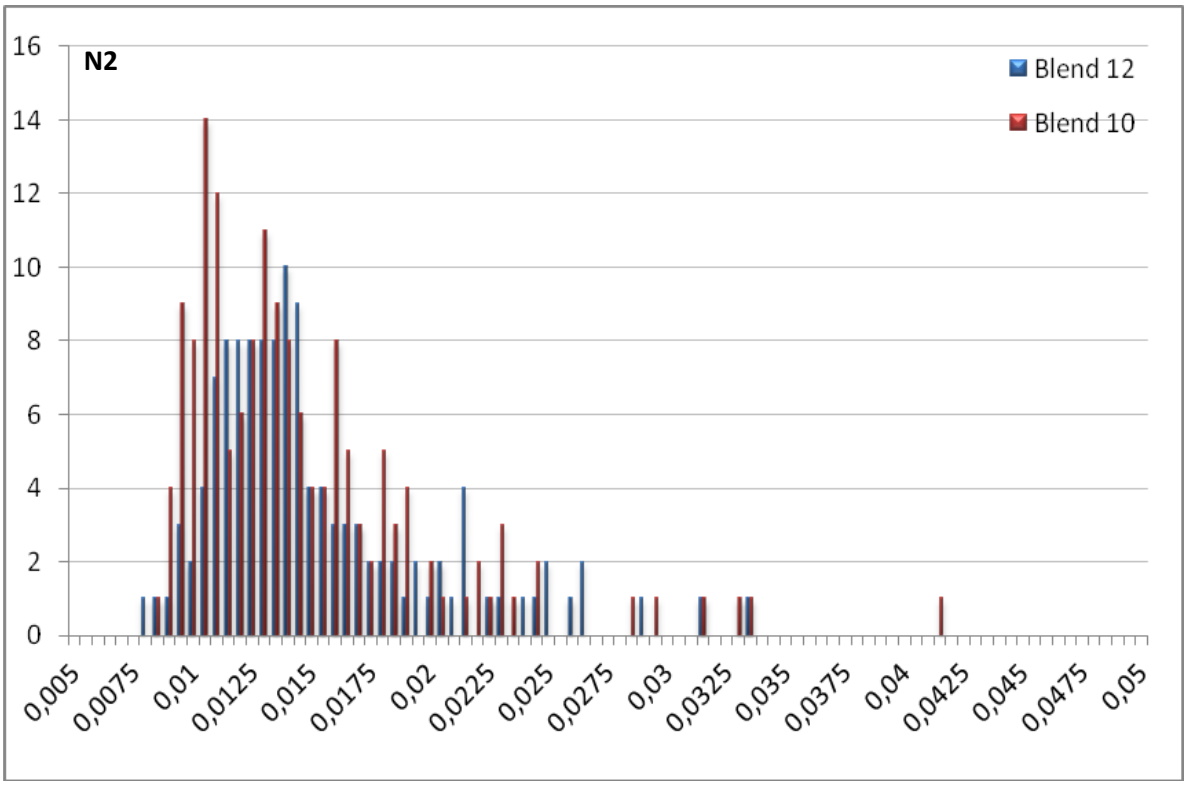
N2
Blend 12
Blend 10
16
14
12
10
8
6
4
2
0
0,005
0,0075
0,01
0,0125
0,015
0,0175
0,02
0,0225
0,025
0,0275
0,03
0,0325
0,035
0,0375
0,04
0,0425
0,045
0,0475
0,05

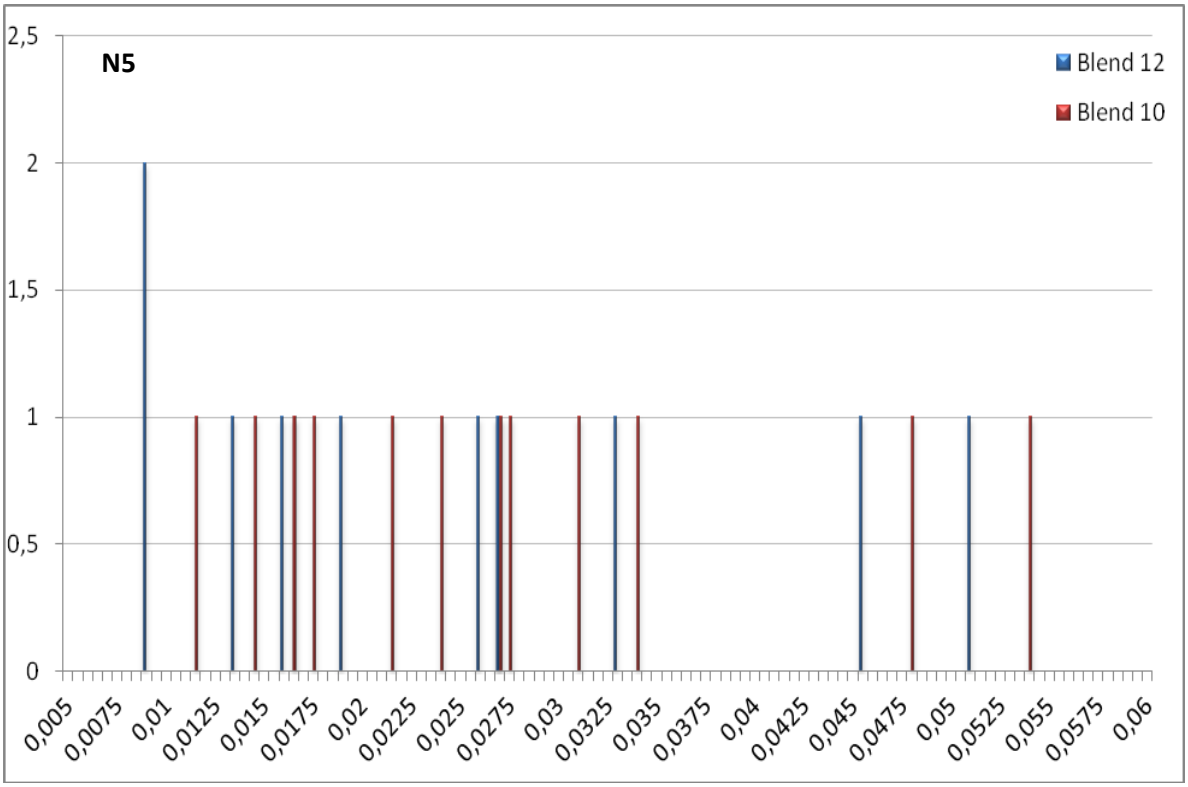
N5
Blend 12
Blend 10
2,5
2
1,5
1
0,5
0
0,005
0,0075
0,01
0,0125
0,015
0,0175
0,02
0,0225
0,025
0,0275
0,03
0,0325
0,035
0,0375
0,04
0,0425
0,045
0,0475
0,05
0,0525
0,055
0,0575
0,06

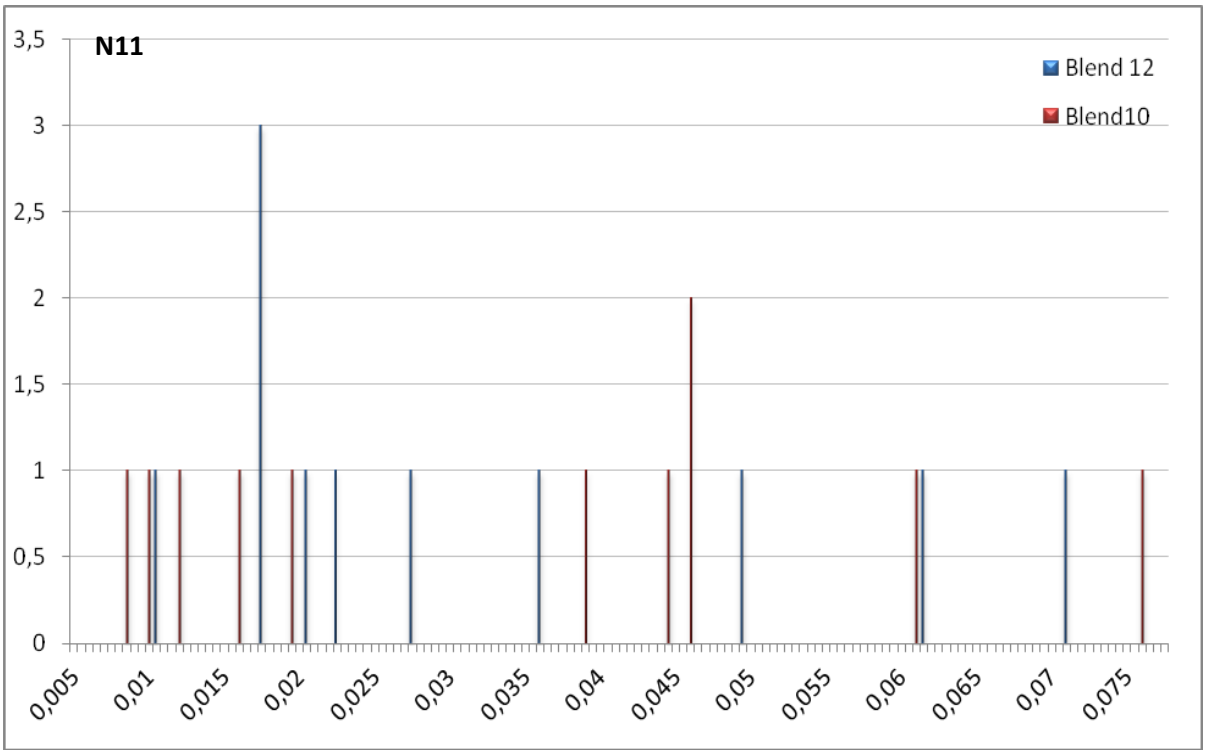
N11
Blend 12
Blend10
3,5
3
2,5
2
1,5
1
0,5
0
0,005
0,01
0,015
0,02
0,025
0,03
0,035
0,04
0,045
0,05
0,055
0,06
0,065
0,07
0,075

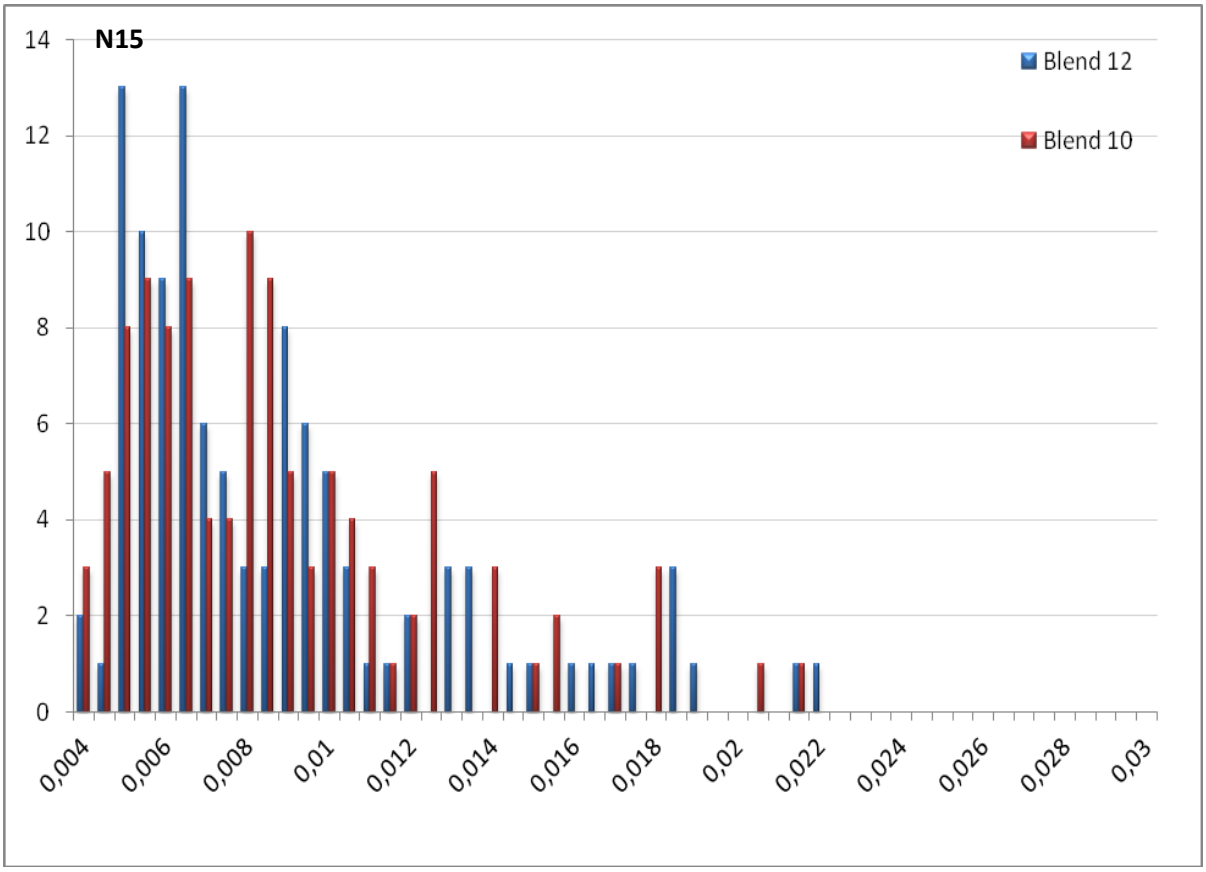
N15
Blend 12
Blend 10
14
12
10
8
6
4
2
0
0,004
0,006
0,008
0,01
0,012
0,014
0,016
0,018
0,02
0,022
0,024
0,026
0,028
0,03

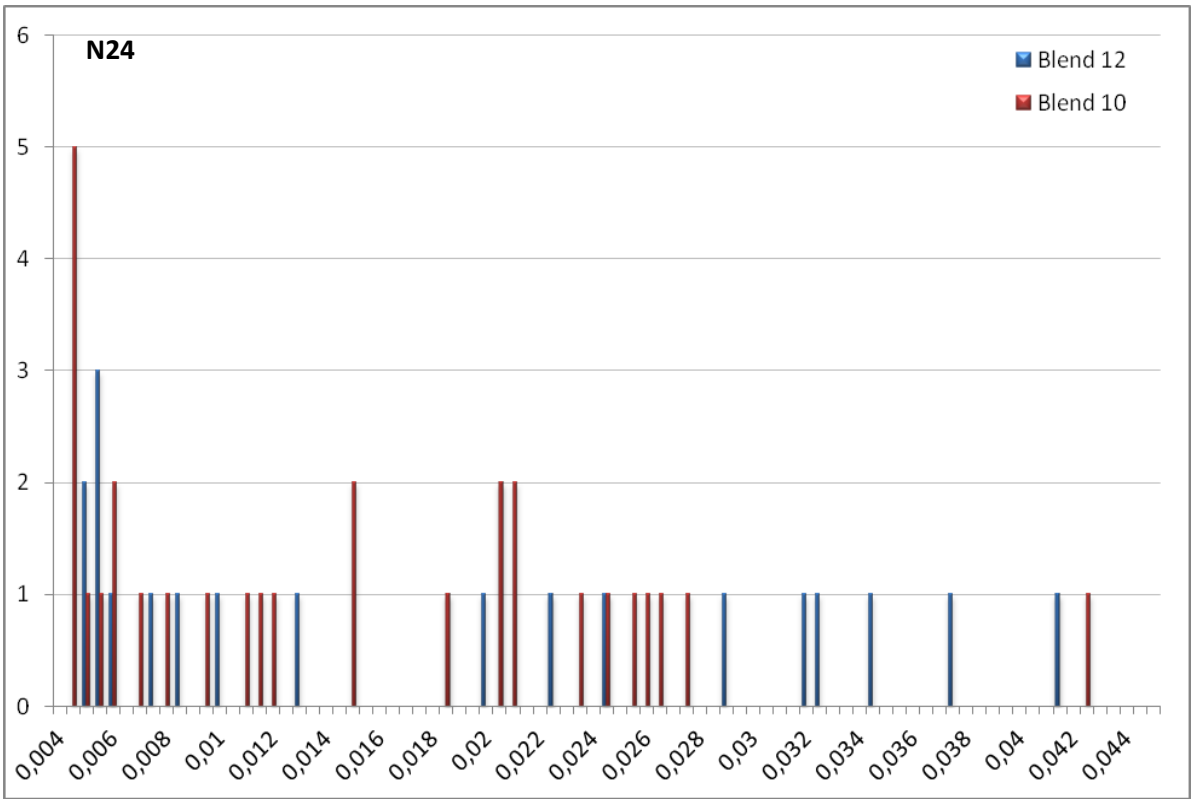
N24
Blend 12
Blend 10
6
5
4
3
2
1
0
0,004
0,006
0,008
0,01
0,012
0,014
0,016
0,018
0,02
0,022
0,024
0,026
0,028
0,03
0,032
0,034
0,036
0,038
0,04
0,042
0,044

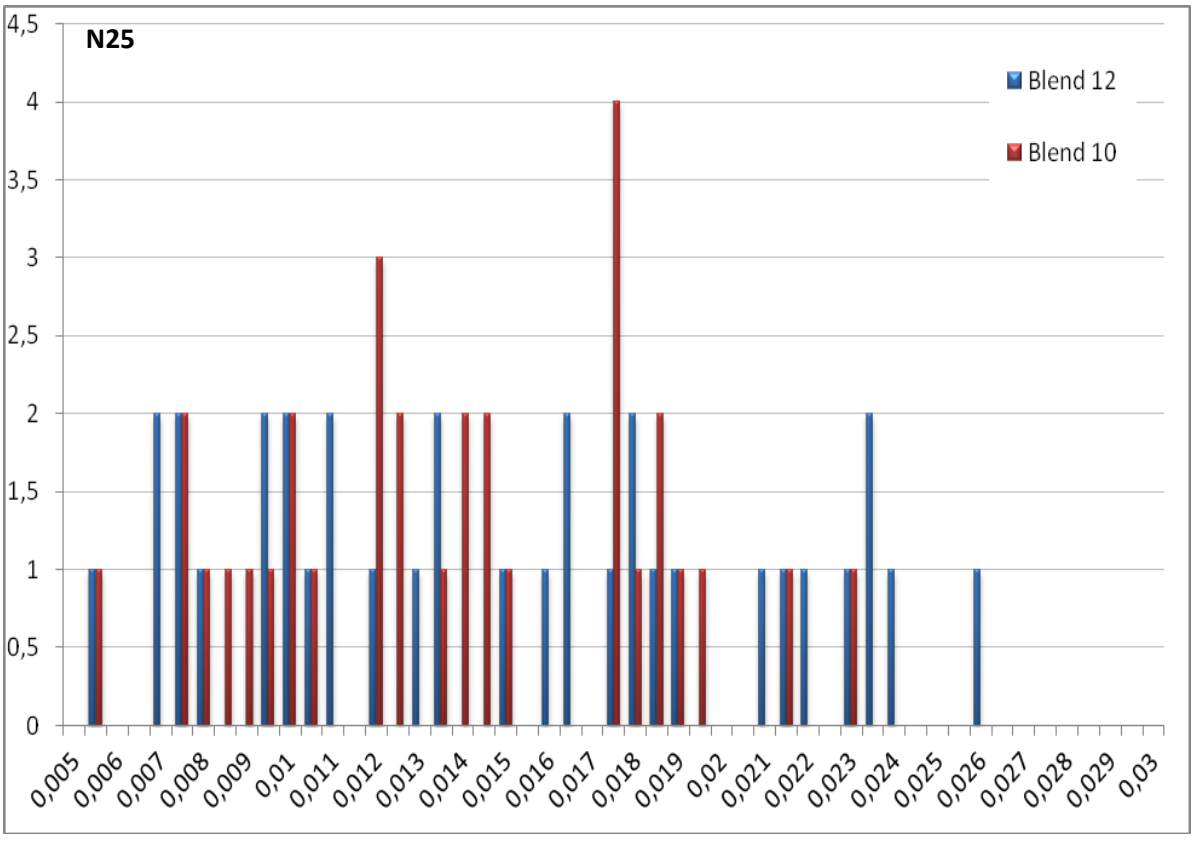
N25
Blend 12
Blend 10
4,5
4
3,5
3
2,5
2
1,5
1
0,5
0
0,005
0,006
0,007
0,008
0,009
0,01
0,011
0,012
0,013
0,014
0,015
0,016
0,017
0,018
0,019
0,02
0,021
0,022
0,023
0,024
0,025
0,026
0,027
0,028
0,029
0,03

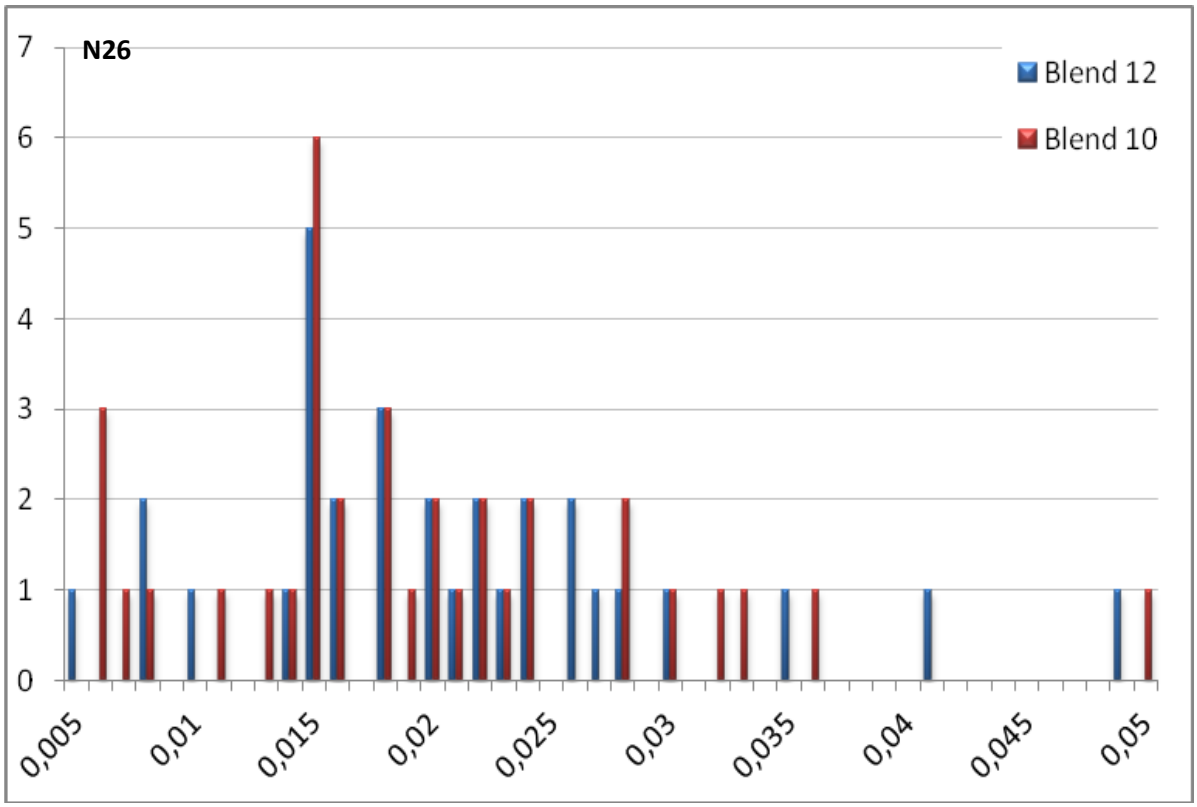
N26
Blend 12
Blend 10
7
6
5
4
3
2
1
0
0,005
0,01
0,015
0,02
0,025
0,03
0,035
0,04
0,045
0,05

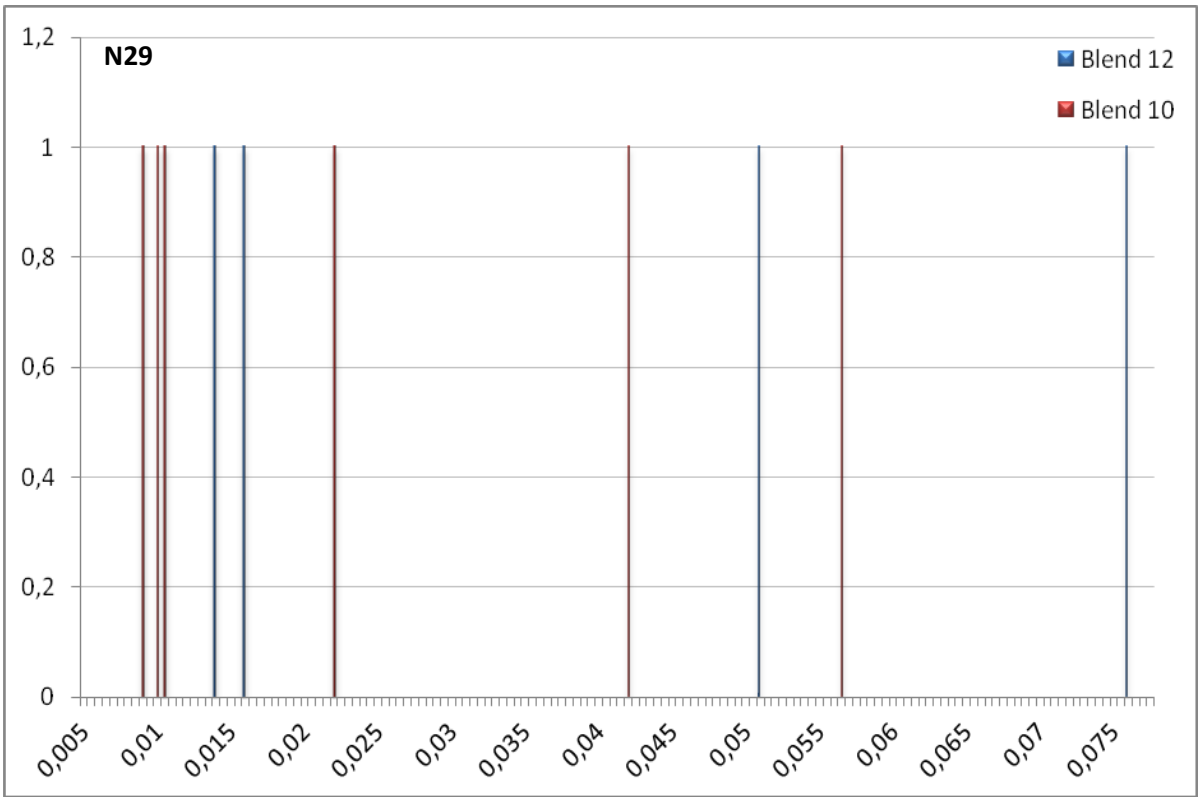
N29
Blend 12
Blend 10
1,2
1
0,8
0,6
0,4
0,2
0
0,005
0,01
0,015
0,02
0,025
0,03
0,035
0,04
0,045
0,05
0,055
0,06
0,065
0,07
0,075

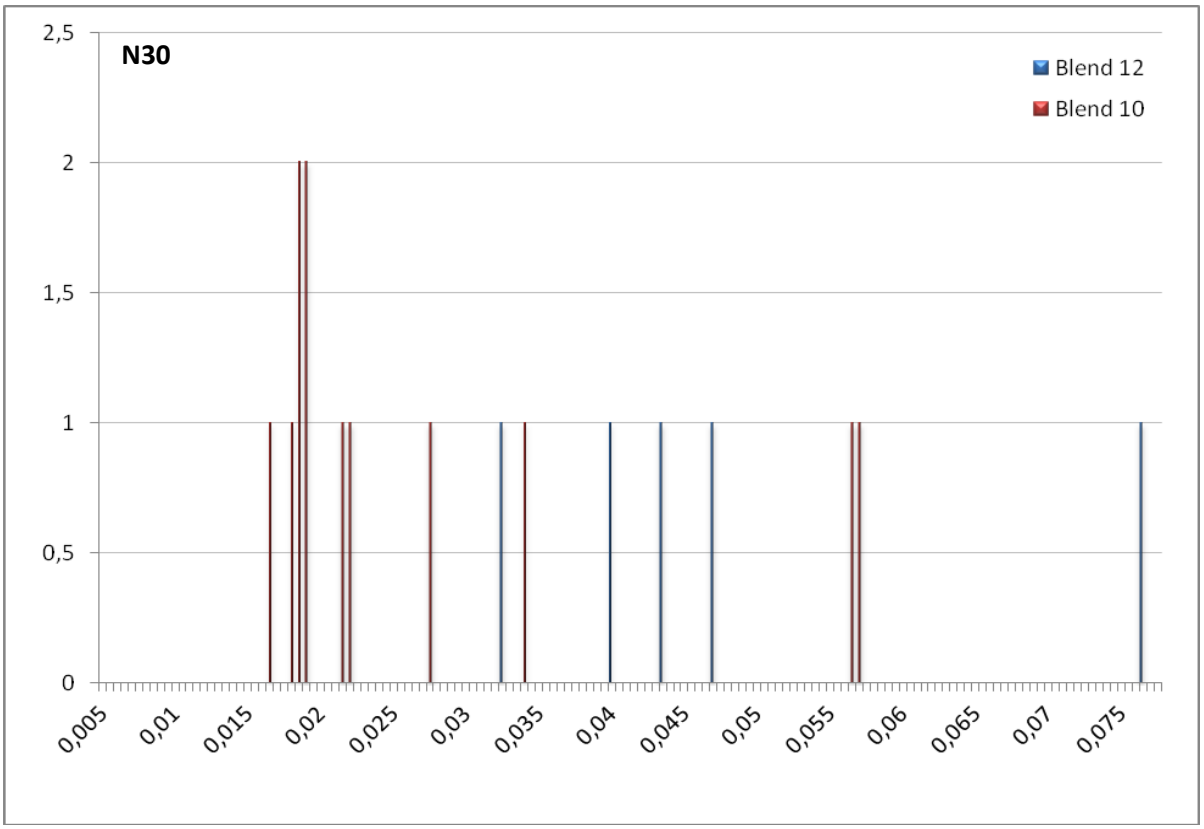
N30
Blend 12
Blend 10
2,5
2
1,5
1
0,5
0
0,005
0,01
0,015
0,02
0,025
0,03
0,035
0,04
0,045
0,05
0,055
0,06
0,065
0,07
0,075

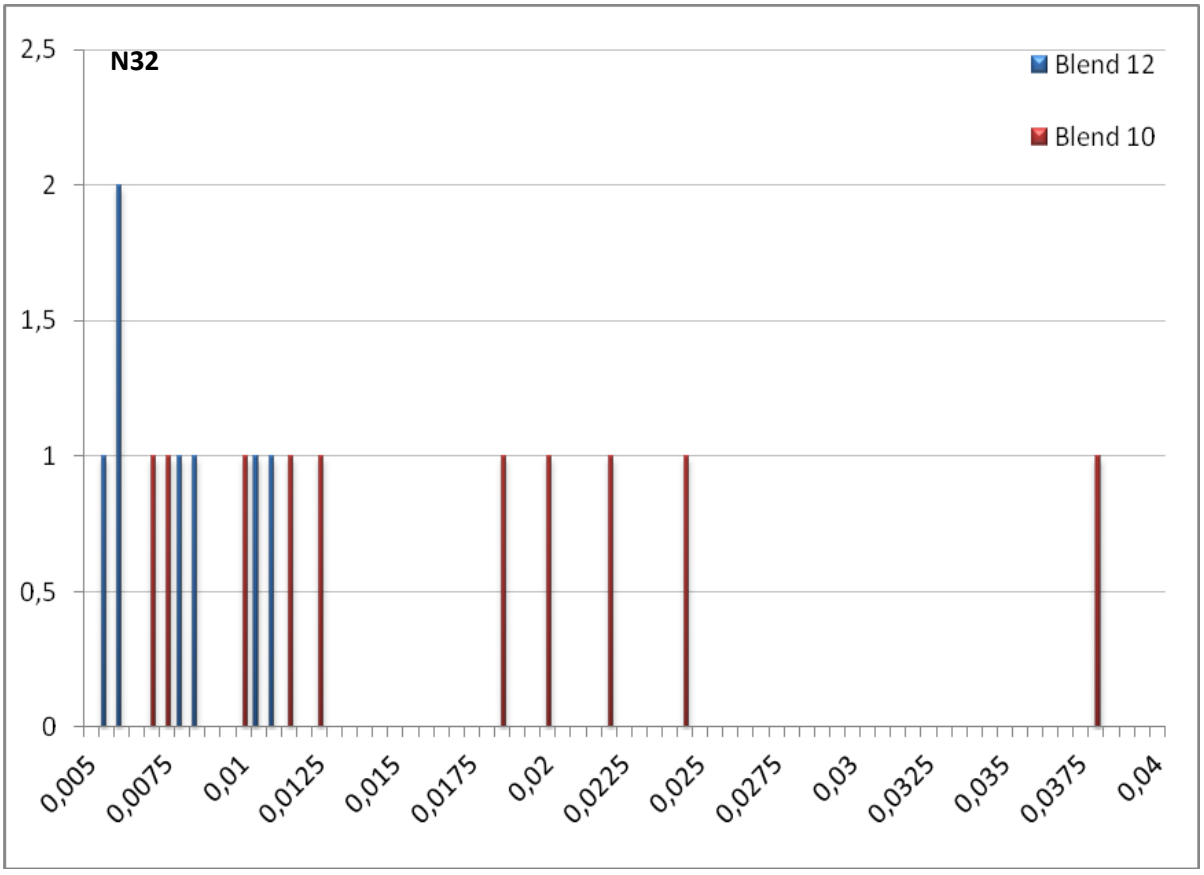
N32
Blend 12
Blend 10
2,5
2
1,5
1
0,5
0
0,005
0,0075
0,01
0,0125
0,015
0,0175
0,02
0,0225
0,025
0,0275
0,03
0,0325
0,035
0,0375
0,04

Corrected tables

Table 5. Overview of comparison of response strengths to blends and single odorants with alpha level corrected for multiple comparisons (α`= 0.0018). For each combination of odorants, if one odorant is significantly more potent than the other, the table displays the color of the stronger odorant.

MDS <>	Blends	Blend 12	Blend 10	Blend 2	Linalool	Germacrene D	Hexenylacetate
Singles	P<0,001						
Blend 12							
Blend 5							
Blend 2							
Linalool			P<0,0018				
Germacrene D		P<0,0018					
Hexenylacetate							
Phenylethanol		P<0,0018	P<0,0018				

Table 6. Overview **of** Spearmans rank order coefficient for each pair of odorants with alpha level corrected for multiple comparisons (α`= 0.0022). Green: significant; red: not significant.

Correlation	Blend 12	Blend 10	Blend 5	Blend 2	Linalool	Germacrene D	Hexenylacetate
Blend 12							
Blend 10	0,87						
Blend 5	0,81	0.4					
Blend 2	0,86	0,78					
Linalool	0,85	0,82		0,95			
Germacrene D	0,45	0,32		0,70	0,61		
Hexenylacetate	0,73	0,95		0,82	0,81	0,40	
Phenylethanol	0,89	0,83			0,60	0,80	0,80